GEOLOGY AND PETROLOGY OF THE KÖSEDAĞ METAVOLCANIC ROCKS TO THE SOUTH OF TOSYA

A THESIS SUBMITTED TO
THE GRADUATE SCHOOL OF NATURAL AND APPLIED SCIENCES
OF
MIDDLE EAST TECHNICAL UNIVERSITY

BY

FARUK BERBER

IN PARTIAL FULFILLMENT OF THE REQUIREMENTS
FOR
THE DEGREE OF MASTER OF SCIENCE
IN
GEOLOGICAL ENGINEERING

AUGUST 2015

Approval of the thesis:

GEOLOGY AND PETROLOGY OF THE KÖSEDAĞ METAVOLCANIC ROCKS TO THE SOUTH OF TOSYA

submitted by **FARUK BERBER** in partial fulfillment of the requirements for the degree of **Master of Science in Geological Engineering Department, Middle East Technical University** by,

Prof. Dr. Gülbin Dural Ünver _____
Dean, Graduate School of **Natural and Applied Science**

Prof. Dr. Erdin Bozkurt _____
Head of Department, **Geological Engineering**

Assoc. Prof. Dr. Kaan Sayıt _____
Supervisor, **Geological Engineering Dept., METU**

Examining Committee Members:

Prof. Dr. M. Cemal Göncüoğlu _____
Geological Engineering Dept., METU

Assoc. Prof. Dr. Kaan Sayıt _____
Geological Engineering Dept., METU

Prof. Dr. Uğur Kağan Tekin _____
Geological Engineering Dept., HU

Assoc. Prof. Dr. Biltan Kürkçüoğlu _____
Geological Engineering Dept., HU

Assist. Prof. Dr. Fatma Toksoy Köksal _____
Geological Engineering Dept., METU

Date: 26.08.2015

I hereby declare that all information in this document has been obtained and presented in accordance with academic rules and ethical conduct. I also declare that, as required by these rules and conduct, I have fully cited and referenced all material and results that are not original to this work.

Name, Last name : Faruk Berber

Signature :

ABSTRACT

GEOLOGY AND PETROLOGY OF THE KÖSEDAĞ METAVOLCANIC ROCKS TO THE SOUTH OF TOSYA

Berber, Faruk
M.S., Department of Geological Engineering
Supervisor: Assoc. Prof. Dr. Kaan Sayıt

August 2015, 102 pages

The Kösedağ Metavolcanics crops out in the southern Central Pontides as a NE-SW trending belt to the south of Tosya. This unit is characterized by a low-grade metavolcanic assemblage interbedded with metasedimentary lithologies. While these metavolcanics are bounded to the north by the North Anatolian Fault Zone, they structurally overlie the metacarbonates of the Dikmen Formation in the south.

Petrographically, the Kösedağ Metavolcanics are characterized by metadacites, metaandesites and metabasalts. The metadacites within this unit include abundant quartz phenocrysts, whereas the metaandesites are plagioclase-phyric. The metabasalts, on the other hand, consists of clinopyroxene and plagioclase as the dominant primary phases. All these metavolcanics have been influenced by low-grade metamorphism. In addition, the Kösedağ Metavolcanics appear to have been affected by mylonitic deformation along the NAFZ.

The Kösedağ Metavolcanics are characterized by a wide range of chemical compositions including basalts, andesites and dacites. The Kösedağ Metavolcanics are subdivided into two groups as Type 1 and Type 2 based on trace element systematics. The Kösedağ Metavolcanics display enrichment in Th and LREE relative to HFSE, and characterized by negative Nb anomalies, suggesting involvement of subduction component. The high Zr/Nb, low Zr/Y and Nb/Y signatures of the Kösedağ Metavolcanics indicate that they have derived from a depleted mantle source similar to N-MORB source.

Geochemical signatures of the Kösedağ Metavolcanics suggest that they have formed above a subduction zone. Considering also their geological characteristics, the Kösedağ Metavolcanics appear to represent remnants of an island arc within a Neotethyan branch during the Late Cretaceous.

Keywords: Central Pontides, metavolcanic rocks, geochemistry, island arc.

ÖZ

TOSYA GÜNEYİNDEKİ KÖSEDAĞ METAVOLKANİK KAYALARININ JEOLOJİSİ VE PETROLOJİSİ

Berber, Faruk
Yüksek Lisans, Jeoloji Mühendisliği Bölümü
Tez Yöneticisi: Doç. Dr. Kaan Sayıt

Ağustos 2015, 102 sayfa

Kösedağ metavolkanik kayaları, güney Orta Pontidler'de, Tosya'nın güneyinde KD-GB uzanımlı bir kuşak boyunca yüzlek verirler. Birim metasedimanter litolojilerle ardalanan metavolkanik kayalardan oluşur. Kösedağ Metavolkanikleri kuzeyde Kuzey Anadolu Fay'ı ile sınırlanırken, güneyde Dikmen Formasyonu'nun metakarbonatlarını tektonik olarak üzerlemektedirler.

Kösedağ metavolkanik kayaları petrografik olarak metadasit, metaandezit ve metabazalt olarak tanımlanmışlardır. Metadasitler bol miktarda kuvars fenokristalleri içerirken, metaandezitlerde hakim mineral plajiyoklastır. Diğer taraftan metabasaltların birincil fazlarını klinopiroksen ve plajiyoklas oluşturmaktadır. Kösedağ Metavolkanikleri düşük dereceli metamorfizmadan etkilenmişlerdir. Birim ayrıca Kuzey Anadolu Fay Zonu boyunca, milonitik deformasyona maruz kalmıştır.

Kösedağ Metavolkanikleri bazalttan, andezit ve dasite kadar değişen geniş bir kimyasal kompozisyon aralığı sunarlar. Kösedağ Metavolkanikleri iz element sistematiğine göre Tip 1 ve Tip 2 olmak üzere ikiye ayrılırlar. Kösedağ metavolkanik kayaları HFSE'lere göreceli olarak, Th ve LREE konsantrasyonlarında zenginleşme gösterirler, ve negatif Nb anomalisine sahiptirler. Bu özellikler onların dalma-batma öğesi taşıdıklarını işaret etmektedir. Yüksek Zr/Nb, düşük Zr/Y ve Nb/Y oranları Kösedağ Metavolkaniklerinin N-MORB kaynağına benzer, tüketilmiş bir manto kaynağından türediklerini gösterir.

Jeokimyasal karakterleri, Kösedağ Metavolkaniklerinin dalma-batma zonu üzerinde oluştuklarını işaret eder. Jeolojik özellikleri de göz önüne alınırsa, Kösedağ Metavolkanikleri'nin Geç Kretase'de bir Neotetis kolu içinde yeralan bir yayın kalıntısı olduğu düşünülebilir.

Anahtar kelimeler: Orta Pontidler, metavolkanik kayalar, jeokimya, ada yayı.

To my brother

ACKNOWLEDGEMENTS

This thesis study was funded by the ÖYP Programme.

Foremost, I would like to express my sincere gratitude to my supervisor, Assoc. Prof. Dr. Kaan Sayıt, for his continuous support invaluable guidance, patience and encouragement during this M.Sc. study. I am extremely grateful for his advice, both on academic and on personal level. His attitude inspired and encouraged me for writing thesis.

I would like to express my thanks to Prof. Dr. M.Cemal Göncüoğlu for his valuable recommendations and ideas regarding the study.

I wish to thank my examining committee members, Prof. Dr. M.Cemal Göncüoğlu, Prof. Dr. Uğur Kağan Tekin, Assoc. Prof. Dr. Biltan Kürkçüoğlu and Assist. Prof. Dr. Fatma Toksoy Köksal for their valuable recommendations and criticism.

I would like to thank my friends Sanem Elidemir, Okay Çimen, Yavuz Kaya, Mustafa Yücel Kaya, Felat Dursun, Mustafa Kaplan, Alican Aktağ, Çidem Argunhan, for their valuable help and being there for me whenever I need any help.

I would like to thank Mr. Orhan Karaman for the preparation of thin sections and valuable help of him as driver during field work.

At last but not the least, I would like to thank my family for their endless encouragements during my study.

TABLE OF CONTENTS

LIST OF FIGURES

FIGURES

LIST OF TABLES

TABLES

CHAPTER 1

INTRODUCTION

Anatolia represents an east-west trending sector within the Alpine-Himalayan orogenic belt, and is located between Laurasia in the north and Gondwana in the south. This belt is characterized by distinct oceanic and continental fragments related to the opening and closure of the Paleozoic and Mesozoic oceanic basins known as the Tethys Oceans (Şengör and Yılmaz, 1981; Göncüoğlu et al., 1997; Okay and Tüysüz, 1999). Anatolia can be subdivided into four continental microplates (from north to south): 1) The Istranca-Istanbul-Zonguldak Terrane (IIZT), 2) The Sakarya Composite Terrane (SCT), 3) The Tauride-Anatolide Terrane (TAT) and 4) the SE Anatolian Autochton. From north to south (Fig. 1-1), the Alpine sutures separating these terranes are the Intra-Pontide Suture Belt (IPSB), Izmir-Ankara-Erzincan Suture Belt (IAESB) and SE Anatolian Ophiolite Belt, respectively (e.g. Göncüoğlu et al., 1997). Of these, the Intra-Pontide Suture Belt is bounded by the Sakarya Terrane in the south and İstanbul Terrane in the north. The ophiolitic suture known as the IAESB occurs between the SCT and the Anatolides-Taurides. This latter oceanic domain includes remnants of an ancient ocean basin known as the İzmir-Ankara section of the Eastern Mesozoic Tethys Ocean (Sengör and Yılmaz, 1981; Dercourt et al., 1986; Robertson et al., 1996; Dilek et al., 1999; Göncüoğlu et al., 1997, 2000; 2006; 2010; Stampfli and Borel, 2002; Bortolotti and Principi, 2005; Schmid et al., 2008; Moix et al., 2008).

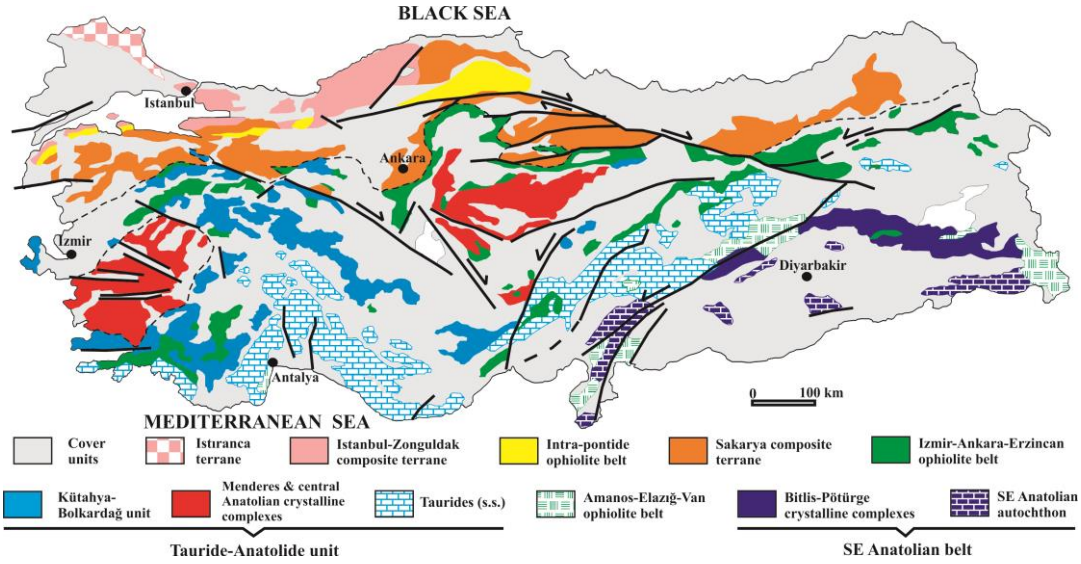

Figure 1-1: Distribution of the main Alpine terranes in Northern Turkey (modified from Göncüoğlu et al., 2010).

The studied unit, namely the Kösedağ Metavolcanics and their cover, is located to the south of Kastamonu-Tosya. They are at the junction of the IPSB and IAESB, where the IIZ, Sakarya and the Central Anatolian Crystalline Complex (CACC) of the Tauride-Anatolide terranes juxtapose. The North Anatolian Transform Fault with its numerous splays runs through the studied area, which complicates the classification of the studied unit into the major tectonic units in the region. In the next paragraphs, an overview of the main tectonic units around the study area will be presented in order to give a brief information about their definition and geodynamic origin.

The Rhodope-Pontide Fragment (Şengör, 1984) or Terrane including the northern part of Ketin's (1966) Pontides is bounded by the Black Sea in the north and the Intra-Pontide Suture in the south. The RPT comprises a Cadomian basement (e.g. Ustaömer and Rogers, 1999; Chen et al., 2002) of North Gondwana origin, covered by an almost complete Paleozoic basement, known as the Paleozoic of Istanbul (e.g. Görür et al., 1997). At the end of Paleozoic, the RPT was amalgamated to Laurasia by the Variscan orogeny. During the Mesozoic, the RPT constituted the active margin of Eurasia facing to the Intra-Pontide branch of Neotethys (Şengör and Yılmaz, 1981; Okay and Tüysüz, 1999). The latter was finally consumed in

Late Cretaceous, leading to the collision between the RPT and the SCT. The earliest common cover of the RPT and the SCT is of Early Cretaceous in age (Tüysüz, 1990; Yiğitbaş et al., 1999).

The Intra-Pontide Suture Zone (IPSZ) is characterized by deformed and/or metamorphic rocks lying along an east-west trending belt and units belonging to a Neotethyan oceanic basin (e.g. Göncüoğlu et al., 1997, 2000, 2008). It extends more than 400 km at northern Turkey from the Kazdağı Peninsula to Boyabat town (Şengör et al., 1982; Yılmaz et al., 1997; Robertson and Ustaömer, 2004; Göncüoğlu et al., 1997). To the east of Boyabat town the rock units of the IPS disappear between the active faults or alternatively merge with the IAESB. The recent data from the oceanic assemblages within the mélange complexes indicate that the life-span of the Intra-Pontide Ocean was from Middle Triassic to early Late Cretaceous (e.g. Göncüoglu et al., 2014). Geochemical data suggest that the ocean was consumed by episodic intra-oceanic subduction events giving rise to supra-subduction-type oceanic crust generation (Göncüoglu et al., 2012; Sayit et al., 2015) and multiple phases of subduction related metamorphism (e.g. Okay et al., 2006, 2013, 2014, 2015; Aygül et al., 2015). The final closure of the Intra-Pontide Ocean very probably occurred at the end of Cretaceous (Göncüoğlu et al., 2014)

The SCT is a "composite terrane" consisting of a Variscan arc basement (e.g. Göncüoglu et al., 1997, 2000; Topuz et al., 2004, 2007; Okay et al., 2006; Göncüoglu et al., 2010; Ustaömer et al., 2012) and its Permian cover (e.g. Göncüoglu et al., 1997, 2010). The remnants of an Early Mesozoic subduction-accretion prism (the Karakaya Complex sensu Okay and Göncüoglu, 2004) are tectonically accreted with the Variscan basement and its Permian-Triassic cover (e.g. Sayit and Göncüoglu, 2009, 2013; Sayit et al., 2011). Early Jurassic-Late Cretaceous cover of the SCT typically represents a north-facing passive margin bounding the Intra-Pontide Branch of Neotethys. During the Late Cretaceous closure of the Intra-Pontide Ocean, its oceanic lithosphere (e.g. Aylıdağ Ophiolite, Göncüoglu et al., 2012) subduction-accretion prism material (e.g. Arkotdağ Melange; Göncüoglu et al., 2012, 2014) were thrusted onto the SCT passive margin. In the Central Pontides, the remnants of this subduction-accretion prism

with metamorphic fore-arc, arc and back-arc assemblages (e.g. Yılmaz, 1980, 1988; Tüysüz, 1990; Ustaömer and Robertson, 1993, 1994, 1999; Yılmaz et al., 1997; Yiğitbaş et al., 1999; Okay et al., 2006; Çelik et al., 2011; Göncüoglu et al., 2012, 2014; Topuz et al., 2013; Marroni et al., 2014) were named recently as the Central Pontide Structural Complex (CPSC) (Tekin et al., 2012) or Central Pontide Supercomplex (Okay et al., 2013), which is in tectonic contact with the studied Kösedağ Metavolcanics and its cover.

The representatives of the IAESB, located to the south of the Kösedağ Metavolcanics have been studied relatively well in terms of geological and geochemical aspects (for a recent review see Rojay, 2013; Parlak et al., 2013; Gökten and Floyd, 2007; Sarıfakioglu et al., 2008, 2014; Uysal et al., 2014, 2015). This suture belt extends from the Aegean coast eastwards for hundreds of kilometres to Erzincan and to northern Iran (e.g. Göncüoğlu et al., 2010). On the other hand, it merges with the Vardar Ocean in the west (e.g. Marroni et al., 2014). The earliest ages of oceanic material within the IAESB are Middle Triassic (e.g. Tekin et al., 2002). As it is the case in the Intra-Pontide Ocean, the Izmir-Ankara-Erzincan Ocean started to close as early as Middle-Late Jurassic (e.g. Çelik et al., 2011; Topuz et al., 2013) by intra-oceanic subduction, generating supra-subduction-type oceanic lithosphere (e.g. Göncüoglu and Türeli, 1993; Yalınız et al., 1996) as late as the Campanian (e.g. Bortoletti et al., 2013). The subduction-accretion prism units of the Izmir-Ankara Ocean were thrusted upon the Anatolide Unit in the Central Sakarya Ophiolitic Complex prior to the Middle Paleocene (e.g. Göncüoğlu et al., 2000, 2006). In the CACC the obduction of ophiolitic material onto the continental crust was prior to the Maastrichtian (e.g. Yaliniz et al., 1999, 2000). The final closure of the IAESB by the collision of the SCT and Tauride-Anatolide units is Middle Eocene, where oceanic relicts of the Izmir-Ankara Ocean, overthrusted the basement rocks of the SCT to the north of Ankara (e.g. Göncüoğlu, 2010).

The TAT is represented in the vicinity of the study area by the CACC. It comprises a Tauride-type continental crust succession with a pre-Cambrian basement and a Paleozoic-Mesozoic platform sequence, metamorphosed at the end of Cretaceous

(Göncüoglu et al., 1991). Mainly supra-subduction-type ophiolitic assemblages (Central Anatolian Ophiolites, Yaliniz et al., 1996; Floyd et al., 1998) of mainly Turonian age, derived from the IAESB (Yaliniz et al., 2000) are found as allochthonous bodies within the CACC. The basement and the ophiolites are intruded by granitoids of Late Cretaceous age (e.g. Köksal et al., 2004, 2012, 2013) indicating a post-Turonian–pre-Maastrichtian age for ophiolite obduction.

1.1. Aim and Scope

The Kösedağ Metavolcanics is located in a tectonically complex area, which had been affected first by the accretion and subsequent closure of Neotethys during the Late Mesozoic, and by the later tectonic processes in relation to North Anatolian Fault (NAF) Zone (Berber et al., 2014; Aygül et al., 2015). Regarding a correlation of the Kösedağ Metavolcanics with the surrounding metamorphic ones, they display similarities to the variably metamorphosed volcanic units cropping out to the north of the study area in the CPSC. However, a possible primary relation is obscured by the transform fault character of the splays of the NAF Zone.

On the other hand, the Mudurnu Volcanics of Lower to Middle Jurassic age within the SCT (Genç and Tüysüz, 2010) show resemblance to the Kösedağ Metavolcanics in terms of lithological and geochemical aspects. However, the precise age of the Kösedağ Metavolcanics and its carbonate cover is a matter of debate. Moreover, the metamorphic nature of the Kösedağ Metavolcanics makes them different than the Mudurnu volcanics. In addition, arc-related volcanics, similar to the Kösedağ Metavolcanics are exposed within the Ankara Mélange within the İzmir-Ankara Suture Belt, which have been identified in recent years (Sarıfakıoğlu et al., 2008; Çelik et al., 2011). Therefore, a detailed examination of the Kösedağ Metavolcanics and their correlation with the volcanics cropping out in different units including the İzmir-Ankara-Erzincan Suture Belt would provide crucial information regarding the distribution of tectonic units in the surrounding areas and help to distinguish between the protoliths of the metamorphic rocks of the Intra-Pontide Suture and İzmir-Ankara-Erzincan Suture belts. Hence, this study area was selected to try to shed light on these critical problems.

Within the scope of this study, a geological map of the Kösedağ Metavolcanics was prepared and petrographic features of the lithologies making up the unit were investigated. Furthermore, geochemical characteristics of the Kösedağ Metavolcanics have been presented for the first time in this study. Consequently, it is aimed here to make petrogenetic implications on the Kösedağ Metavolcanics and to enlighten the geological evolution of the area between the IPSB and IAESB.

1.2. Previous Studies

Geological studies in the vicinity of town of Tosya have been mainly about tectonics and economic geology. Furthermore, some reports of MTA regarding the study area also exist. The first studies performed in Tosya and the surrounding areas intended to investigate the nickel formations by Coulant (1984) and Pilz (1937). Blumenthal prepared 1/100.000 scaled geological maps of the area in different years (1939, 1948, 1950). Ayaroğlu (1980) mentioned the economic importance of the area in his study.

Yoldaş (1982) was the first to use the name Karabürçek Formation for the lithological assemblage composed of chlorite-albite-quartz-epidote schist, chlorite-carbonate-quartz schist, metavolcanic rocks, diabase, spilite, andesite and slightly recrystallize limestone. He suggested that the age of the Karabürçek Formation is Lower Triassic by regional correlation.

Yılmaz and Tüysüz (1984) described the Karabürçek Formation as the Kösdağ Metamorphics. They proposed that the age of the Kösdağ Metamorphics is Liassic or pre-Liassic.

Hakyemez et al. (1986) mentioned that the Karabürçek Formation consists of schist, carbonate rocks and metavolcanics, which is exposed in a large area extending from Kınık village to northwestern of Şemsettin neighborhood. These authors defined the Yaylacık Formation, which crops out around the Avşar and Kınık villages, as represented by calcschist, sandstone, metasandstone, metaconglomerate, metasiltstone and metavolcanics. They stated that the lower contact of the Karabürçek Formation is tectonic, whereas the Karabürçek

Formation is transitional to the overlying Yaylacık Formation. Within the carbonates of the Yaylacık Formation they observed the microfauna consisting of *Protopeneroplis* sp., *Neotrocholina* sp**.,** *Nummoloculina* sp., *Nautiloculina* sp., *Trocholina* sp., *Pseudocyclammina* sp., *Valvulina* sp., *Textularia* sp., *Lagenidae* sp., *Clypeina* sp., *Actinoporella* sp., *Bacinella* sp.), which suggests a Late Jurassic-Early Cretaceous age.

Berber et al. (2014) showed that the Kösedağ Metavolcanics are characterized by a wide range of subalkaline lavas, including basalts, andesites and dacites. They proposed two distinct chemical types on the basis of trace element systematics, and suggested that both types have involved subduction component in their genesis. They interpreted the Kösedağ Metavolcanics, which are interbedded with recrystallized pelagic limestone, chert and mudstone, as remnants of an arc-related magmatism. They also mentioned the resemblance of the Kösedağ Metavolcanics to the Lower to Middle Jurassic Mudurnu volcanics in terms of both lithological and geochemical characteristics, and suggested that the Kösedağ Metavolcanics can be metamorphic equivalents of the Mudurnu volcanics, provided that the Kösedağ Metavolcanics are also of the same age.

Aygül et al. (2015) used the name Kösdağ Formation for the metavolcanic rocks in the core of an overturned anticline, overlain by the Late Cretaceous Dikmen Formation. They mentioned that it is tectonically overlain by Middle Jurassic and Albian-Turonian subduction complexes of the CPSC to the north, and tectonically underlain by the ophiolitic mélange. They further suggested that the contact between the Kösdağ Formation and the overlying Dikmen Formation, represented by metacarbonates, slate and volcanogenic sandstone is stratigraphic. These authors reached a similar conclusion drawn by Berber et al. (2014) and interpreted the Kösedağ Metavolcanics (equivalent to Kösdağ Formation) as arc-related products of an intra-oceanic subduction within the Izmir-Ankara-Erzincan Ocean. They suggested that the Late Cretaceous (93.8±1.9 and 94.4±1.9) U-Pb radiometric ages acquired from two metarhyolite samples reflect the age of magmatism, whereas the Ar-Ar age of 69.9±0.4 Ma represents the age of low-grade metamorphism.

Some regional studies did not directly study the Kösedağ Metavolcanics but they included and described this unit in their studies. For example, Ustaömer and Robertson (1999) regarded the Kösdağ unit as a Late Cretaceous Neotethyan volcanic arc bounded by the Kirazbaşı Mélange to the south. Okay et al. (2006), in their study on the Central Pontides, mapped the the Kösedağ Metavolcanics as the Permo-Triassic metabasite-phyllite association that they named the Çangaldağ and Kargı Complexes and the Upper Cretaceous accretionary complex consisting of basalt, chert, shale and serpentinite. Çelik et al. (2011), on the other hand, interpreted the Kösedağ Metavolcanics as the Jurassic-Eocene sedimentary sequence of the Sakarya Zone.

The NAF Zone on the northern boundary of the Kösedağ Metavolcanics is a very important structural feature in North Anatolia (e.g. Barka, 1992). It is a several kilometres wide zone with several right lateral strike-slip faults (e.g. Ellero et al., 2015), that have produced an extensive belt of mylonitic rocks. Barka (1992) regarded the age of the fault zone as the Late Miocene to Early Pliocene. This idea is also consistent with a number of studies which ascribe the initiation time of the NAF Zone to early late Miocene (13 Ma) (Şengör et al., 1985; Dewey et al., 1986).

1.3. Study Area

The study area is exposed to the southeast of town of Tosya town which is located on the Istanbul-Samsun main road and approximately 70 km south of Kastamonu city. It is bounded by NAF to north and covers an area of approximately 80 km^2 in the G-32 a1, G-32 a2 quadrangles of 1/25.000 scale topographic maps of Turkey.

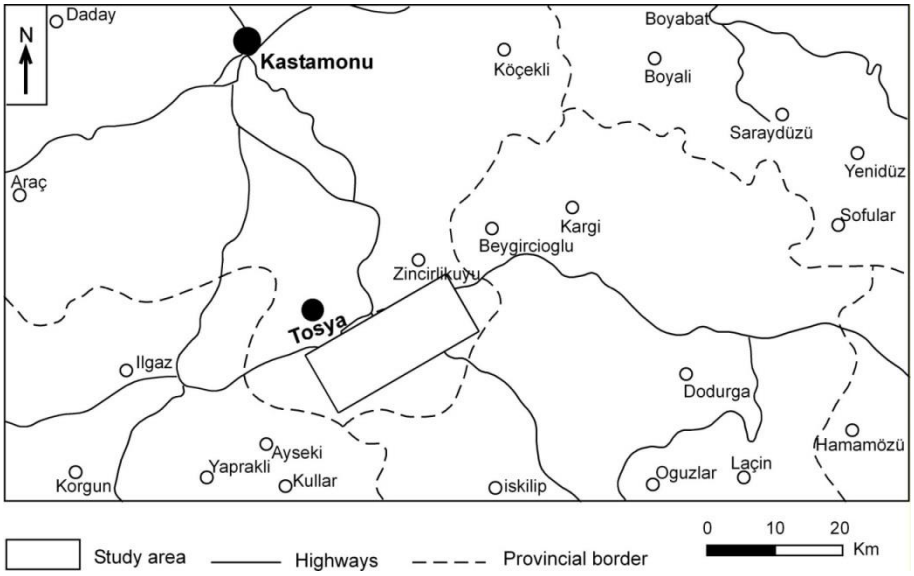

Figure 1-2: Location map of the study area

The study area can be reached by an asphalt road connecting town of Tosya and Iskilip. In the investigated area, the main villages are Aşağıdikmen, Dedem, Sofular and Yukarıdikmen, while Aşağıdikmen Hill, Dedemköy Hill, Topçuoğlugöynüğü Hill constitute the main peaks in the study area.

1.4. Field Work

The field work was performed in 2013 summer period, and a 1/25.000 scaled geological map of the study area was prepared. During the fieldwork, approximately 195 rock samples were collected, which include mainly metavolcanics and to a lesser extent volcaniclastics, recrystallized limestones, mudstones and cherts.

1.5. Laboratory Work

Laboratory work can be subdivided into two main phases as petrographic and geochemical studies. Regarding the petrographic studies, more than 80 thin-sections were studied from rock samples collected from the study area. Thin-sections, prepared at the Department of Geological Engineering, METU were

investigated under the Nikon polarizing microscope. Thin-section microphotographs, on the other hand, were taken by the Olympus camera attached to an Olympus polarizing microscope.

After petrographical investigations, 15 samples were chosen for the geochemical analysis. The samples were broken into small pieces by using a hammer, and sent to ACME Analytical Laboratories (Canada) for pulverization and subsequent analysis to get major, trace and rare earth element concentrations by ICP-ES and ICP-MS.

CHAPTER 2

GEOLOGICAL FEATURES

2.1. Regional Geology

The Kösedağ Metavolcanics and its cover are bounded to the north by the splays of the NAF and by the tectonic slivers of the CPSC (Fig. 2-1). The NAF, which is a 1200 km long active strike-slip fault, has had a major effect on the geology of the study area. The lithologies affected by the fault have been intensely sheared and undergone mylonitization, which is especially evident in the northern boundary of the study area.

The Kösedağ Metavolcanics is overthrust by the Upper Cretaceous mélanges and fore-arc sediments (Aygül et al., 2015; Fig. 2-1), corresponding to the "Kirazbaşı Complex" of (Tüysüz, 1985, 1986; Tüysüz and Tekin, 2007) in the area to the NE of the NAF and the study area. To the south, the Kösedağ Metavolcanics is bounded by the Dikmen Formation with a tectonic contact. The relationship of the Dikmen Formation with the ophiolitic mélange unit is also tectonic, which is well observed in the proximity of Yağcılar and Çukurköy villages. The unit is characterized by an ophiolitic mélange accompanied by blocks of serpentinites, gabbros, pillow-basalts, pelagic limestones and radiolarian cherts, which are thrust onto the recrystallized limestones of Dikmen Formation (Tüysüz, 1990) that may represent the cover of the Kösedağ Metavolcanics (Aygül et al., 2015). In this chapter, geological characteristics of the units within the CPSC that surround the Kösedağ Metavolcanics will be outlined in an order from north to south. This will

be then followed by the geological features of the Kösedağ Metavolcanics and the Dikmen Formation.

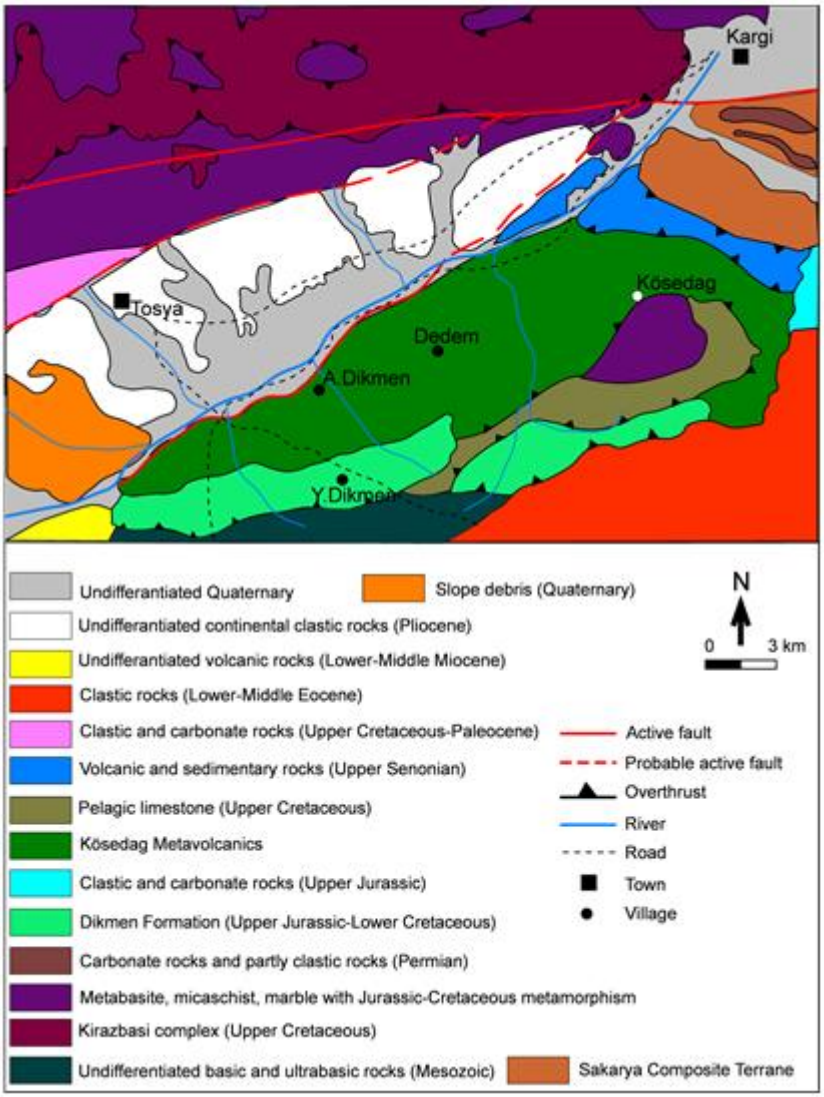

Figure 2-1: Modified from 1/500.000 Geological Map of Turkey MTA Publication, MTA, 2003

2.1.1. Central Pontide Structural Complex (CPSC)

The CPSC is an association of several tectonic units, which covers a wide area in the Central Pontides (Tekin et al., 2012). These variably metamorphosed units are from N to S: the Çangaldağ Complex, the Elekdağ ophiolite, Domuzdağ Complex,

Martin Complex, Esenler Complex, Saka Complex, Kızılırmak ophiolite and Kirazbaşı Complex (Fig. 2-2). The Çangaldağ Complex is exposed to north of town of Taşköprü and characterized by an over 10 km thick assemblage composed of volcanic, volcaniclastic and fine-grained clastic rocks that have metamorphosed under low-greenschist-facies conditions (Yılmaz, 1988; Ustaömer and Robertson, 1993; Okay et al., 2013). The complex is unconformably overlain by the Lower Cretaceous sedimentary rocks to the north (Okay et al., 2013). Ustaömer and Robertson (1999) proposed a pre-Late Jurassic age for the formation of Çangaldağ Complex on the basis of Middle-Jurassic granitic rocks intruding the complex (Yılmaz, 1980; Yılmaz and Boztuğ, 1986; Aydın et al., 1995). Ustaömer and Robertson (1993, 1994) suggest a Middle Jurassic age (168 and 169 Ma) based on zircons extracted from dacite porphyries. In their recent study, however, Okay et al. (2013) suggested an Early Cretaceous (Valanginian-Barremian) metamorphic age for this unit based on Ar-Ar age performed on white micas from phyllites. The Çangaldağ Complex was interpreted by Yılmaz (1980, 1988) and Tüysüz (1990) as an ophiolite, whereas Ustaömer and Robertson (1997, 1999) interpreted the unit as an intra-oceanic magmatic arc. Okay et al. (2006), on the other hand, regarded the Çangaldağ Complex as similar to the Nilüfer Unit which has been interpreted as a Paleo-Tethyan oceanic plateau (Okay, 2000) or a series of oceanic islands (Pickett and Robertson, 2004; Sayit and Göncüoglu 2009; Sayit et al., 2010).

The Elekdağ Ophiolite (Yılmaz and Tüysüz, 1984) is a SW-NE trending body consisting of serpentinite, serpentinized layered peridotite, serpentinized massive peridotite, dykes of massive metagabbro, layered gabbro lenses, isolated dolerite, microgabbro and pegmatitic gabbro. The unit has been subjected to high-pressure/low-temperature metamorphism. The Elekdağ Ophiolite is thrust over mélange units in the south. On the other hand, its northern contact with Çangaldağ Complex is a thrust. A Late Cretaceous age was suggested as the age of HP/LT metamorphism by (Okay et al., 2006; 2013). Elekdağ ophiolite was proposed to represent by supra-subduction zone ophiolite (Ustaömer and Robertson, 1999).

The Domuzdağ Complex is composed of quartz-mica schist, metabasite, marble, metachert and ophiolites displaying eclogitic metamorphism (Okay et al., 2006).

This metamorphic unit crops out in an area covering the north of the Tosya town, north of Kargı and west of Boyabat. In previous works, the southern part of the Domuzdağ Complex was defined under different names, namely the Bekirli Formation (Tüysüz and Yiğitbaş, 1994) and Domuzdağ-Saraycıkdağ Complex (Ustaömer and, Robertson, 1997). The Domuzdağ Complex is tectonically overlain by the Esenler Complex that is characterized by blueschist-facies metamorphics including phyllite, metasandstone and subordinate metabasite and marble (Okay et al., 2013). On the other hand, to south it is underlain by the Kirazbaşı Complex. Ustaömer and Robertson, (1999) suggested a Palaeozoic-earliest Triassic age for subduction accretion complex called Domuzdağ-Saraycık Complex. However, Okay et al. (2006) suggested a Middle Cretaceous age (circa 105 Ma) for the metamorphism of the Domuzdağ Complex based on Ar-Ar and Rb-Sr isotopic data, which is similar to that of the Martin Complex. The Domuzdağ Complex was interpreted as a subduction complex by Tüysüz (1990), Tüysüz and Yiğitbaş (1994), and Ustaömer and Robertson (1997, 1999).

The Martin Complex is mainly composed of slate and phyllite with lesser amount black recrystallized limestone, metasiltstone and fine-grained metasandstone (Okay et al., 2013). It is considered as a Triassic or older basement (Tüysüz, 1999; Ustaömer and Robertson, 1994, 1999; Yılmaz et al., 1997; Yiğitbaş et al., 1999; Uğuz et al., 2002). In a recent study, Okay et al. (2013) proposed an Albian (107±4 Ma) age for the metamorphism of the unit.

The Esenler Complex crops out to the SE of Kastamonu and it consists of phyllite, metasandstone, metabasite and marble. The complex is characterized by Middle Cretaceous (Albian) metamorphism (Okay et al., 2013). The Esenler Complex tectonically overlies the Domuzdağ Complex in the north. The Esenler Complex displays the same metamorphism age (105 Ma) with that of Domuzdağ Complex.

The Saka Complex is composed of micaschists, marble, calc-schist, metabasite and serpentinite slivers, which crops out around the Daday Massif (Okay et al., 2013). Ar-Ar ages from muscovite indicated a Middle Jurassic (162 and 170 Ma) age

(Okay et al., 2013). The Saka Complex was interpreted by Okay et al. (2013) as an accretionary complex.

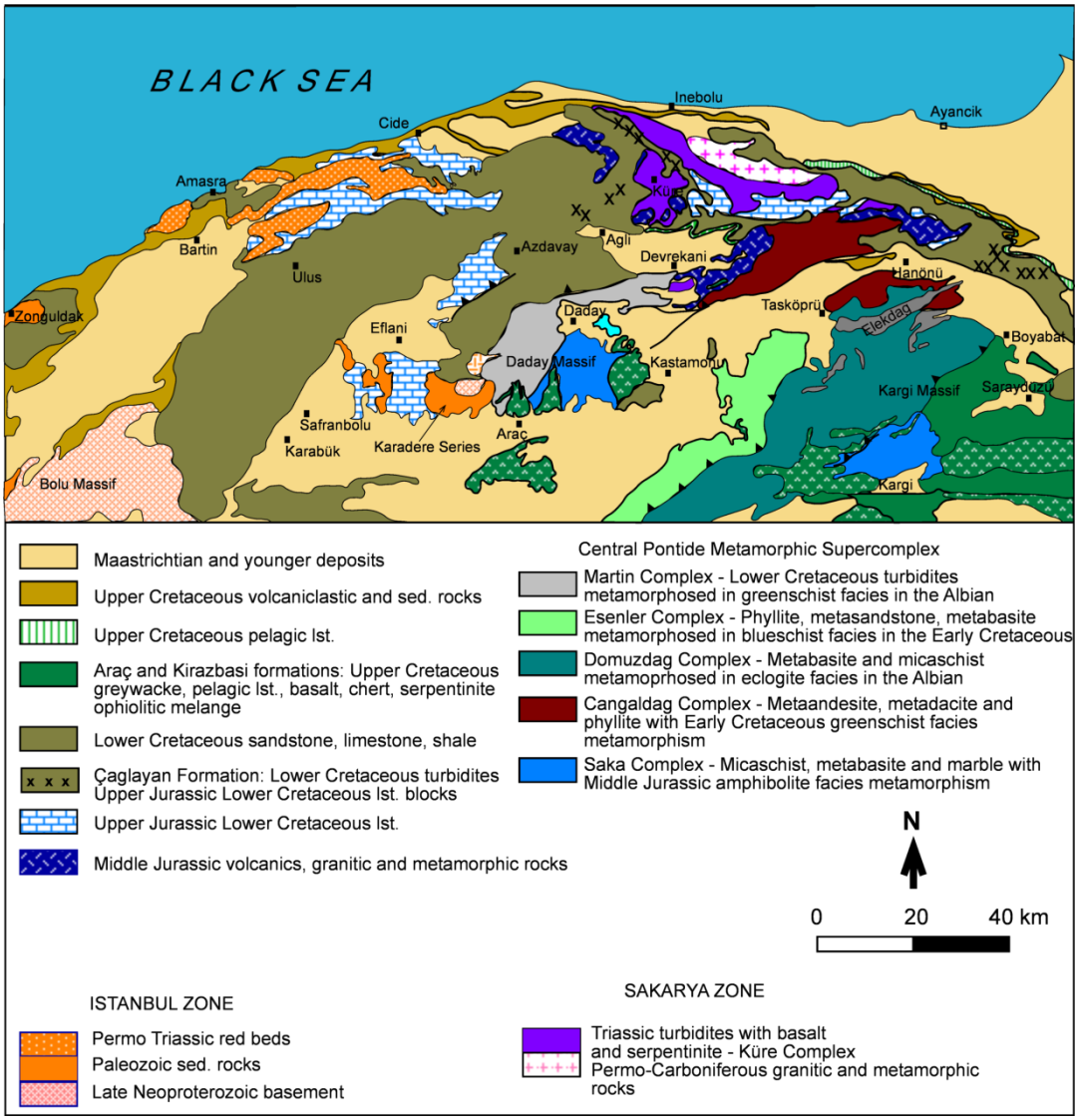

Figure 2-2: Distribution of tectonic units in the Central Pontides (after Okay et al., 2013).

The southern part of the CPSC in the vicnity of Kargı is composed of a number of Triassic-Early Cretaceous metamorphic units imbricated with the late Early Cretaceous Kirazbaşı Complex (Tüysüz, 1993; Tüysüz and Tekin, 2007). The Kirazbaşı Complex thrust over the Kösedağ Metavolcanics (Tüysüz and Tekin, 2007, Fig. 2-1) and is overthrust by the high-grade metamorphics of the Domuzdağ Unit. To the NW of the study area the same unit is named as the Arkot Dağ

Mélange, wheras the ophiolitic slice on top of it is described as the Aylı Dağ Ophiolite (Göncüoğlu et al., 2014; Catanzariti et al., 2014; Marroni et al., 2014; Sayit et al., 2015). The Kirazbaşı Complex and its continuation towards W comprise ophiolitic assemblages and deep marine sedimentary rocks accompanied by blocks of different origin. Apart from these, syn-depositional blocks and tectonic slices including metamorphic rocks and Upper Jurassic-Lower Cretaceous limestones from the Central Pontide basement, along with some silisiclastic turbidites are found within the Kirazbaşı Complex. The Kirazbaşı Complex was regarded as a Triassic unit by Tüysüz and Yiğitbaş (1994), and Early Cretaceous by Okay et al. (2006). However, Tüysüz and Tekin (2007), on the basis of radiolarians obtained from the matrix and blocks of the Kirazbaşı Complex, suggested late Valanginian-early Barremian, middle Albian-latest Cenomanian ages.

The main tectonic unit to the S of NAF and the Kösedağ Metamorphic Unit is the Kızılırmak Ophiolite (Tüysüz, 1990) of the IAESB. It actually is an ophiolitic mélange, characterized by slide-blocks of serpentinized harzburgite, cumulate pyroxenite, dunite, isotropic and layered gabrro and deformed greenschist facies metabasaltic pillow lava in a clastic matrix. This unit crops out in Bayat, Eldivan, along the Kızılırmak River in Pelitcik village, near town of Kargı. The presence of *Globotruncana* obtained from the pelagic limestones interbedded with basaltic pillow lavas suggests a Campanian-Maastrichtian age for the Kızılırmak Ophiolite (Tüysüz, 1990).

Younger units in contact with the Kösedağ Metavolcanics and its cover are the Eocene volcanics outcropping to the southeast of the study area and the Miocene volcanics located to the southwest of it. The Miocene volcanics are pyroclastics known as the Uludere (Sevin and Uğuz, 2011). The Uludere pyroclastics are composed of andesitic, dacitic tuff, tuffite, agglomerate, volcanic conglomerate, basalt, andesite and dacitic lavas.

2.2. GEOLOGICAL OBSERVATIONS IN THE STUDY AREA

2.2.1. The Kösedağ Metavolcanic Rocks

The Kösedağ Metavolcanics (Berber et al., 2014) are represented by metavolcanic rocks consisting of metadacites, metaandesites and metabasalts that have been affected by low-grade metamorphism and variably degree of deformation. These lithologies were previously named as the Kösdağ metamorphics (Yılmaz and Tüysüz, 1984). The Kösedağ Metavolcanics differ from the other metamorphic units in the region by the presence of dynamic metamorphism. The Kösedağ Metavolcanics cover an area of approximately 20 km^2 and is exposed in the vicinity of Aşağıdikmen, Yukarıdikmen, Sofular and Dedem Villages (Fig. 2-3). Since the alternation of different metavolcanics occurs at short intervals, they were not mapped as distinct entities, but given collectively under the name "metavolcanics" (Fig. 2-3, 2-4).

The Kösedağ metavolcanic rocks are bounded to the north by an active splay of the NAF. The fault can be recognized to the NW of the study area, near the Aşağıdikmen village, where it has affected the Kösedağ Metavolcanics. The effect of faulting is reflected by the occurrence of shear zones in which the metavolcanic lithologies have been heavily mylonitized. The presence of foliation is common in these rocks, which has been developed in response to the deformation associated with the faulting. Also, in some places, the mylonitized rocks include boudinaged parts that are observable at the outcrop scale. It must also be noted that while the sheared lithologies display the signs of ductile deformation, this effect becomes weaker away from the shear zone. In contrast to the foliated and boudinaged nature of the former (sheared) lithologies, the latter ones (non-sheared) exhibit massive outlines, reflecting the original appearance of the metavolcanics.

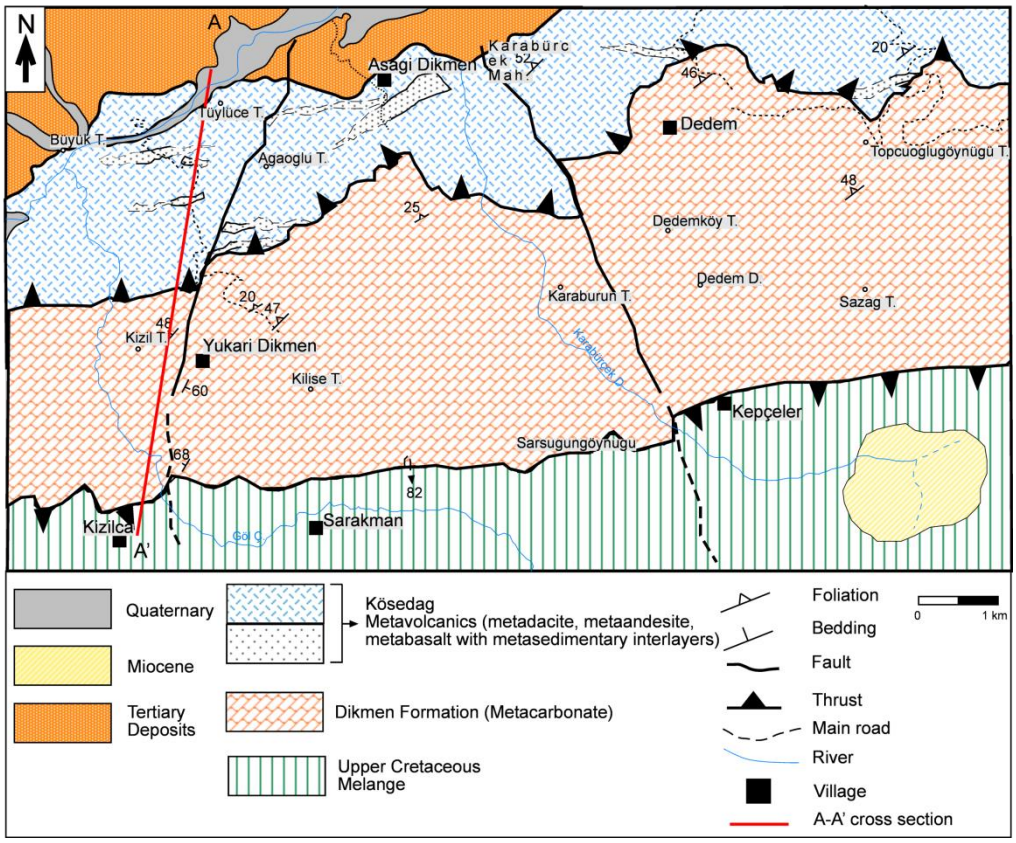

Figure 2-3: Geological map of the study area.

Metadacites are exposed in a large part of the study area. In the field, the metadacites display white, light brownish and greenish colors. Greenish ones actually resemble to metaandesites and can be easily confused if not examined in detail. Inside metadacites, quartz phenocrysts can be identified even in hand specimen, which provide a robust distinction relative to metaandesites. The metadacites are characterized by quartz grains which can be observed by naked eye, with their smoky colors and vitreous appearance. These lithologies are sporadically distributed with the other metavolcanics in the field. The metadacites are observed to be cut by calcite veins in several places. Metadacites exhibit foliation. Well-preserved outcrops of these metavolcanics are found on the road to the Yukarıdikmen Village (Fig. 2-5).

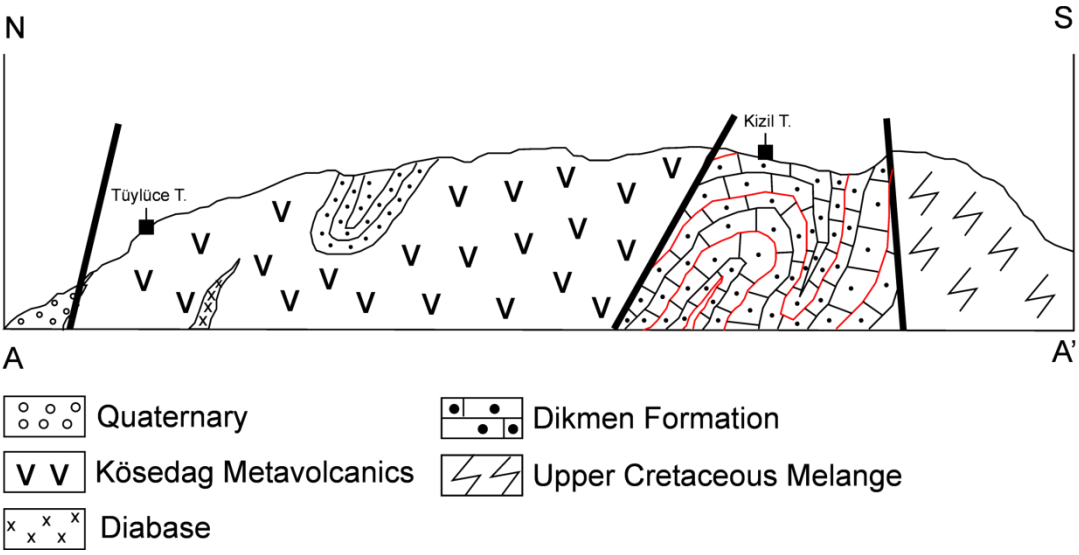

Figure 2-4: Cross section of the study area.

Figure 2-5: Light-colored metadacites with well-developed foliation observed on road to the Yukarıdikmen Village.

Metaandesites probably forms the most common member observed within the Kösedağ Metavolcanics. Most of the metaandesites are fine-grained and have shades of green colors implying the effects of low-grade metamorphism (Fig. 2-6).

Similar to metadacites these metavolcanics also display mylonitic texture which can be observed at outcrop scale (Fig. 2-7). Feldspar is bounded by new sericite minerals, so they exhibit augen appearance. Some kinds of metaandesites display purple colors. Micas leads to shiny appearance in metaandesites.

Figure 2-6: Photograph of typical greenish colored metaandesite displaying foliation.

The metabasalts are recognized by their dark colours in constrast to metaandesites and metadacites that are lighter-colored (Fig. 2-8). The colors of metabasalts on fresh surfaces change from greenish to dark grey. While some metabasalt samples have foliation, others are non-foliated. The influence of low-grade metamorphism on the metabasalts can be identified by the occurence of greenish metamorphic minerals such as epidote and chlorite. These metabasic lithologies appear to be originally porphyritic and aphanitic. In some cases, relict pyroxene phenocrysts can be recognized by naked eye.

Figure 2-7: Sheared metaandesites around the Aşağıdikmen village. Note the boudinaged parts developed in response to ductile deformation associated with the faulting.

Figure 2-8: An exposure of fine-grained metabasalt with dark green color from the south of Kuşçular village. Note the presence of shear zone to the left of metabasalt.

In the study area, the metavolcanics display cross-cut relationships. In some places, metadacites are found to cross-cut metaandesites, and metabasalts cross-cut metadacites (Fig. 2-9). Accordingly, it can be suggested that at least some metabasalts represent the youngest magmatic products among the Kösedağ Metavolcanics. Neverthless, in many areas the presence of intense shearing makes it difficult to decide the relationship as to whether the investigated metavolcanic rock is a dyke or lava flow.

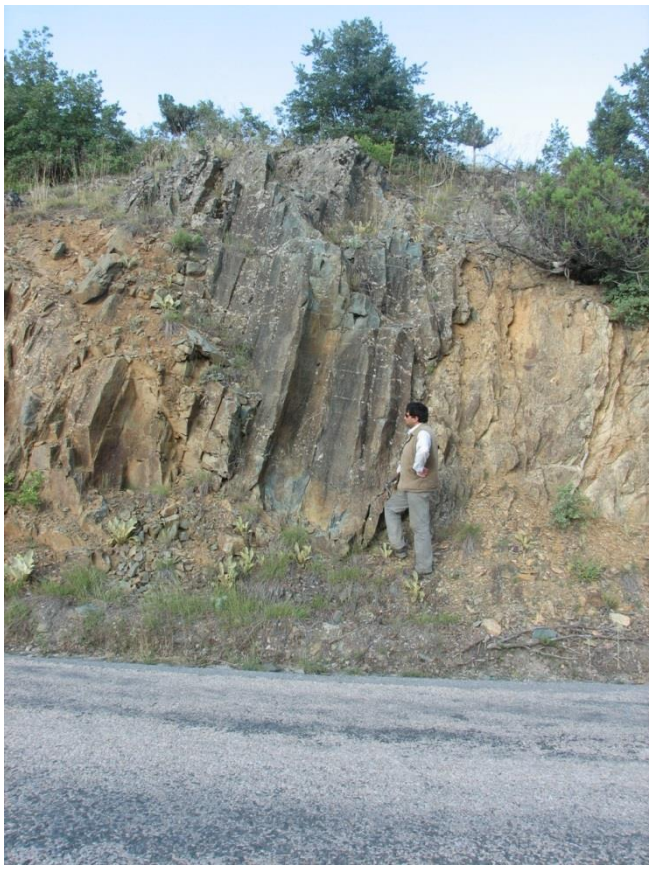

Figure 2-9: Metabasalt dyke cross-cutting the light-colored metadacites.

Apart from the metadacites, metaandesite and metabasalts, which form the bulk of the Kösedağ Metavolcanics, there are also volcaniclastic and sedimentary lithologies interbedded with the metavolcanic rocks. The volcaniclastic lithologies

are characterized by the occurrence of mineral and volcanic rock fragments generally set in a volcanic matrix (Fig. 2-10).

The nature of the fragments are especially is well observed in the lava breccias that include angular clasts (Fig. 2-11). The clasts are represented by dark green metabasalt fragments with vesicular texture. Nearby the shear zones, the clasts within these fragmental lithologies appear to be elongated, while the relatively less effected parts reflects the original, angular appearance.

Figure 2-10: Field view of volcaniclastic rock including volcanic clasts.

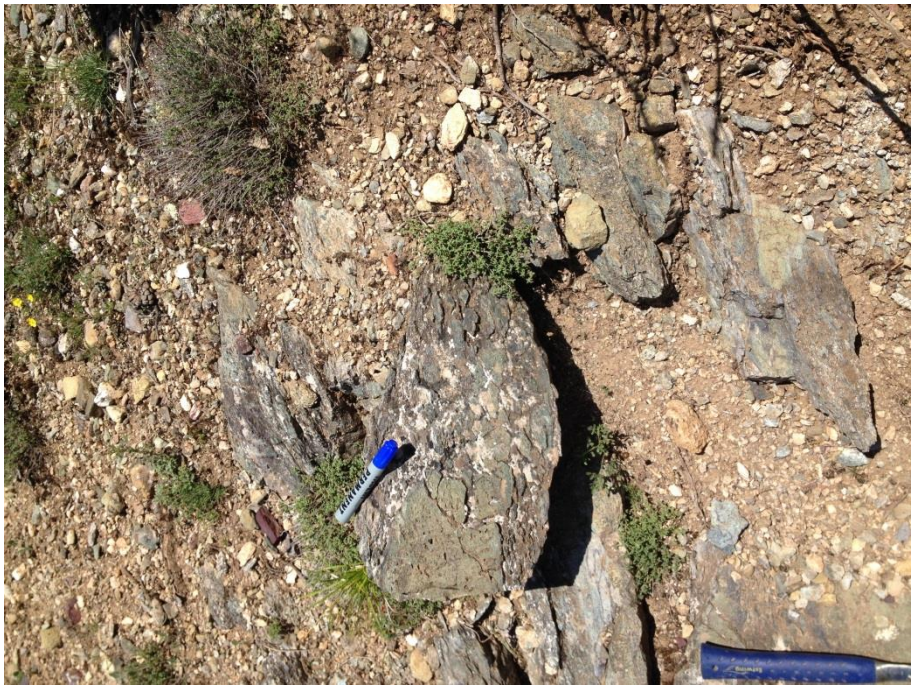

Figure 2-11: Lava breccia including metabasalt fragments with gas vesicles embedded in a carbonate matrix.

The sedimantary lithologies that are interbedded with the Kösedağ metavolcanic rocks are represented by purple-colored chert and mudstone (Fig. 2-12). In some parts, these lithologies are observed as bands, which are generally medium-bedded, are exposed on the main road reaching the Yukarıdikmen village. In some places, pinkish-colored mudstones are observed to include chert nodules (Fig. 2-13). Although the intense tectonic activity in the region has largely destroyed the primary structures within these lithologies, in the relatively preserved parts, cherts are found to consist of radiolarian ghosts (Fig. 2-14).

Figure 2-12: Kösedağ Metavolcanics alternating with reddish mudstone and chert.

Figure 2-13: Red chert nodules within the pinkish, thin-bedded mudstone on the road to the Yukarıdikmen village.

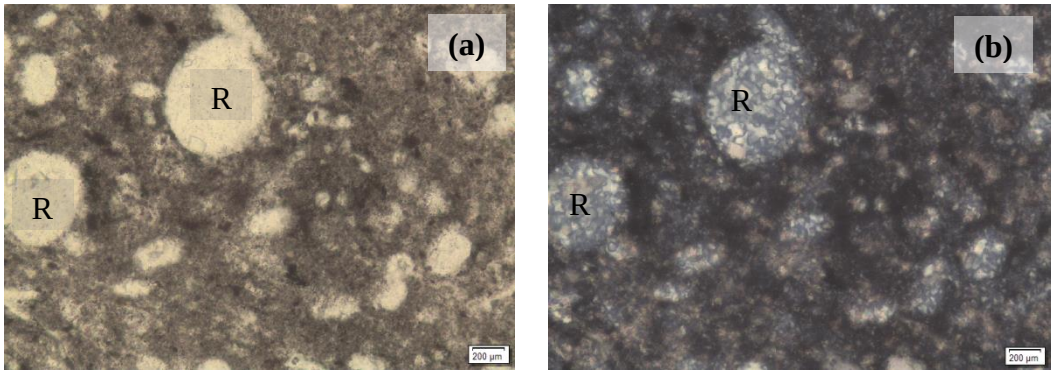

Figure 2-14: Microphotograph of radiolarian (R) skeletons with calcite in chert lithologies a) in PPL view, b) in XPL view.

In the study area, the northern contact of the Kösedağ Unit is characterized by splays of NAF Zone that forms the southern boundary of the Tosya Basin. Thus, in the mapped area, the contact of the Kösedağ Metavolcanics with the CPSC is not observed. However, further north, the Kösedağ Unit was reported to be structurally overlain by the CPSC (Okay et al., 2006; Aygül et al., 2015). The oldest cover unit in primary depositional contact with the Kösedağ Metamorphic Unit is the Middle Eocene clastic rocks to the east and SE of the study area (Fig. 2-1).

No stratigraphic contact between the Kösedağ metavolcanic rocks and Dikmen Formation was observed. Therefore, it is not possible to suggest a relative age for the Kösedağ Metavolcanics on the basis of the limestones. Sevin and Uğuz (2011) also indicate that the Hacıhasan Formation, which is partly equivalent of Kösedağ metavolcanic rocks, displays tectonic contact relationship with upper and lower units. Hakyemez et al. (1986) named this unit as Karabürçek Formation and suggest Malm-Neocomian age based on presence of transition between Karabürçek Formation and overlying Yaylacık Formation consisting of limestone, calc-schist, sandstone, metasandstone, metaconglomerate, metavolcanic. Yılmaz and Tüysüz, (1984) named the unit as Kösdağ metamorphite and proposed Liasssic or pre Liassic age for the unit. Tüysüz (1990) proposed Late Mesozoic Neotethyan age for Kösdağ arc. Aygül et al. (2015) also indicate Late Cretaceous (93.8±1.9 and 94.4±1.9 Ma) U-Pb ages for magmatism and 69.9±0.4 Ma metamorphism age implying Danian-Maastrichtian by $^{40}Ar/^{39}Ar$.

2.2.2. The Dikmen Formation

The Dikmen Formation was named by Tüysüz (1990) and it is characterized by yellowish, light grey to pinkish colored carbonates, which are exposed in an area of about 35 km^2 in the southern part of the study area, including the Yukarıdikmen and a major part of the Dedem villages. The unit, in general, appears to be a micritic limestone. In some parts, however, these micritic parts alternate with clayey to sandy carbonates and light pinkish mudstone. Cherts are also encountered within the formation, and it is generally observed as lenses within the

metacarbonates. Furthermore, in some places, especially the clayey-silty parts show well developed foliation in response to the shearing (Fig. 2-15). The Dikmen Formation have been affected by metamorphism, which is evidenced by the intense recrystallization and destruction of the primary micritic textures as well as the fossils inside.

Figure 2-15: Outcrop of yellowish colored, thin bedded, strongly foliated and recrystallized limestone of Dikmen Formation to the north of Yukarıdikmen village.

Aygül et al. (2015) proposed that Dikmen Formation stratigraphically overlie Kösedağ metavolcanic rocks. During the present study, however, no primary, stratigraphic relation could be observed between the Kösedağ Metavolcanics and Dikmen Formation. In contrast, the contact relationship between the Dikmen Formation and Kösedağ metavolcanic rocks appear to be tectonic and it is well observed on the ridge in the vicinity of Kızılca and west of the Yukarıdikmen village. Metacarbonates in this locality dip to the north with angles between 40 to

60°. Furthermore, they are observed to be folded, which is evidenced by the repetition of the lithologies (Fig. 2-16).

Figure 2-16: Recrystallized limestone including cherty and muddy parts. Yellowish parts represent carbonate, reddish ones characterize mudstone.

The boundary between the Dikmen Formation and the ophiolitic melange is also tectonic and can be observed at the Kızılca ridge to east and north of the Çukur village. It is also important to note that in some parts of the study area, the Dikmen Formation may be observed to lie structurally above the Upper Cretaceous mélange of the IAESB. This tectonic relationship is also supported by our study on the road between Yukarıdikmen and Sarakman as well as on the N-S trending dirt-roads on the ridges of Kızıltepe (Fig. 2-17, Fig. 2-18).

No fossils could be obtained from the Dikmen Formation in the present study due to their recrystallized nature. Hakyemez et al. (1986)'s suggestion of the Upper Jurassic-Lower Cretaceous age was actually acquired from the carbonate unit lying to the west of the study area, known as Akbayır Formation (Akyürek et al., 1982).

In contrast, Uğuz et al. (2002) suggested an Early Cretaceous age for the Yaylacık Formation. Tüysüz (1990, 1993) also proposed a similar age, ascribing the Dikmen Formation to Cenomanian age based on fossil findings.

Apart from the formation ages of the studied units, the age of their primary juxtaposition is not clearly understood. The contact between the Kösedağ Metavolcanics and Dikmen Formation as well as the Dikmen Formation and the ophiolitic mélange unit appears to have been affected by multiple events.

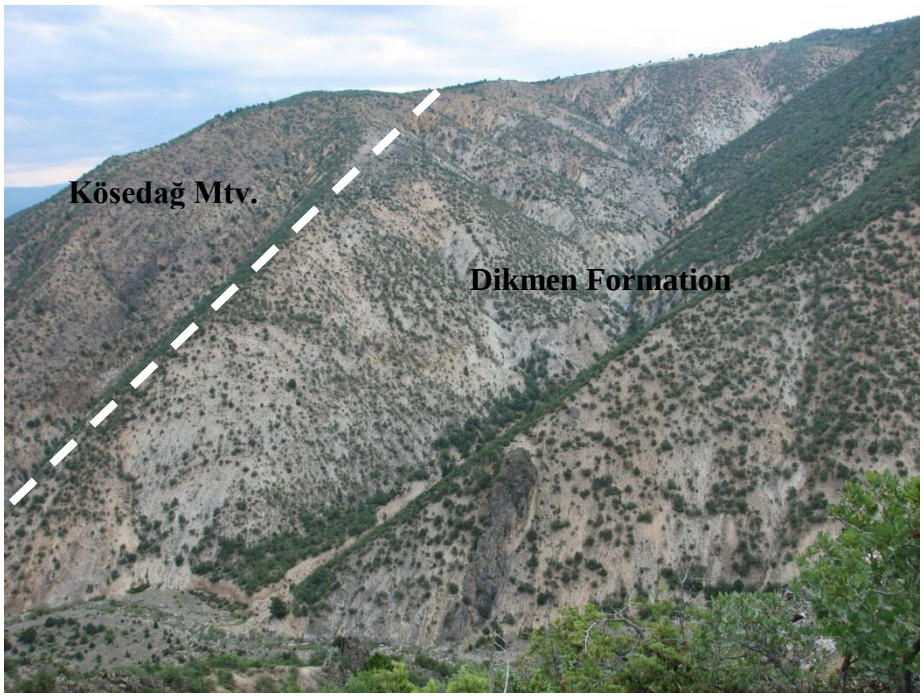

Figure 2-17: Tectonic contact relationship between Kösedağ Metavolcanics and Dikmen Formation cover in the north of Kızılca.

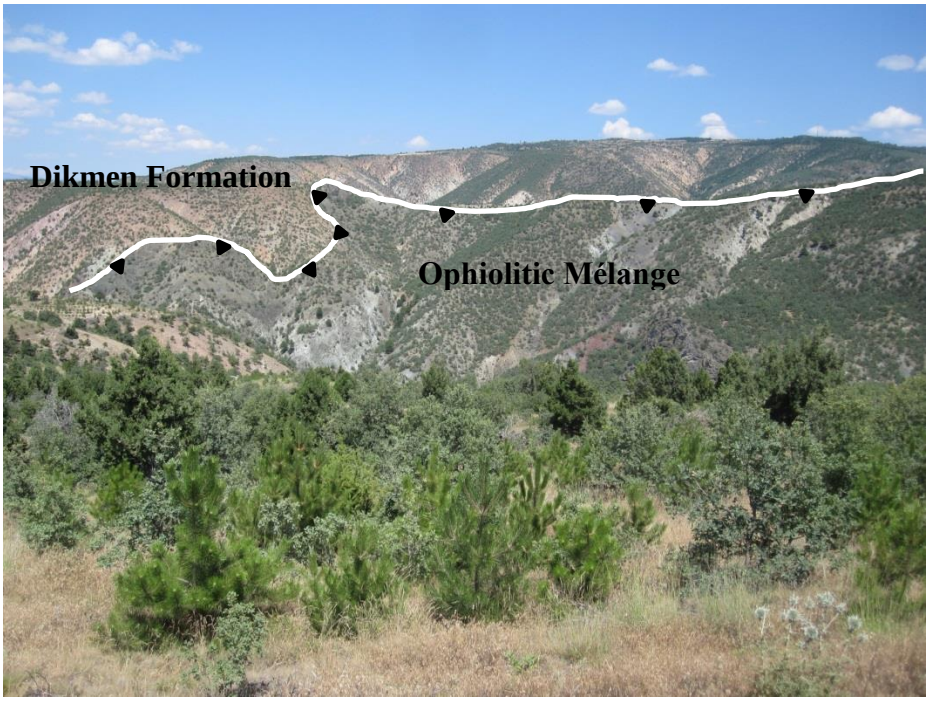

Figure 2-18: Tectonic contact relationship between the Dikmen Formation and ophiolitic mélange as viewed from the Kızılca ridge. Note that the Dikmen Formation is structurally underlain by the ophiolitic mélange.

CHAPTER 3

PETROGRAPHY

In order to reveal the petrographic features of the metavolcanic rocks from the Kösedağ Metavolcanics more than 80 thin sections were prepared and examined under the polarizing microscope. The rock types presented in this section only include metavolcanic rocks, which make up the bulk of the unit, and the other lithologies (i.e. volcaniclastics, carbonates, mudstones and cherts) were not included. The examined Kösedağ Metavolcanics are represented by metadacites, metaandesites and metabasalts, which reflect variable metamorphism and/or deformation histories. Thus, in this chapter, mineralogical assemblage and textural properties of these metavolcanics along with their alteration/metamorphism and deformation features were studied in detail.

3.1. Metabasalts

In hand specimen, the Kösedağ metabasalts are characterized by dark green color, which reflects the presence of secondary mineral phases, such as chlorite, epidote and actinolite. Both massive and foliated types were encountered. Porphyritic texture, which is represented by large phenocrysts set in a fine-grained groundmass, is a common feature of volcanic rocks. It is suggested that phenocrysts are generated by slow cooling in deeper parts and the groundmass is produced by rapid cooling, accordingly has fine-grained nature (Vernon, 2004). These basaltic lithologies are aphanitic. It must be also noted that the exact determination of primary mineral assemblage is difficult due to the fine-grained nature of the basalts, and the presence of low-grade metamorphism and/or deformation.

Under the microscope, the primary mineral constituents of the metabasalts are plagioclase and clinopyroxene. Plagioclase is present as both phenocryst and microlith in the groundmass. It is distinguished by first-order interference colors combined with polysynthetic twinning under cross-polarized light (XPL). It generally forms subhedral to euhedral crystals. In some cases, plagioclase is seen as randomly oriented laths with varying sizes, indicating seriate texture (Fig. 3-1). Moreover, in some samples, it is seen that plagioclase is heavily altered to secondary minerals, including sericite and epidote.

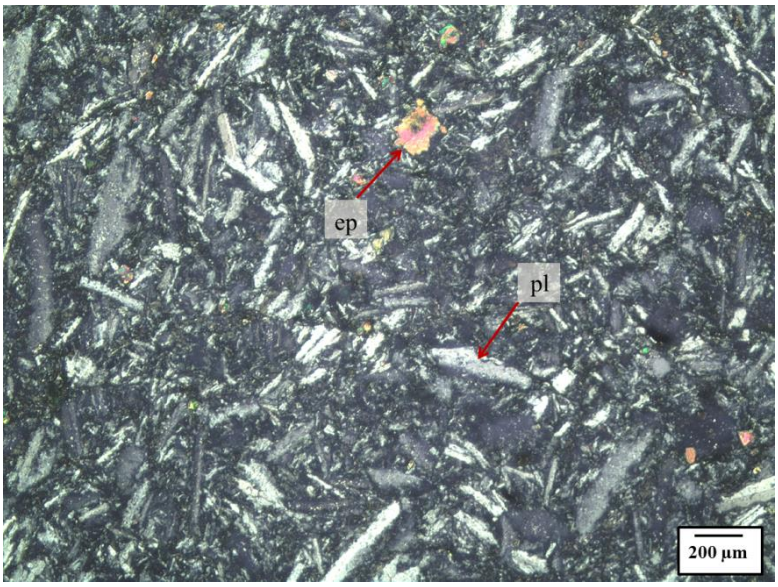

Figure 3-1: Clusters of randomly oriented plagioclase in a fine grained matrix of non-foliated metabasalt. Also seen is seriate texture defined by variable-sized plagioclase laths (Sample 6-7c; 4X, XPL, ep: epidote, pl: plagioclase).

Other prominent constituent of the metabasalts is clinopyroxene. This mineral appears colorless under plane-polarized light (PPL) and displays moderate to high relief. Under crossed polars, it exhibits moderate birefringence with second-order interference colors. Moderately-developed cleavages are common. Extinction angle of clinopyroxene ranges from 35 to 45°. In clinopyroxene, twinning is observed (Fig. 3-2). Fractures are also present. It is a typical phenocryst phase in the

metabasalts. It is also seen to create clusters, defining glomeroporphyrtic texture (Fig. 3-2).

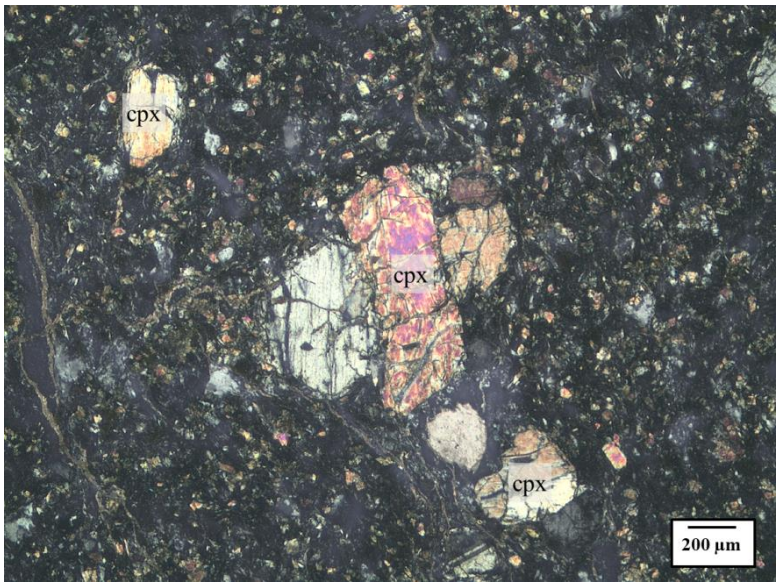

Figure 3-2: Photomicrograph of fractured clinopyroxene phenocrysts forming glomeroporphyrtic texture. The fine grained matrix is composed of epidote and clinopyroxene. (Sample 136; 4X, XPL, cpx: clinopyroxene).

Opaque minerals are also noticed in the metabasalts. The ones with cubic outlines may indicate the presence of magnetite or pyrite. Otherwise, the exact determination of opaque minerals is difficult to determine under polarizing microscope.

Plagioclase and clinopyroxene are the primary minerals of the metabasalts, whereas epidote, actinolite, chlorite, sericite and calcite are present as the secondary minerals (Fig. 3-3). Of these secondary mineral phases, chlorite and epidote are present in all Kösedağ metabasalts, whereas actinolite appears to join this assemblage only in some samples. This may suggest that the Kösedağ metabasalts have been metamorphosed mostly under sub-greenschist-facies conditions. Representative minerals of typical greenschist-facies conditions are rarely found.

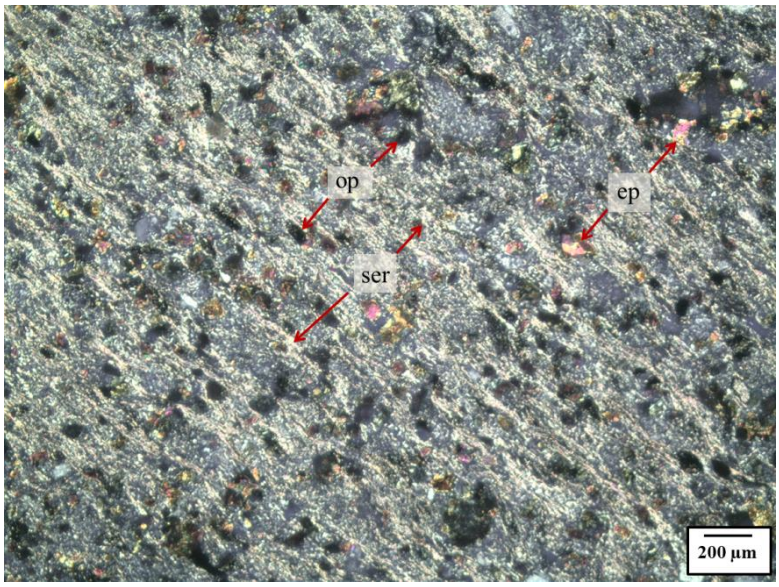

Figure 3-3: Metabasalt showing flakes of sericite and chlorite aligned parallel to the foliation, together with abundant opaque grains. Chlorite displays anomalous interference colors, whereas epidote shows its characteristic patchy birefringence (Sample 76; 4X, XPL, ep: epidote, op: opaque, ser: sericite).

Chlorite and epidote occur as the typical secondary mineral phases replacing pyroxene and plagioclase. The pale green color of chlorite is diagnostic with slight pleochroism. It shows low-angle oblique extinction with first-order anomalous interference colors. Plagioclase is also replaced by sericite, which is another alteration product seen in some thin-sections. Epidote is easily identified by its high relief and yellowish colors under PPL. It displays patchy birefringence under crossed polars. It is seen in thin-sections as altering plagioclase and clinopyroxene. Clinopyroxene is also replaced by actinolite showing acicular (needle-like) habit. As mentioned before, the presence of these secondary minerals points out low-grade metamorphism. Gas vesicles are present and appear to be filled by epidote in most cases, and chlorite (Fig. 3-4).

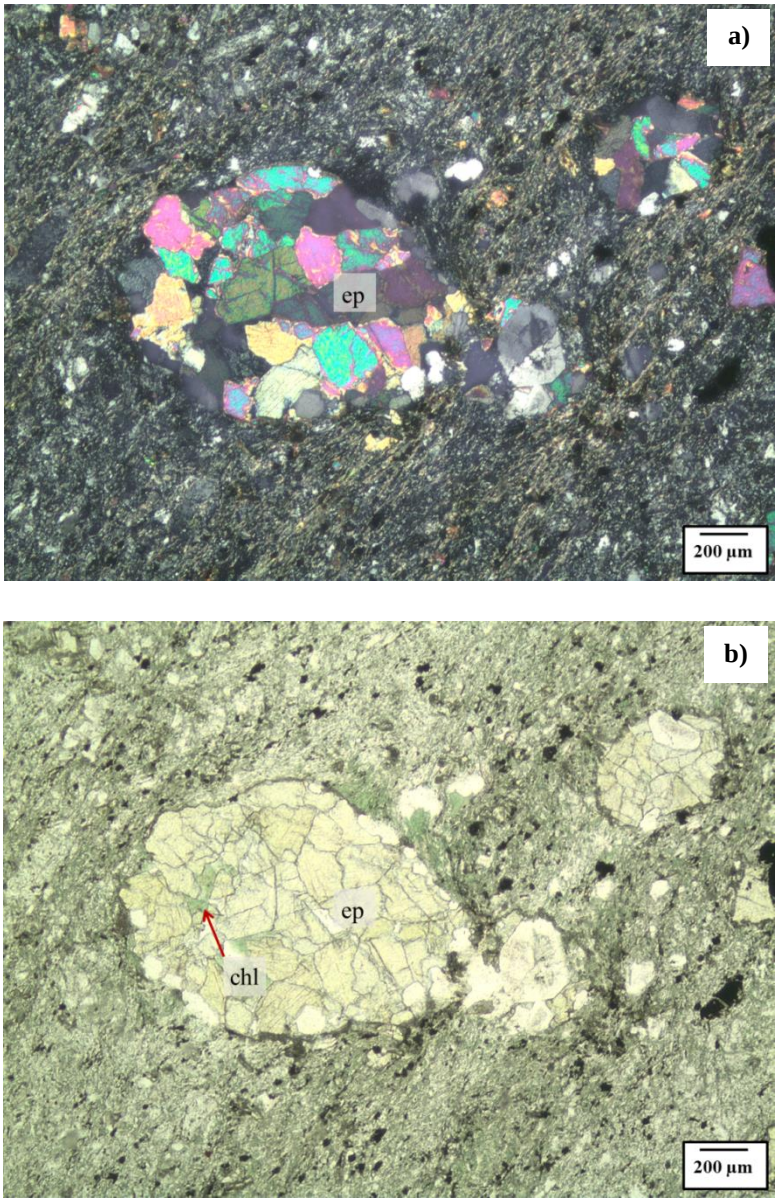

Figure 3-4: (a) Gas vesicles filled by epidote and chlorite in metabasalt (Sample 65; 4X, XPL, ep: epidote). (b) Epidote exhibits high relief with yellowish colors, whereas chlorite is distinguished by greenish colors. Note also abundant opaque minerals in the groundmass. (Sample 65; 4X, PPL, chl: chlorite, ep: epidote).

3.2. Metaandesites

Metaandesites, which constitute the most common metavolcanic rock type in the study area, are varicolored, exhibiting greenish and dark-greyish colors in hand specimen. They are aphanitic and largely include foliated and to a lesser extent

nonfoliated varieties. If the original textures of these rocks are taken into consideration, the crystallinity of these rocks appears to change between hypocrystalline and holocrystalline.

Plagioclase is a major constituent of the metaandesites and occurs as subhedral to euhedral crystals. In some places, plagioclase exhibits concentric zoning, indicating the presence of bands with distinct chemical composition. This type of zoning is essentially observed in plagioclase (e.g. Vernon, 2004), though there are many other minerals displaying this feature (e.g. Clark et al., 1986; O'Brien et al., 1988). In addition, plagioclase is encountered as porphyroclast (Fig. 3-5), which indicates the effect of ductile deformation on the metaandesites. The rocks that have experienced ductile deformation are typically characterized by large relict minerals embedded in a fine-grained matrix. This microstructure defines porphyroclastic texture. In this relationship, the relict crystals are known as porphyroclast.

Similar to metabasalts, chlorite and epidote constitute the common secondary mineral phases in Kösedağ metaandesites (Fig. 3-6). Sericite is also found and, it is observed to have variably replaced plagioclase (Fig. 3-7). Sericite forms as the product of sericitization which is an important type of hydrothermal alteration in igneous rocks (e.g. Creasey, 1966; Meyer and Hemley, 1967). Epidote, which is generally observed filling the vesicles in metabasalts, is found as replacing plagioclase and clinopyroxene in metaandesites. Chlorite, with characteristic anomalous interference colors, is found abundantly in metaandesites. The metaandesites have fine-grained groundmass composed of epidote, plagioclase, chlorite.

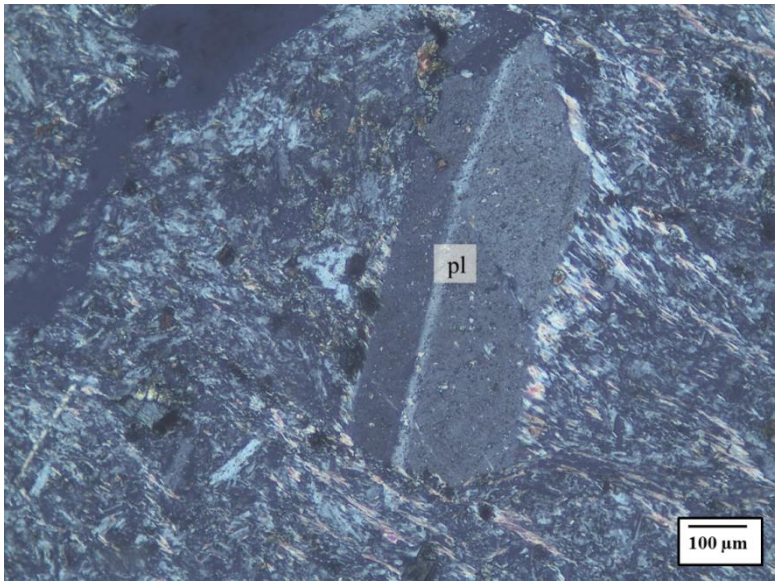

Figure 3-5: Photomicrograph illustrating porphyroclastic texture in metaandesite. Note also the polysynthetic twinning on plagioclase porphyroclast (Sample 110; 10X, XPL, pl: plagioclase).

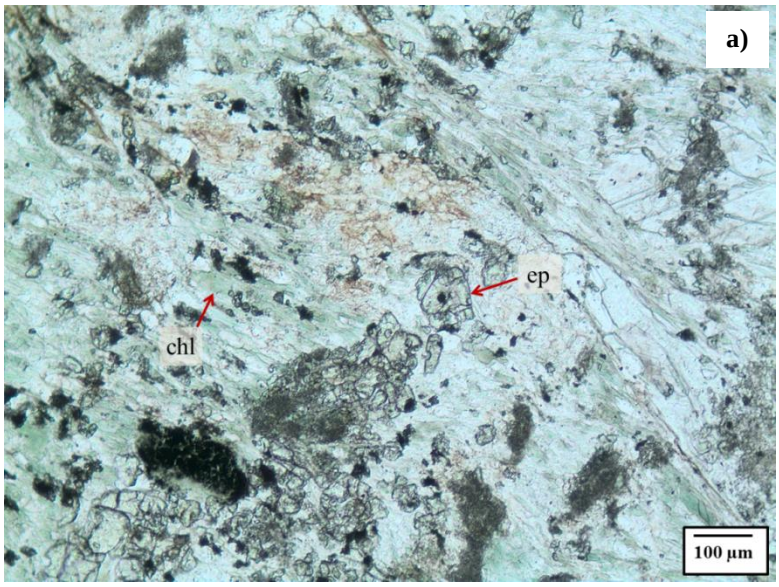

Figure 3-6: (a) Photomicrograph of pale green chlorite and yellowish epidote identified its characteristic feature high relief with opaque minerals (Sample 6-7a; 10X, PPL, cal: calcite, chl: chlorite, ep: epidote). (b) Chlorite is characterized by anomalous interference colors, calcite displaying rhombohedral cleavage and epidote identified by patchy birefringence (Sample 6-7a; 10X, XPL, cal: calcite, chl: chlorite, ep: epidote).

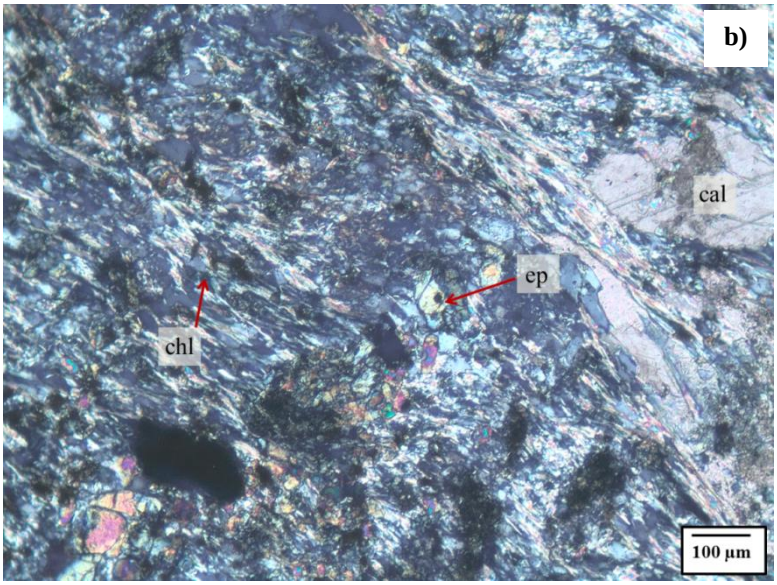

Figure 3-6: (continued).

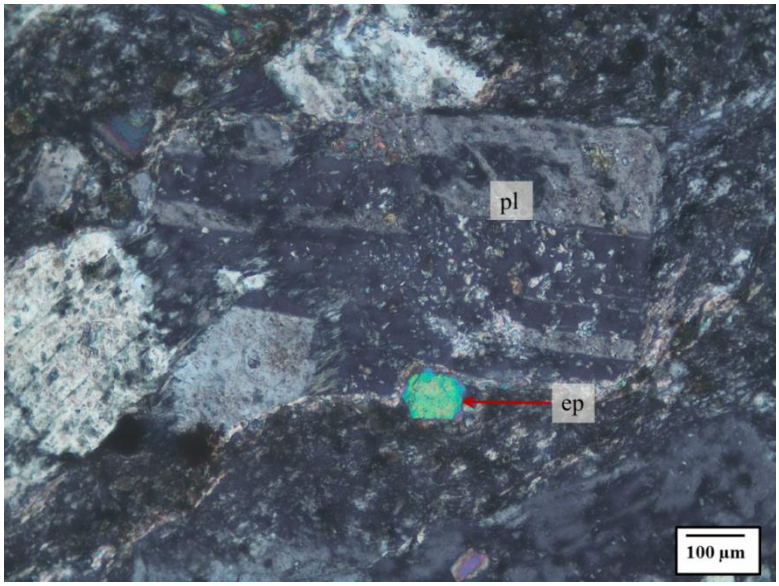

Figure 3-7: Plagioclase partially altered by sericite and epidote. Also found is larger epidote next to plagioclase (Sample 153; 10X, XPL, ep: epidote, pl: plagioclase).

3.3. Metadacites

In hand specimen, metadacites are generally white in color. Some metadacites, however, reflect somewhat similar appearance to those of metaandesites with greenish colors. In spite of this similarity, the presence of quartz grains, which are

even visible to the naked eye, helps to distinguish these lithologies from the metaandesites. Metadacites are aphanitic with visible, large grains of K-feldspar, plagioclase and quartz. They show foliation similar to most metaandesites and some metabasalts. Quartz is abundant in metadacites and can be easily recognized by naked eye, with shade of grey colors. At their original state, metadacites display porphyritic and microcrystalline texture.

The main primary constituents of metadacites are characterized by quartz, plagioclase and to a lesser extent K-feldspar. Opaque minerals are also present. Quartz is the common primary mineral phase, which generally occurs as porphyroclasts surrounded by aligned sericite minerals. In metadacites, quartz and K-feldspar minerals are enveloped by secondary mica minerals implying mylonitic texture (Fig. 3-8), which is an indication for strong ductile deformation (e.g. Passchier and Trouw, 2005). Frequently but by not always, it reflects rounded, anhedral outlines, whereas to a lesser extent occurs as subhedral crystals. Under XPL, large rounded porphyroclasts of quartz showing undulose extinction (Fig. 3-9) can be encountered in the metadacites. They are surrounded by finer-grained quartz minerals, displaying mortar texture (Fig. 3-9) (e.g. Barker, 1990). Because of its strong resistance to alteration, under PPL quartz appears quite fresh. There is no primary mafic phase found in metadacites; they are all replaced entirely by chlorite and epidote group minerals.

Plagioclase is the second common primary mineral phase in the metadacites. It is mostly found as subhedral to anhedral crystals. Like quartz, plagioclase also appears to have been affected by dynamic metamorphism, and present as porphyroclasts. Relatively less altered plagioclase grains display polysynthetic twinning. Rarely, sector twinning is also observed on plagioclase (Fig. 3-10).

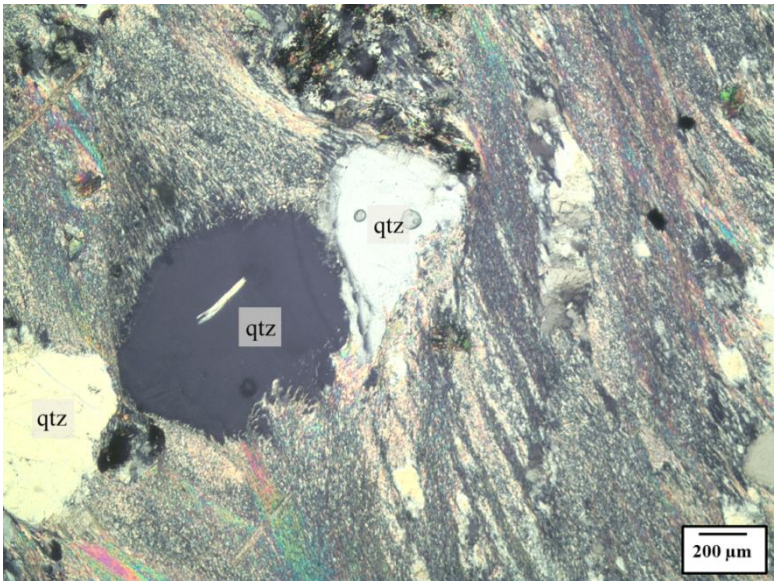

Figure 3-8: Mylonite formed by intense deformation of the metadacite, showing aligned white mica adjacent to quartz porphyroclast (Sample 32; 4X, XPL, qtz: quartz).

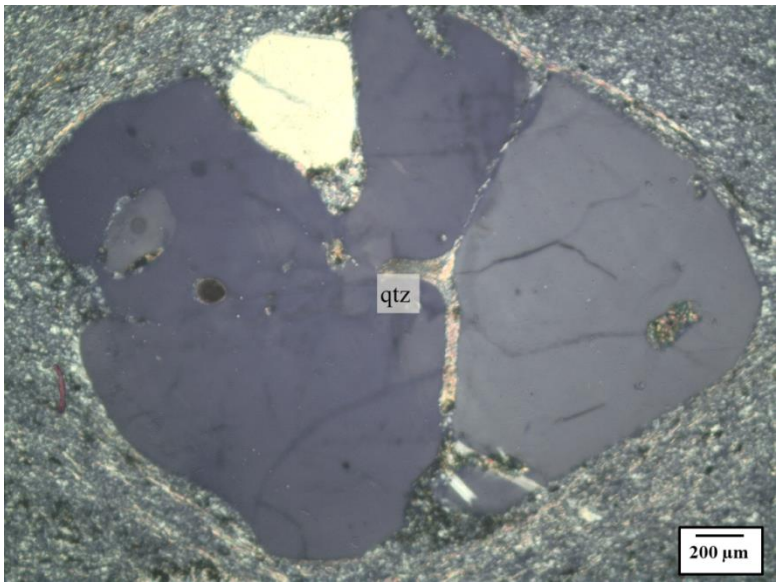

Figure 3-9: Undulose extinction observed on quartz porphyroclast displaying effects of deformation (Sample 197; 4X, XPL, qtz: quartz).

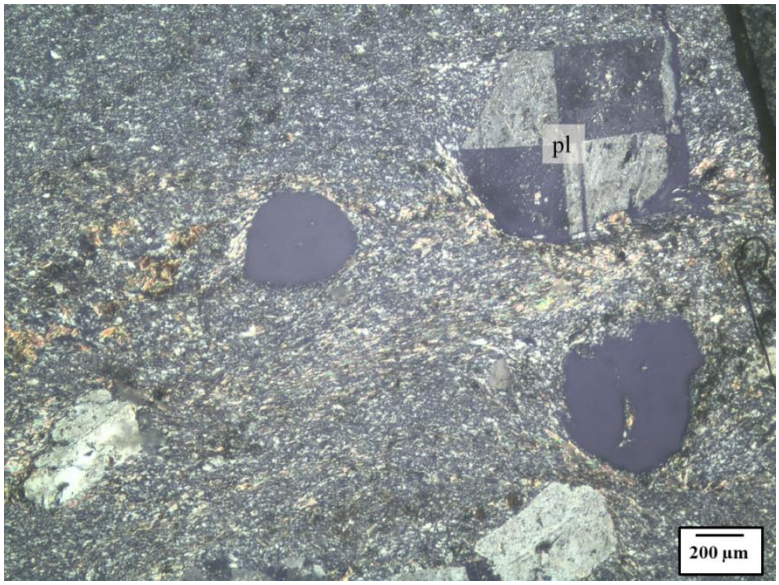

Figure 3-10: Sector twinning in a plagioclase crystal surrounded by secondary sericite minerals in metadacite (Sample 214; 4X PPL, pl: plagioclase).

Secondary mineral assemblage in metadacites comprises chlorite, epidote, sericite and calcite, which is actually similar to that of metaandesites. Chlorite is an abundant secondary mineral phase in metadacites, which is identified by pale green colors under PPL, while it exhibits anomalous interference colors under XPL (Fig. 3-11b). The anomalous purple interference color may indicate Fe-rich nature of chlorite. Epidotization is also common, which appear to have affected plagioclase and clinopyroxene. Based on the secondary mineral assemblage in metadacites, it can be suggested that they have been affected by low-grade metamorphism.

Calcite occurs as a secondary mineral, replacing mafic phases and plagioclase via-late stage hydrothermal solutions by the presence of CO_2. While it is colorless under PPL, calcite is identified by very high-order interference colors under XPL. Twinkling, which is a characteristic feature of calcite, may also be observed in

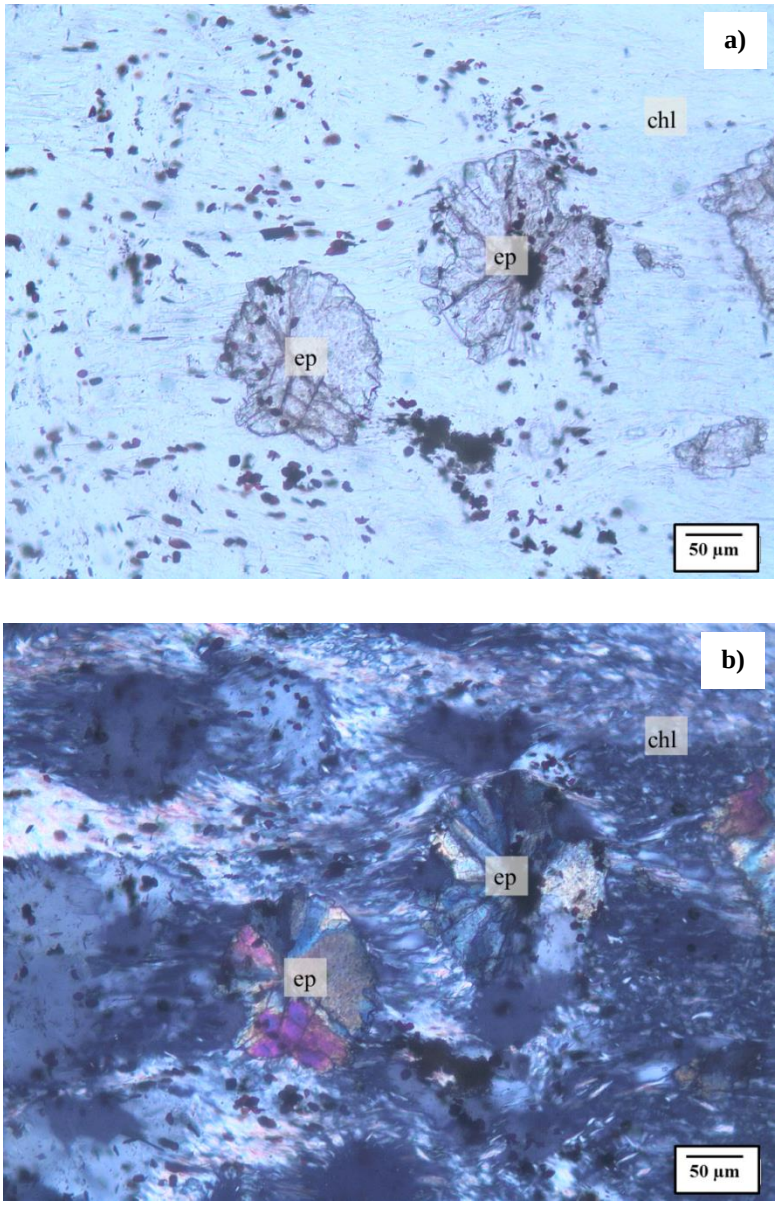

Figure 3-11: (a) Photomicrograph of rosette epidote exhibiting high relief with well aligned sericite minerals and pale green chlorite lying parallel to the foliation (Sample 32; 20X, PPL, chl: chlorite, ep: epidote). (b) Rosette epidote displaying patchy birefringence accompanied by chlorite showing anomalous interference colors (Sample 32; 20X, XPL, chl: chlorite, ep: epidote).

metadacites. Another important point is rhombohedral twinning (Fig. 3-12) which is the cleavage type intrinsic property of calcite. Furthermore, zircon appears as a common accessory mineral of metadacites.

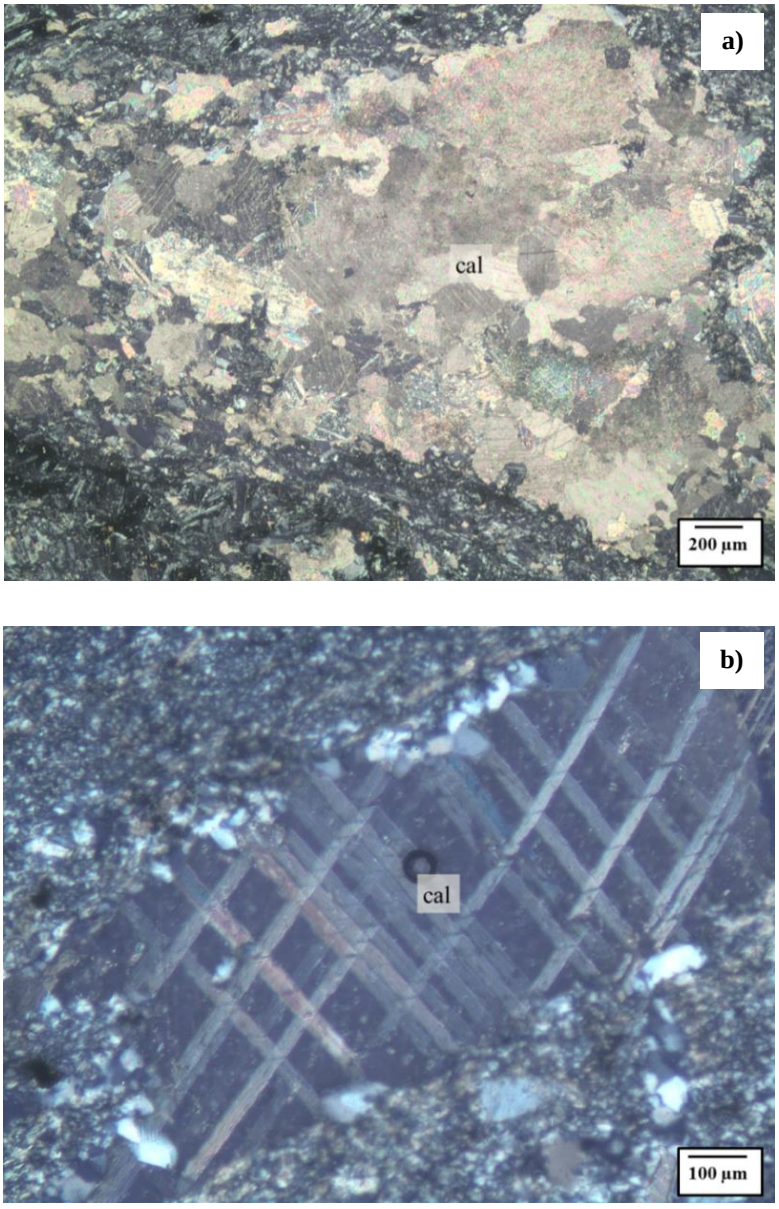

Figure 3-12: a) Intense carbonate replacement in metadacite (Sample 211; 4X, XPL, cal: calcite). (b) Photomicrograph of calcite (extremely high-order interference colors) exhibiting perfect rhombohedral cleavage, which is surrounded by recrystallized quartz grains. (Sample 24; 10X, XPL, cal: calcite).

The matrix is composed of quartz, albite, sericite and chlorite. Muscovite flakes are oriented, defining foliation (Fig. 3-13).

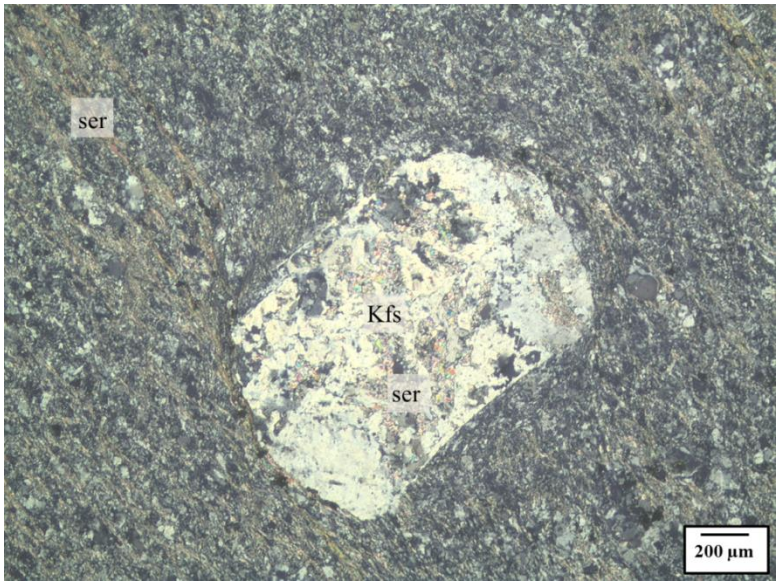

Figure 3-13: Metadacite including porphyroclast of K-Feldspar with first-order interference colors, Note the intense sericitization on K-feldspar, which is characterized by small patches with high-order interference colors. The porphyroclast are set in a fine-grained matrix including aligned sericite and opaque minerals (Sample 212; 4X, XPL, Kfs: K-Feldspar, ser: sericite).

In the Kösedağ metadacites, pressure shadows are present and appear to have formed around K-Feldspar porphyroclasts (Fig. 3-14). Pressure shadows are common in metamorphic rocks (Williams, 1972), which forms around rigid minerals (Bard, 1986). During magmatic evolution, minerals that are stable may be unstable with decreasing temperature, which may cause them to interact with the melt. This process is known as magmatic corrosion and can be observed in the Kösedağ metadacites, which is evidenced by the presence of corroded quartz grains (Fig. 3-15).

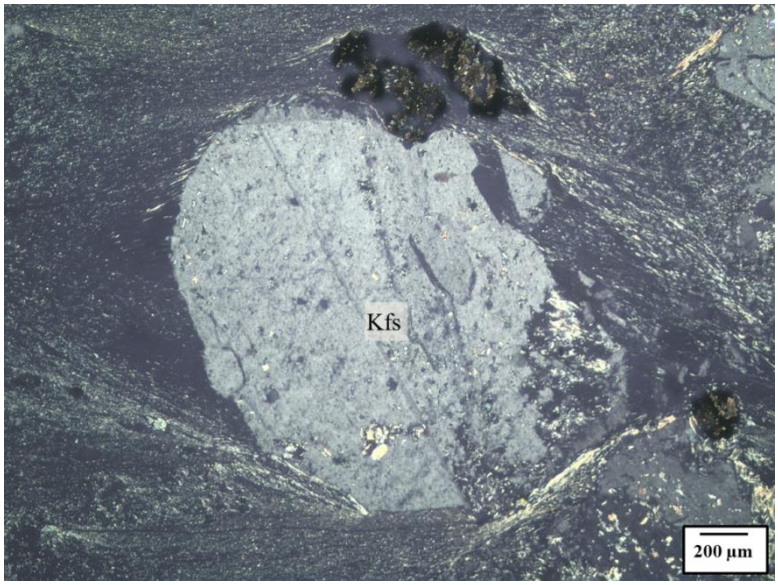

Figure 3-14: Pressure shadows around K-Feldspar porphyroclast in metadacite (Sample 49; 4X, XPL, Kfs: K-Feldspar).

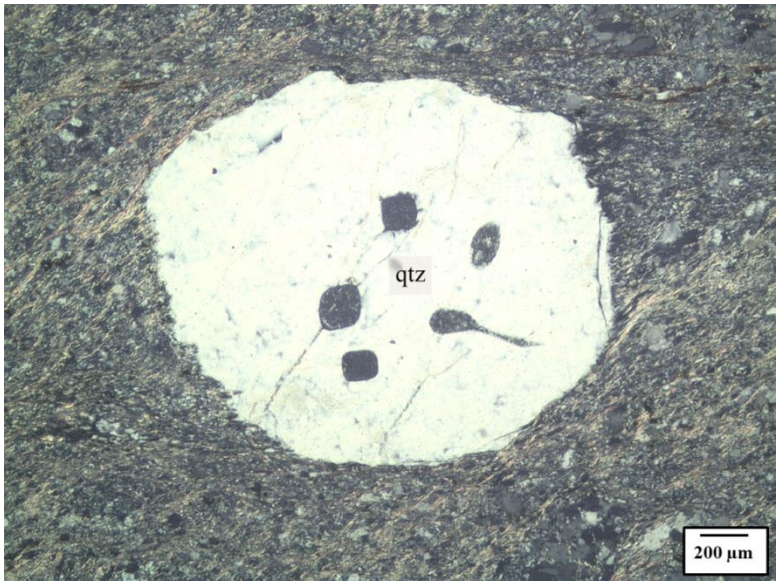

Figure 3-15: Rounded, embayed quartz porphyroclast in metadacite. While rounding probably results from the dynamic metamorphism, the internal corrosion is related to the dissolution during interaction with magma (Sample 185; 4X, XPL, qtz: quartz).

CHAPTER 4

GEOCHEMISTRY

4.1. Methods

In this part, 15 variably metamorphosed rock samples collected from the Kösedağ Unit were investigated to reveal their geochemical characteristics by using a number of schemes, including Harker diagrams, multi-element diagrams, and tectonomagmatic discrimination diagrams. The selected lithologies for geochemical interpretation include metabasalts, metaandesites and metadacites, which represent a wide spectrum of both primitive and evolved products. The whole-rock geochemical analyses of the metavolcanics were performed in the ACME Analytical Laboratories (Vancouver, Canada). Major elements analyses of these metavolcanic rocks were performed by inductively-coupled plasma optical emission spectrometry (ICP-OES), while trace elements (including REE) were measured by inductively-coupled plasma mass spectrometry (ICP-MS). All major element data were presented on volatile-free basis for the rest of discussion and interpretation of diagrams. The analysis results are given in the appendix (Table A-1).

4.2. Chemical Effects of Alteration

The studied rocks display variable loss on ignition (LOI) values ranging from 1.4 to 5.5 wt.%, indicating that the studied rocks may have been subjected to secondary processes, such as hydrothermal alteration and metamorphism. This result is also confirmed by petrographic observations such that the investigated metavolcanics

include secondary mineral assemblages like chlorite, epidote and calcite, which indicate the presence of alteration. Large ion lithophile elements (LILE) (e.g. Sr, K, Rb, Ba) are not reliable to interpret petrogenetic history of the investigated rocks because of their mobile nature (e.g. Wood et al., 1976; Thompson, 1991). High field strength elements (HFSE) and REE are thought behave immobile during low-grade metamorphism or hydrothermal alteration (Pearce and Cann, 1973; Floyd and Winchester, 1978). Thus, owing to the presence of post-magmatic effects on the Kösedağ Metavolcanics, relatively immobile elements, such as HFSE and REE will be mainly used to interpret their petrogenetic characteristics.

4.3. Classification of the Kösedağ Metavolcanics

In order to classify the studied samples, instead of the TAS diagram, the plot of Winchester and Floyd, (1977) that is based on immobile elements were used to avoid effects of secondary processes. This classification scheme indicates that the Kösedağ metaextrusives are all sub-alkaline and represented by four distinct chemical compositions; basalt, basaltic andesite, andesite and rhyodacite/dacite (Fig. 4-1). This chemical classification scheme, in general, seems to be consistent with the petrographical classification. It must be noted that hereafter chemical classification will be taken into consideration.

The studied rocks show a wide spectrum of chemical composition ranging from mafic to felsic, including basalts, andesites, dacites with MgO contents between 0.17-10.3 wt.%. Based on immobile trace element element systematics the studied rocks are subdivided into two main groups as Type 1 and Type 2 (Fig. 4-2). Both groups exhibit sub-alkaline affinity (Nb/Y=0.07-0.19 for Type 1; Nb/Y=0.05-0.13 for Type 2) and display enrichment in Th with respect to Nb (Th/Nb=0.61-1.44 for Type 1; Th/Nb=0.29-1.93 for Type 2; Average N-MORB Th/Nb=0.05; Sun and McDonough, 1989). Type 2 have wider spectrum of Th/Nb ratio compared to Type 1. In addition, light rare-earth elements (LREE) are enriched relative to HFSE (e.g. Nb, Zr, Hf and Ti) and heavy REE (HREE) (Fig. 4-2, Fig. 4-3) (La/Nb=2.19-4.7 for Type 1; La/Nb=2.92-5.93 for Type 2; Average N-MORB La/Nb=1.07; Sun and McDonough, 1989). The presence of negative Eu anomaly is observed on both

groups. REE patterns of the two groups are also similar. Despite these similarities, however, there appear to be some differences between the two groups. While Type 2 displays some degree of depletion in Zr and Hf, Type 1 is characterized by depletion in P. Furthermore, Type 1 displays greater enrichment in Th relative to Nb.

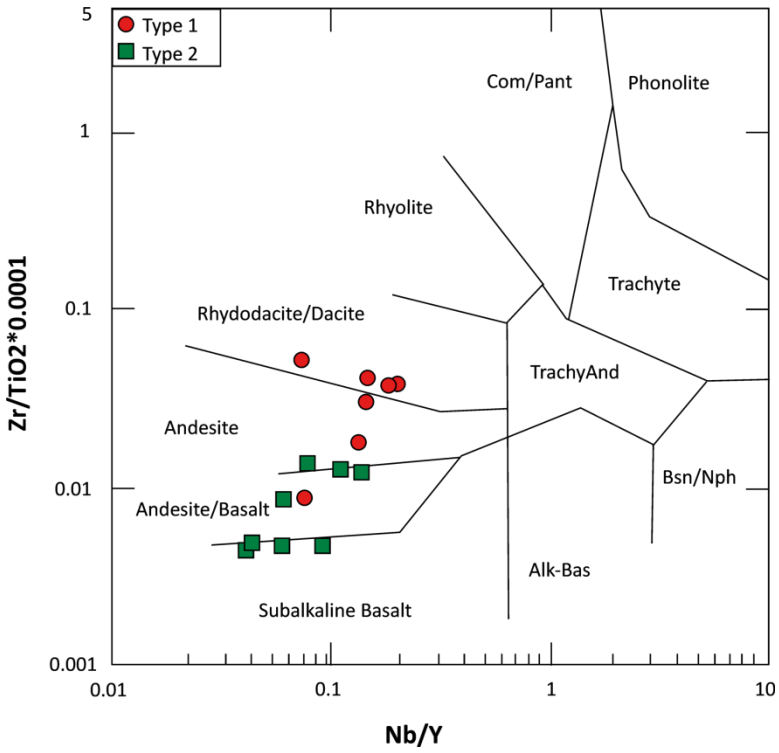

Figure 4-1: Chemical classification of the Kösedağ Metavolcanics on the basis of immobile elements (after Winchester and Floyd, 1977).

4.4. Elemental Variations

As mentioned above, the studied rocks are divided into two groups as Type 1 and Type 2. The SiO_2 content of Type 1 (56.1 to 78.3 wt.%) and that of Type 2 (48.1 to 71.4 SiO_2 wt.%) are similar. Total alkali values ($Na_2O + K_2O$) range from 3.18 to 6.66 wt. %. Type 1 samples have MgO contents ranging from 0.57 to 5.21 wt.%. On the other hand, Type 2 samples display wider spectrum of MgO contents

relative to Type 1 samples, nearly covering their range (1.95-10.3 wt.%; average MgO for Type 2 = 4.72 wt.%). While Type 1 samples have TiO_2 contents between 0.28 and 0.73 wt. %, the TiO_2 contents of Type 2 change between 0.45 - 1.25 wt.%, exhibiting a somewhat wider spectrum. P_2O_5 contents of Type 1 samples range from 0.05 to 0.17, Type 2 samples have P_2O_5 contents changing between 0.11% - 0.29 wt.%, reflecting a wider range.

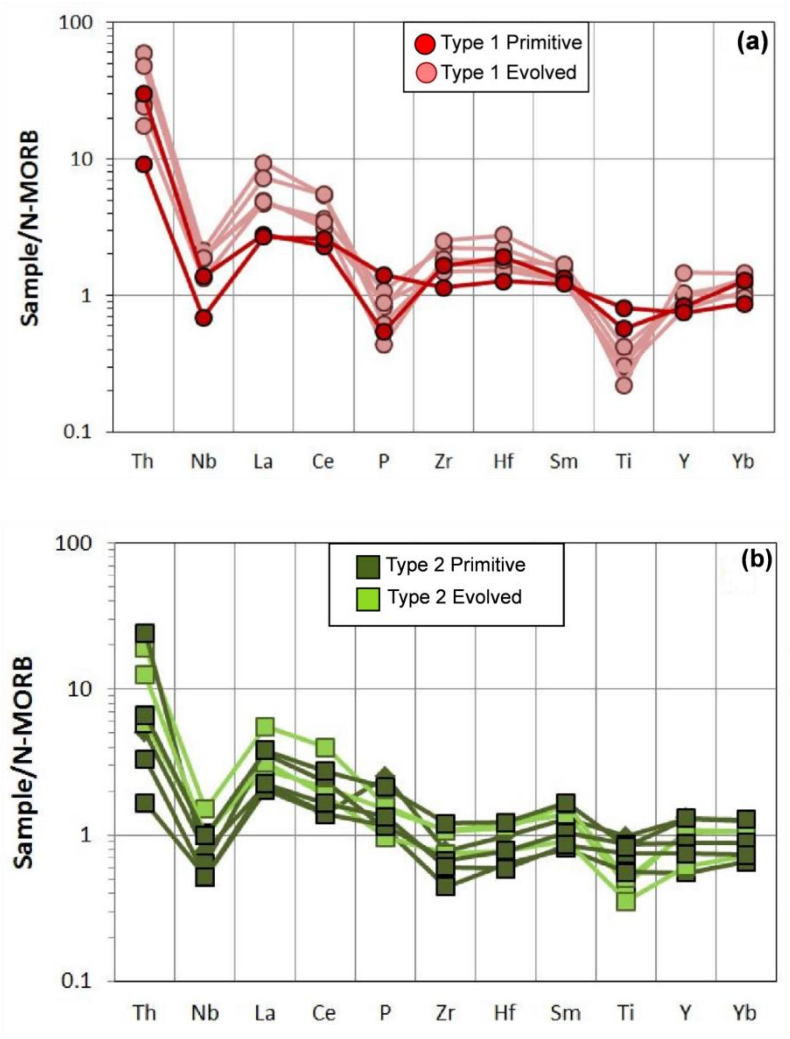

Figure 4-2: N-MORB normalized multi-element variation patterns of Type 1 and Type 2 samples (normalization values from Sun and McDonough, 1989).

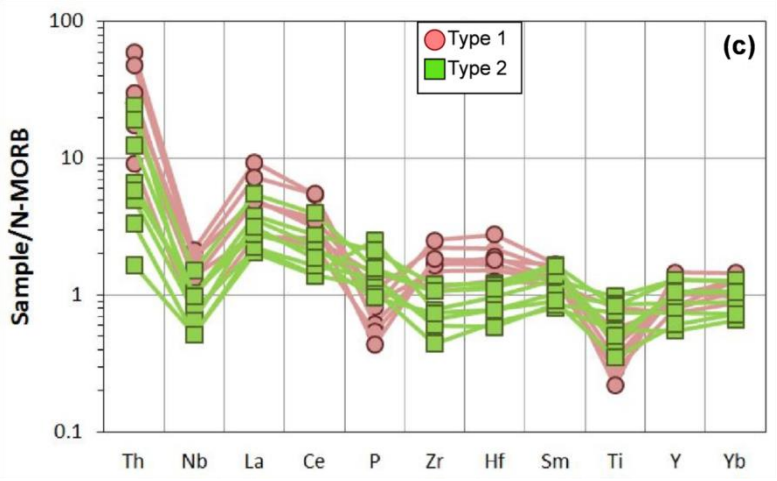

Figure 4-2: (continued).

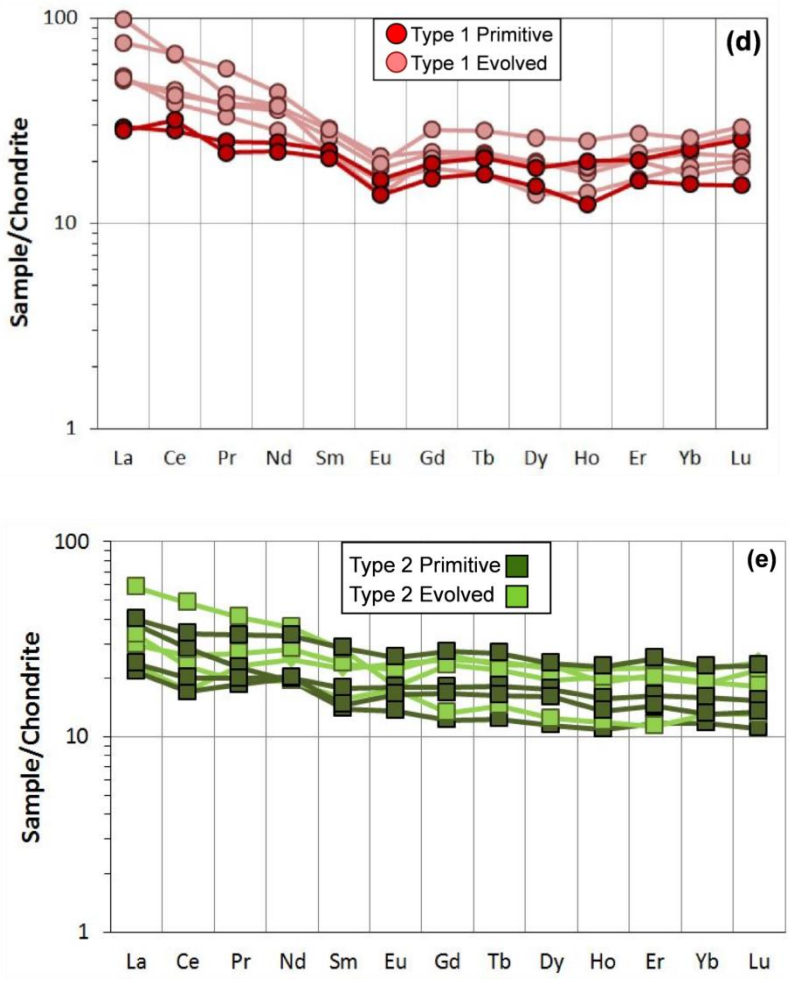

Figure 4-3: Chondrite normalized REE patterns of Type 1 and Type 2 samples (normalization values from Sun and McDonough, 1989).

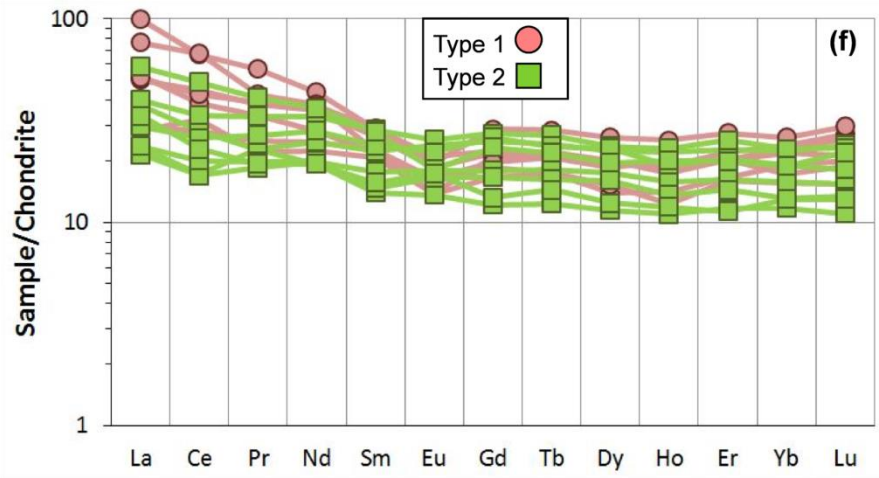

Figure 4-3: (continued).

The Harker diagrams, which include variations of SiO_2 (or MgO) against other major oxides and trace elements, can be used to indicate the evolution of the magma (Fig. 4-4). Since SiO_2 displays a wide range, it is used here as a differentation index in the Harker diagrams. As seen in Fig. 4-4, both negative and positive trends can be observed in the binary diagrams of SiO_2 versus major oxides, such as TiO_2 (Fig. 4-4a), Fe_2O_3 (Fig. 4-4b), Al_2O_3 (Fig. 4-4c), MgO (Fig. 4-4d) and MnO (Fig. 4-4e) which can be interpreted in terms of fractional crystallization of specific mineral phases during magmatic evolution.

Co prefers to enter Fe^{2+} lattice sites because of their similarity in terms of electronegativity and ionic radii (McDougall and Lovering, 2007). The negative trend between Co and SiO_2 (Fig. 4-5d) therefore, can be related to fractionation of ferromagnesian and iron oxide minerals. This idea is supported by the decrease in Ni and Cr against SiO_2, which may suggest fractionation of olivine and pyroxene during the early stages of magma evolution.

Negative trends are also seen in the plots of MgO and Fe_2O_3 versus SiO_2. While the SiO_2 concentration increases, the Fe_2O_3 and MgO contents decrease, which may indicate the fractionation of ferromagnesian minerals. In both groups, as SiO_2 increases, Al_2O_3 (Fig. 4-4c) content decreases. This negative trend may be related to plagioclase fractionation. Decrease in V (Fig. 4-5b), Y (Fig. 4-5a) and Zr (Fig. 4-

5e) with decreasing SiO_2, on the other hand, can be explained by fractionation of Fe-Ti oxides.

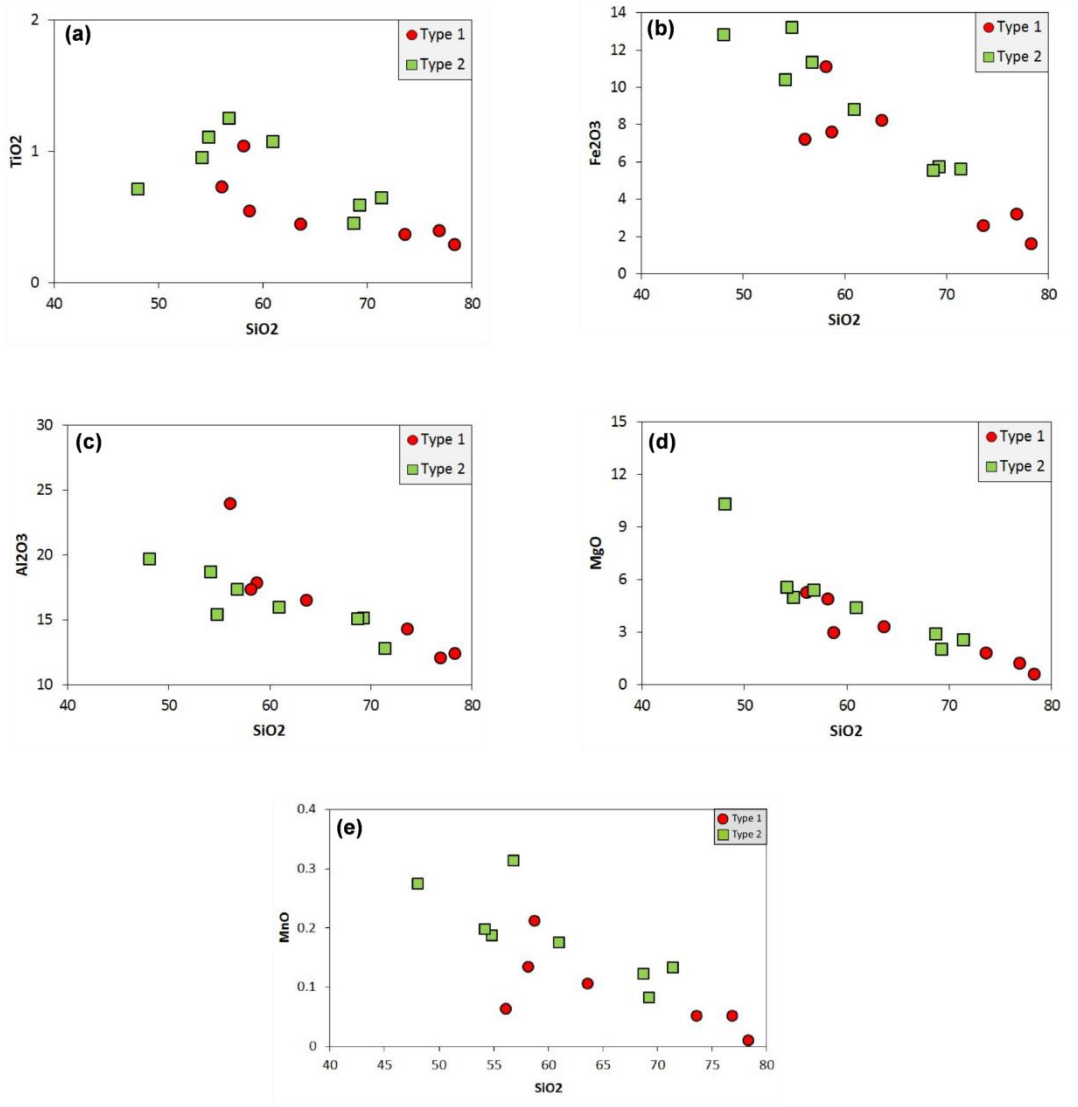

Figure 4-4: Harker diagrams showing relationship between SiO_2 and major oxides.

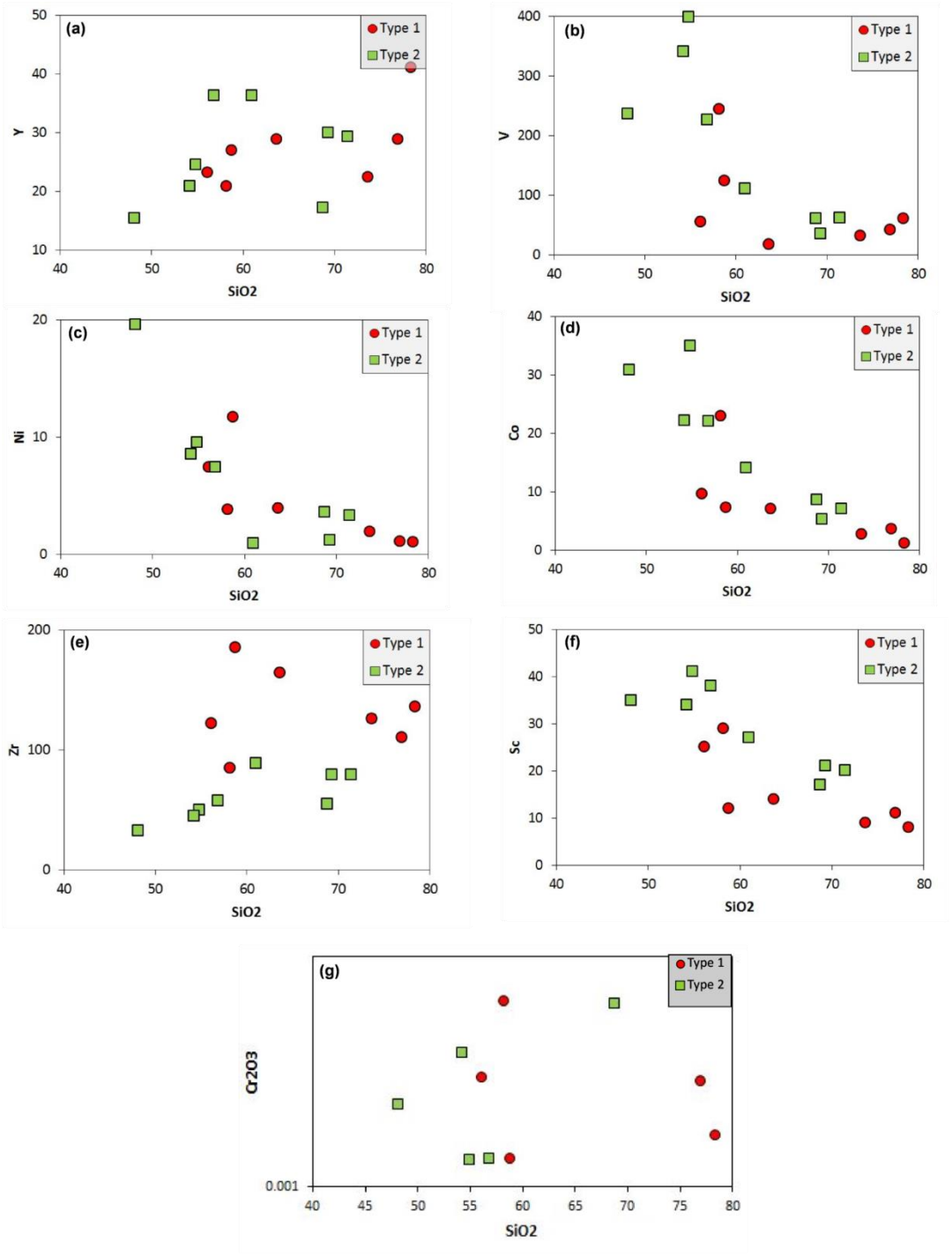

Figure 4-5: Harker diagrams showing relationship between SiO_2 and selected trace elements.

To sum up, the variations in major oxides and trace elements demonstrate that fractional crystallization of olivine, pyroxene, plagioclase and Fe-Ti oxides may

have played an important role in the magmatic evolution of Kösedağ Metavolcanics.

4.5. Source and Petrogenesis

As mentioned above, the Kösedağ Metavolcanics reflect a wide range of SiO_2 content, which is also reflected by the occurrence of lithologies represented by dacites, andesites and basalts. Because of this large range, only the most primitive samples in the dataset were taken into consideration in order to make interpretatiton about the source characteristics. By selecting the samples with higher MgO and lower SiO_2 contents, it is aimed to eliminate assimilation and fractional crystallization processes as much as possible. If the relative compatibilities of trace elements is considered during partial melting of lherzolite, Nb is known to be more incompatible than Zr (Sun and McDonough, 1989). Therefore, high Zr/Nb ratios may indicate involvement of depleted sources, as is the case for N-MORBs (31.8; Sun and McDonough, 1989). Lower Zr/Nb ratios, on the other hand, may suggest contribution from the enriched mantle sources, as seen in OIBs (5.83 Sun and McDonough, 1989). The Zr/Nb ratios of Type 1 samples change between 38.1 and 52.9, while this ratio ranges between 21.8 and 41.2 for Type 2 samples. These values are somewhat similar to Zr/Nb ratio of N-MORB that have been generated from depleted mantle sources (Fig. 4-6). Therefore, it can be inferred that the Kösedağ Metavolcanics have mainly derived from depleted sources, such as N-MORB source.

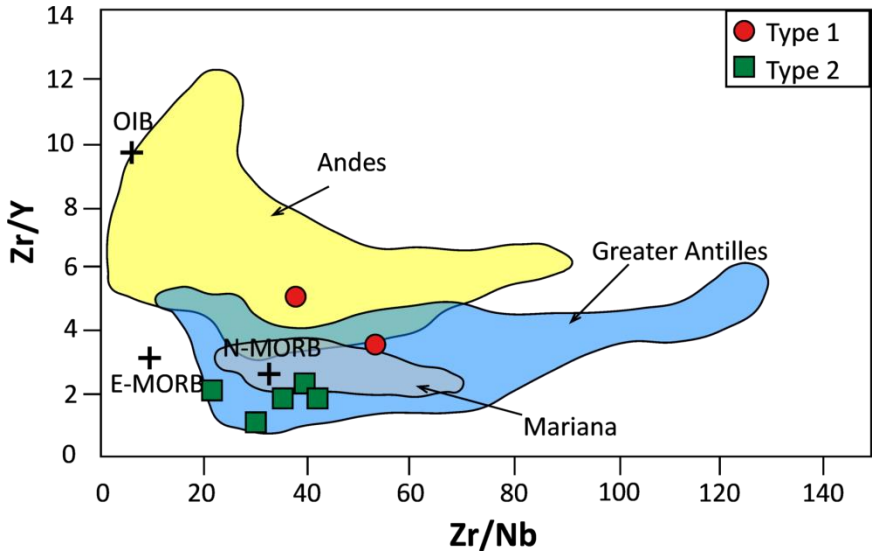

Figure 4-6: Zr/Y-Zr/Nb diagram. Greater Antilles data from Jolly et al (1998) and Jolly (2001); Andes from compilation of Winter (2001); Mariana from Pearce et al (2005).

Another parameter to assess the nature of the source can be Zr/Y ratio. High Zr/Y ratios imply enriched mantle sources, such as that of OIBs (OIB Zr/Y = 9.66; Sun and McDonough, 1989). Lower Zr/Y ratios, however, points out depleted mantle sources, like that of N-MORBs (N-MORB Zr/Y = 2.64; Sun and McDonough, 1989) (Fig. 4-6). Zr/Y ratio of Type 1 samples change between 4.07 and 5.25, while Type 2 samples range from 1.58 to 2.44. Therefore, on the basis of Zr/Y ratio, it can be suggested that Type 2 samples have been dominantly derived from depleted mantle sources, whereas Type 1 samples may have also included some contribution from enriched mantle sources. Nb/Y ratios can be used in a similar manner to Zr/Y such that low Nb/Y ratios are associated with depleted mantle sources, whereas high Nb/Y ratios may be suggestive of enriched sources (N-MORB Nb/Y = 0.08, OIB Nb/Y = 1.65; Sun and McDonough, 1989) (Fig. 4-7). The range of Nb/Y for Type 1 samples is between 0.08 and 0.14, while Type 2 samples changes between 0.05 to 0.10. This is result in aggrement with the idea that the Kösedağ Metavolcanics have acquired a dominant contribution of the depleted sources. However, Type 1 samples, in general, reflect more depleted characteristics.

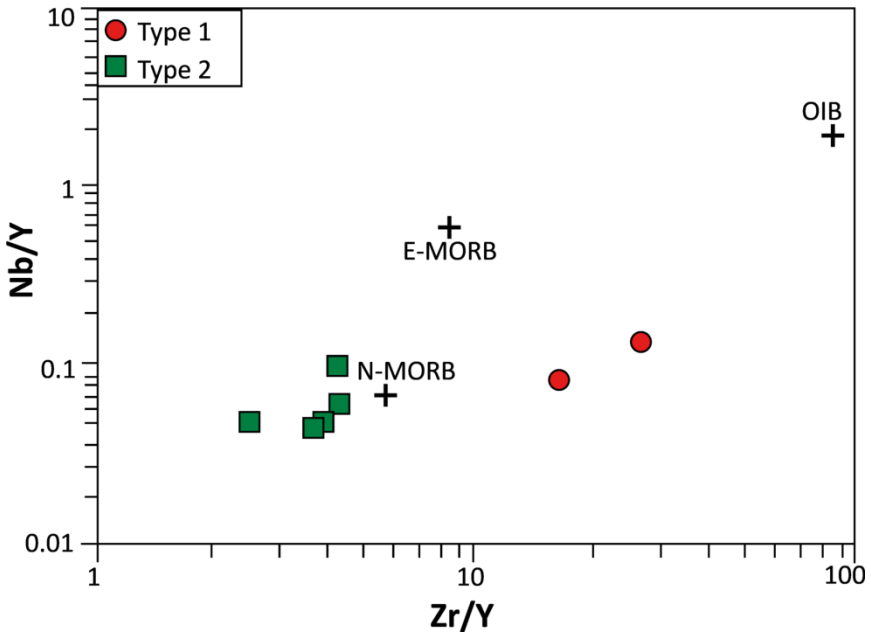

Figure 4-7: Nb/Y versus Zr/Y diagram (Average N-MORB, E-MORB, OIB values from Sun and Mc Donough, 1989).

Another issue to consider is whether the Kösedağ Metavolcanics have derived from a spinel- or garnet-bearing mantle source. In this regard, Sm/Yb ratio can be useful to identify the presence of spinel or garnet in the source. High Sm/Yb ratios may suggest the occurrence of garnet as a residual phase in the source region (e.g. McKenzie and O'Nions 1991). This is because HREEs are strongly compatible with garnet (e.g. Irving and Frey, 1978; McKenzie and O'Nions, 1991). Therefore, the presence of garnet in the source would lead to strong depletion in HREE compared to LREE due to retention of HREE in garnet (Wilson, 1989; Spath et al., 1996). However, this is not the case observed in the Kösedağ samples, which suggests mantle depths shallower than the stability of garnet. Therefore, it can be proposed that the Kösedağ metavolcanic rocks have generated from a spinel-lherzolitic mantle source rather than a garnet-lherzolite [$(Sm/Yb)_N$ = 0.99-1.34 for Type 1, 1.00-1.24 for Type 2; OIB = 4,63; Sun and McDonough, 1989)].

Depletion in Nb (and Ta) relative to adjacent LILEs and LREEs (e.g. Th and La) is a characteristic feature of subduction zone magmas (e.g. Pearce, 1982), which is related to fluid/melt transport in the shallow parts of subduction zones (Baier et al., 2007). This feature is also observed in the Kösedağ Metavolcanics that reflect Nb and Ta depletion compared to LILE and LREE (Fig. 4-2, Fig. 4-3). The relative depletion of Nb (and Ta) in subduction-related magmas is generally attributed to accessory phases that can effectively partition these elements, such as rutile. The fluids coming from the dehydrating slab have low Nb and Ta abundances (Becker et al., 2000; Scambelluri and Philippot, 2001). Therefore, the presence of negative anomalies observed on the Kösedağ metavolcanic rocks may indicate the involvement of subduction zone component in their mantle source (Fig. 4-2).

Th/Yb-Nb/Yb diagram gives useful information about source characteristics and subduction related processes (Pearce 1983; Pearce and Peate, 1995) (Fig. 4-8). The trace elements Nb and Th display similar geochemical behaviour during partial melting of MORBs and OIBs (Wood et al. 1979; Pearce et al., 2005). While Nb is both fluid- and subduction-immobile, Th is fluid-immobile but subduction-mobile incompatible trace element. Th and Nb behave similarly during within-plate processes, but crustal contamination and subduction processes lead to enrichment in Th, without effect on Nb. Yb, which is a subduction-immobile element, is used as a normalizing factor to decrease fractional crystallization and crystal accumulation effects (Pearce and Peate 1995; Pearce et al., 2005). In this context, Th can be derived from the subducted slab. Nb and Yb, on the other hand, derive from the mantle. Therefore, with the aid of Th/Yb-Nb/Yb plot, the influence of subduction component can be revealed based on the relative displacement from the compositional array defined by the magmas from non-subduction settings (i.e. MORBs and OIBs). Therefore, on the Th/Yb-Nb/Yb diagram, if there is no subduction component and crustal contamination, samples would plot on this array. However, Both Type 1 and Type 2 samples plot outside the array, indicating the effect of subduction process and/or crustal contamination (Fig. 4-8).

It must be noted that Type 2 samples display higher Th/Yb values for a given Nb/Yb compared to Type 1. This may show that the contribution of subduction

component (or crustal effects) on Type 2 samples have been greater. In addition, Nb/Yb ratios of Kösedağ Metavolcanics are largely lower than that of average N-MORB (N-MORB Nb/Yb = 0.76; Sun and Mcdonough, 1989). Low Nb/Yb ratios are characteristic of depleted mantle sources. Thus, this result also supports the predominant involvement of depleted sources in the petrogenesis of the Kösedağ Metavolcanics. It must also be noted that the lower Nb/Yb values characteristics of Type 2 in general relative to Type 1 may suggest that the more depleted nature of the former (Fig. 4-8).

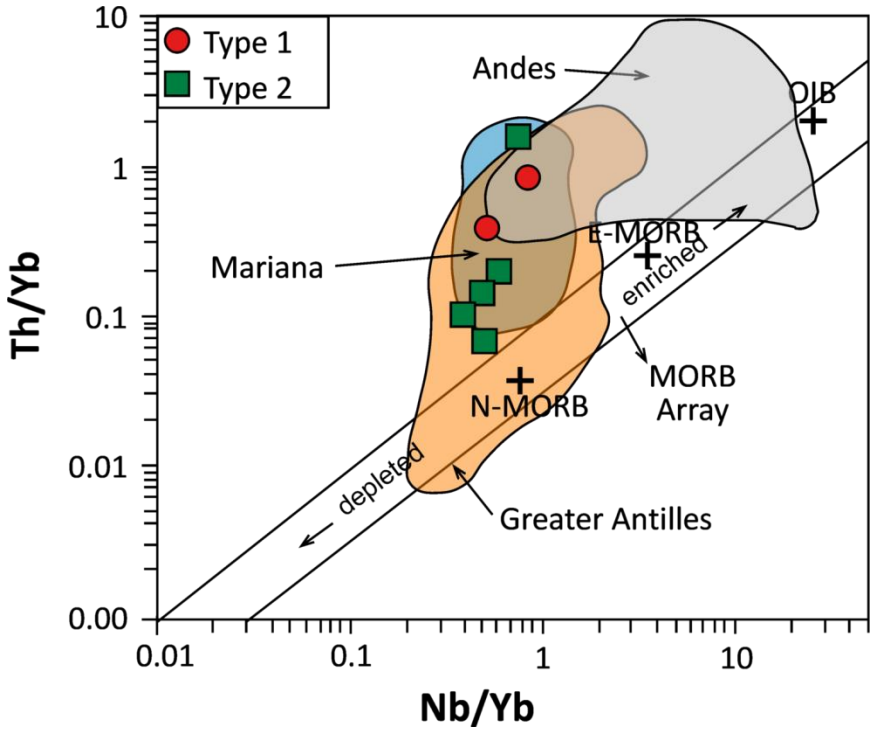

Figure 4-8: Th/Yb versus Nb/Yb diagram (after Pearce and Peate, 1995). Average N-MORB, E-MORB and OIB values from Sun and Mc Donough (1989). Greater Antilles data from Jolly et al (1998); Jolly (2001); Andes from compilation of Winter (2001), Mariana from Pearce et al (2005).

Subduction-related magmas are characterized by LILE enrichment relative to HFSE (Pearce and Peate, 1995). Accordingly, high La/Nb ratios are typical features of magmas generated above subduction zones (Average Mariana Arc La/Nb = ~2.50). While La/Nb ratio of Type 1 samples range from 2.19 to 4.19, that of Type 2 samples range from 3.06 to 5.93 (Fig. 4-9a). Such high values may

indicate the presence of subduction component incorporated into the source region of the Kösedağ metavolcanic rocks. Similarly, high Th/Nb values may also display the presence of subduction component (Average Mariana Arc Th/Nb = 0.25). Average Th/Nb values for Type 1 Kösedağ samples is 0.62, while it is 0.91 for Type 2. These high values, therefore, may suggest the presence of subduction component in the mantle source of the Kösedağ Metavolcanics (Fig. 4-8). It must also be noted that high La/Nb and Th/Nb ratios may also imply the influence of crustal contamination (Hart et al., 1989; Saunders et al., 1992). Bulk continental crust is characterized by relatively high La/Nb and Th/Nb ratios (1.45 and 0.32, respectively) (Taylor and McLennan, 1995). Therefore, although these values in the Kösedağ samples are much higher relative to the bulk continental crust, the effect of crustal contamination cannot be entirely excluded at this point.

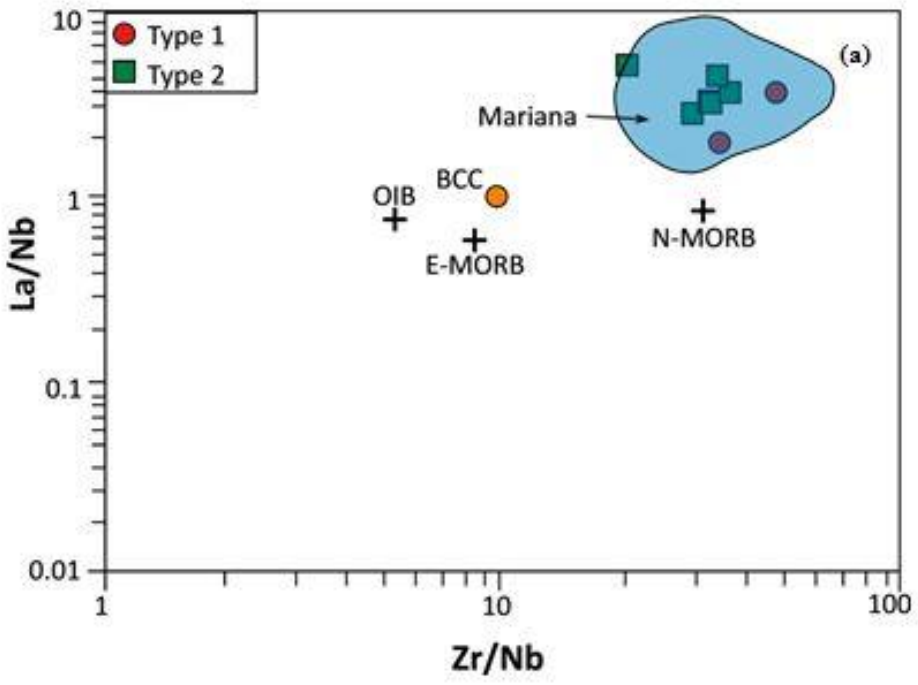

Figure 4-9: a) La/Nb versus Zr/Nb diagram b) Th/Nb versus Zr/Nb diagram. Average N-MORB, E-MORB, OIB values from Sun and Mc Donough (1989). BCC values from Taylor and McLennan (1995).

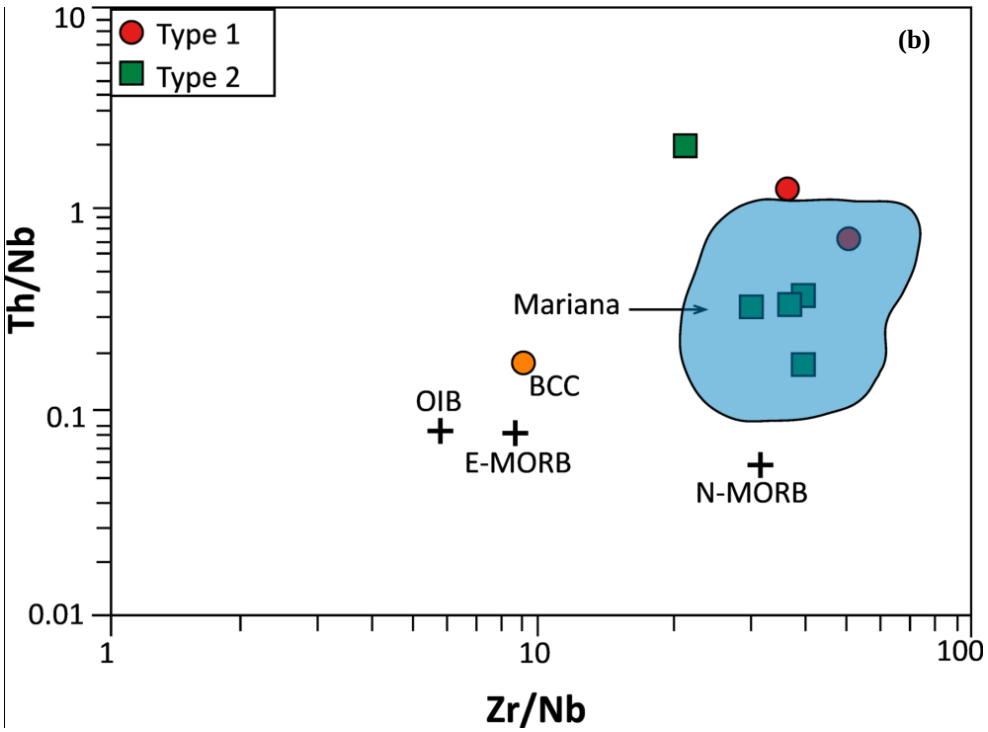

Figure 4-9: (continued).

4.6. Tectonomagmatic Discrimination of the Studied Samples

The Kösedağ Metavolcanics display spiked trace element patterns when normalized to N-MORB (Fig. 4-10). Selective enrichments in Th and LREE over HFSE suggest that the mantle source has been modified by subduction component (i.e. fluids, melts) derived from subducted slab (Best, 1975; Hawkesworth et al., 1977). Such features are not observed on the oceanic magmas generated away from subduction zones (i.e. N-MORBs and OIBs). In addition, the enrichment levels in OIBs are apparently higher compared to the Kösedağ samples (Fig. 4-10). Therefore, neither mid-ocean ridge nor oceanic island setting seem very likely for the petrogenesis of the Kösedağ metavolcanic rocks.

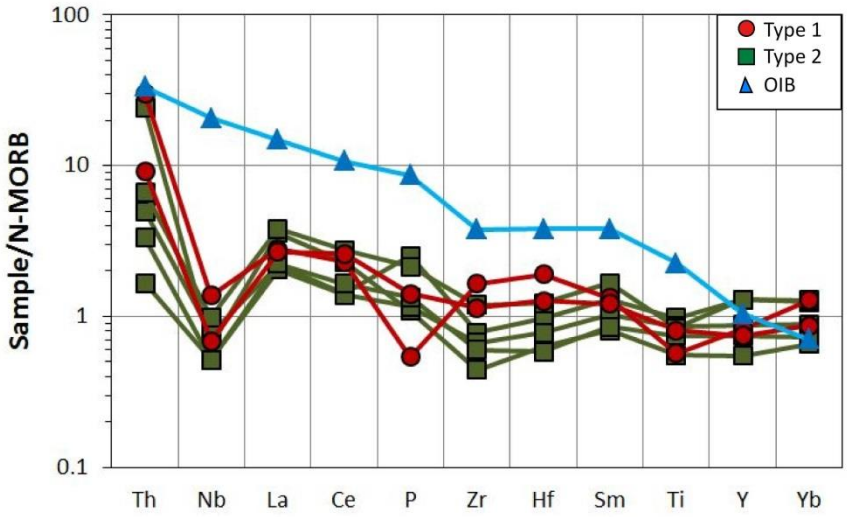

Figure 4-10: Comparison of trace element patterns of the Kösedağ metavolcanic rocks with average OIB (Normalization and OIB values from Sun and McDonough (1989).

When the Kösedağ Metavolcanics are compared to the magmas from rift environments, the marked anomalies present in both Type 1 and Type 2 samples are not found in a rift system like East African Rift (Furman et al., 2006) (Fig. 4-11). Thus, this result appears to be in contrast with the idea that the Kösedağ Metavolcanics are rift-related. However, some magmas developed on the rift flanks and shoulders, such as those of Rio Grande, may exhibit negative Nb anomalies (Gibson et al., 1993), thus they may look like somewhat similar to the subduction zone lavas in this respect. Although subduction signature may exist in the rift-related magmas, their incompatible element concentrations are much higher those of Kösedağ metavolcanic rocks. Therefore, a rift-related origin is not supported for the petrogenesis of the Kösedağ Metavolcanics.

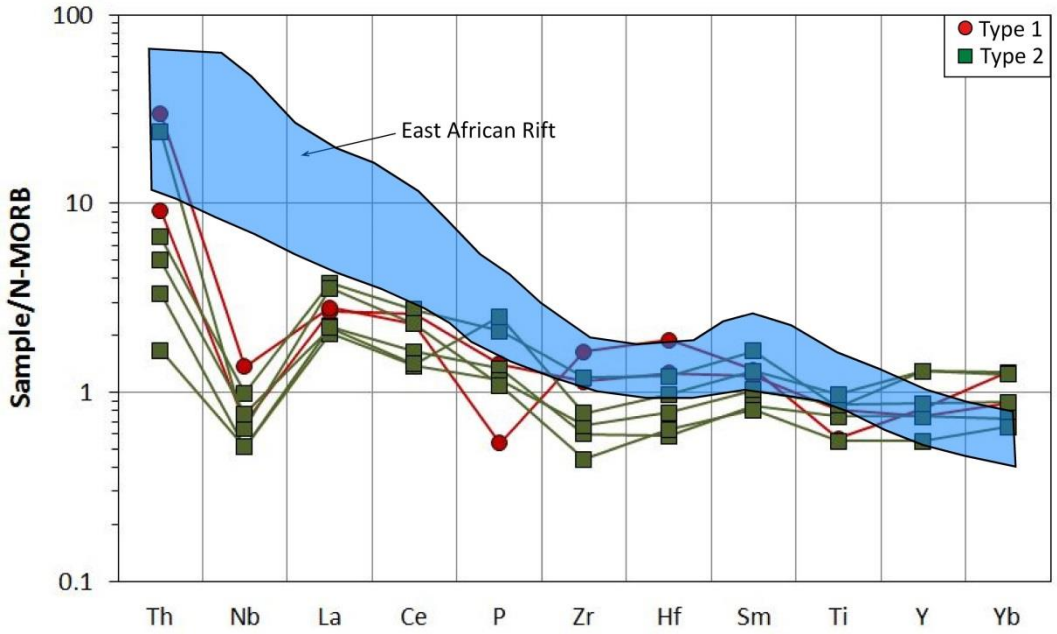

Figure 4-11: N-MORB normalized (Sun and McDonough, 1989) multi-element variation patterns of Kösedağ metavolcanic rocks and East African Rift (Furman et al., 2006).

As mentioned above, the generation of Kösedağ metavolcanic rocks has not been attributed to the tectonic environments, including mid-ocean ridge, ocean island and continental rift. Instead, the most appropriate tectonic environment for the petrogenesis of the Kösedağ metavolcanic rocks appear to be an arc setting, which is supported by a number of reasons. First, saw-tooth distribution on spider diagram could be an evidence showing arc-like tectonic setting (Fig. 4-2). Arc-related volcanics are distinguished by their low abundance of HFSE relative to LILE and LREE (Stolz et al., 1996), implying that their mantle source have been modified by subduction component. Both groups exhibit Th enrichment implying arc basalts. This is well illustrated in the Th/Yb-Nb/Yb diagram (after Pearce and Peate, 1995) in which all Kösedağ samples plot inside the fields represented by arc volcanics. The idea that the Kösedağ Metavolcanics are arc-related is also supported by tectonomagmatic diagrams. In these plots, nearly all Kösedağ samples fall inside the volcanic arc basalt field (Fig. 4-12).

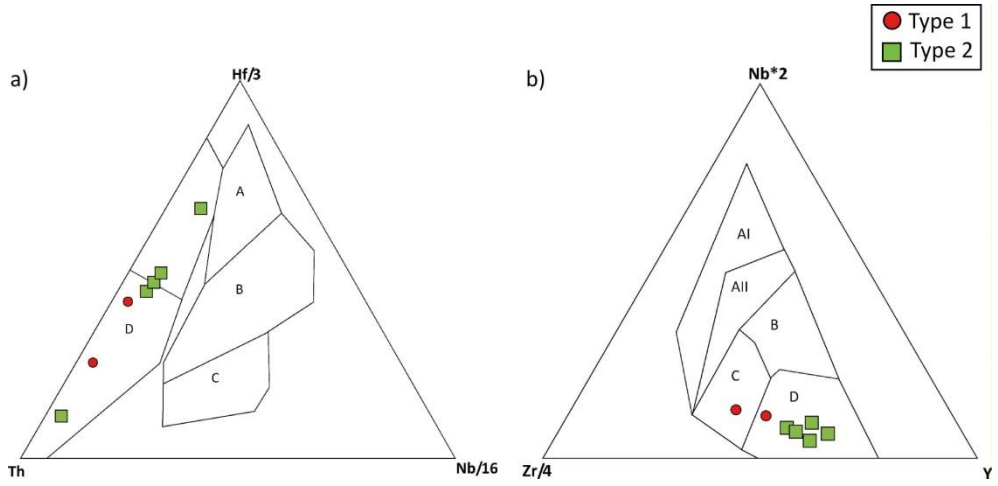

Figure 4-12: a) Tectonic discrimination diagram for the studied rocks (after Wood et al. 1979. Fields: A:N-MORB; B:P-MORB; C:WPD; D:Destructive plate margin basalts). b) Tectonic discrimination diagram for studied rocks (after Meschede, 1986. Fields; AI and AII:WPB; B:P-MORB; C:WPT and VAB; D:N-MORB and VAB).

The trace element evidence suggests that the Kösedağ Metavolcanics have been generated above a subduction zone. However, it is known that arcs magmatism can occur in both continental and oceanic settings. Thus, in order to get further evidence about the affinity of the Kösedağ magmatism, the studied samples were compared with the modern arc samples, such as Greater Antilles, Mariana and Andes (Fig. 4-13, Fig. 4-14). Although the overall process is similar in both continental and oceanic arc settings, the presence of incompatible element-enriched continental crust creates the distinction between continental and island arcs. The level of enrichment in LILE and HFSE in continental arcs are higher than those of island arcs. When compared to island arcs, Ta, Nb, Zr, Hf contents are more abundant in continental arcs, which can be due to the contribution of continental crust and/or subcontinental lithospheric mantle (SCLM) (e.g. Pearce, 1983; Wilson, 1989).

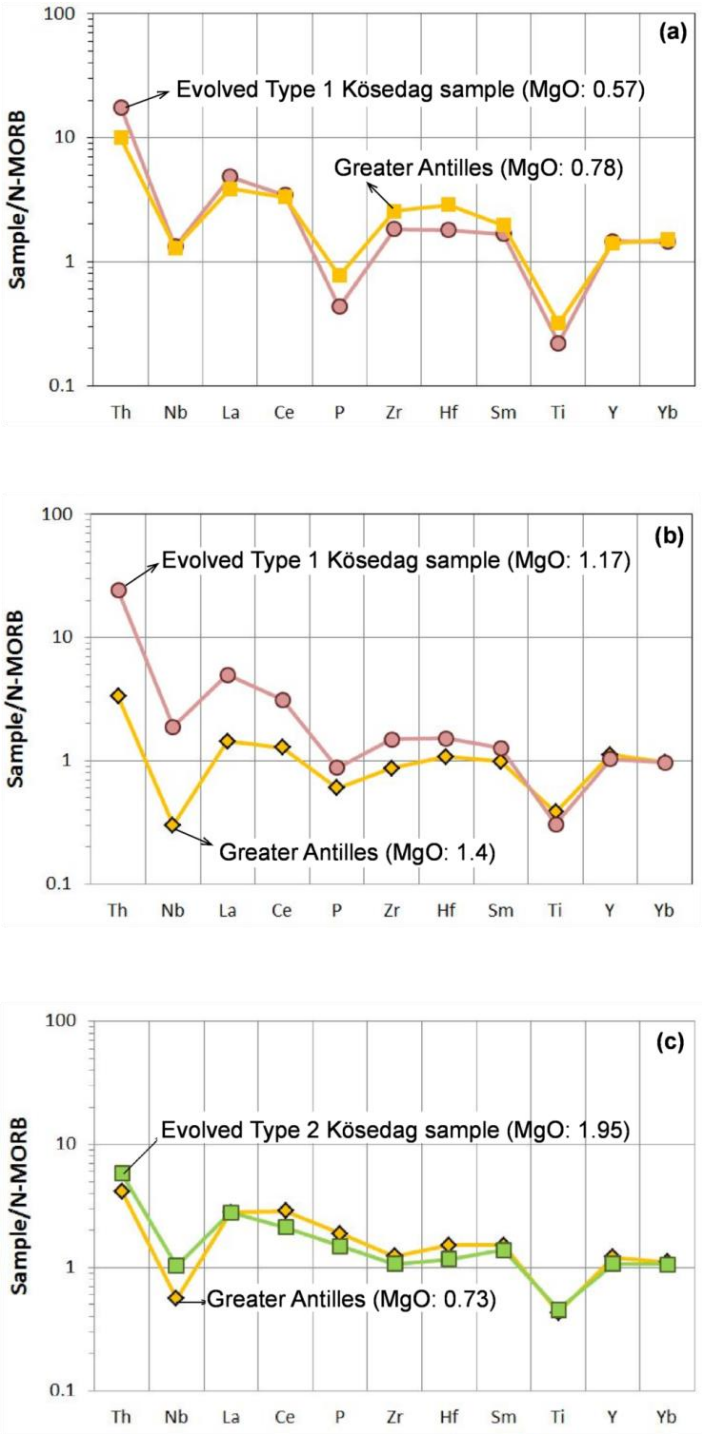

Figure 4-13: Comparison of evolved Kösedağ samples with Greater Antilles (Jolly et al., 1998; Jolly, 2001) and Mariana (Pearce et al., 2005).

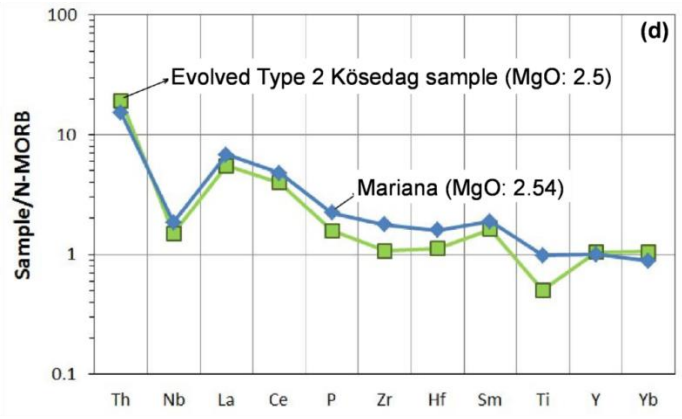

Figure 4-12: (continued).

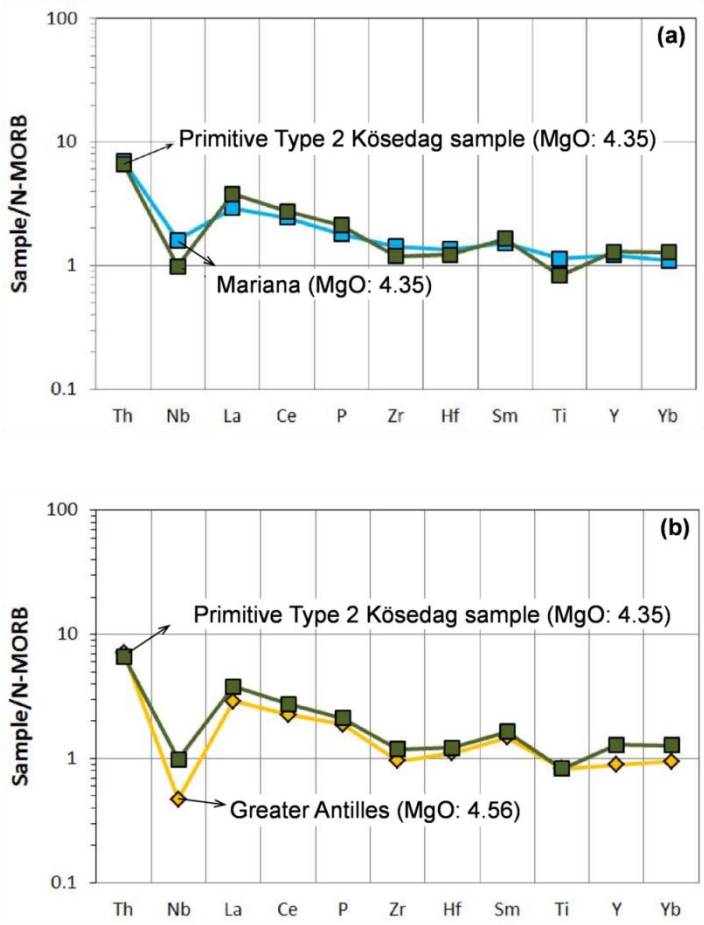

Figure 4-14: Comparison of primitive Kösedağ samples with Greater Antilles (Jolly et al., 1998; Jolly, 2001) and Mariana (Pearce et al., 2005).

In addition, trace element ratios may give some insight in this regard. For example, oceanic arcs are typically characterized by low Nb/Yb ratios (Average Greater Antilles Nb/Yb = 0.68: Jolly et al., 1998; Jolly, 2001; Average Mariana Nb/Yb = 1.22; Pearce et al., 2005) (Fig. 4-8), whereas continental arcs show higher values (Average Andes Nb/Yb = 3.22). The Kösedağ Metavolcanics display low Nb/Yb ratios (an average of 0.6), thus implying island arc affinities. This result is also confirmed by Zr/Nb ratio. The high values of Zr/Nb are indicative of an oceanic origin, whereas low values imply arcs of continental character (Average Greater Antilles Zr/Nb = 52.89; Jolly et al., 1998; Jolly, 2001; Average Mariana = 39.13; Pearce et al. 2005; Average Andes Zr/Nb = 30.8; Winter, 2001) (Fig. 4-9). The average Zr/Nb ratio of the Kösedağ samples is 37.34, therefore suggesting an island arc origin rather than a continental arc.

CHAPTER 5

DISCUSSION

In this chapter, geological, petrographical and geochemical features of the Kösedağ metavolcanic rocks will be discussed in order to shed light into their geodynamic setting and relationship with the surrounding units. In addition, the findings of the previous studies were also evaluated and compared in the light of the new data obtained in this study.

5.1. Contact relations

Reviewing the available data obtained yet, the Kösedağ Metavolcanics are represented by a volcano-sedimentary assemblage. The bulk of the unit is composed of metabasalt, metaandesite and metadacite. The three distinct metavolcanic lithologies (namely basalts, andesites, dacites) alternate with each other in short distances in the field. However, due to intense tectonism, the contacts between them are mostly observed to have been sheared (Fig. 2-2). These metavolcanic rocks are intercalated with volcaniclastics, mudstone, chert and pelagic limestone. The Kösedağ Metavolcanics include secondary mineral phases, including epidote, chlorite and actinolite, which reflect low-grade metamorphic nature of the unit. The volcanic-dominant content and low-grade metamorphic nature of the Kösedağ Metavolcanics, were also noted in the previous studies. For example, the unit was regarded to be mainly composed of felsic and mafic lavas by Yılmaz and Tüysüz, (1984). Hakyemez et al. (1986) similarly defines the unit (their Karabürçek Formation) as composed of metamorphics, consisting of chlorite-albite schist, quartz-epidote schist, chlorite-carbonate-quartz schist, metavolcanites,

diabase, spilite and andesite with recrystallized limestone and quartz bearing metaandesites. The presence of sedimentary alternations within the metavolcanic lithologies as observed in the present study was also noted by the previous studies. Tüysüz (1985) mentioned that the mafic lavas are generally alternated with thin to thick bedded, reddish pelagic limestones (Tüysüz, 1985). He also stated that these pelagic limestones are almost entirely recrystallized, which is confirmed by the present study. Aygül et al. (2015) also noted the presence of metavolcanic rocks within the unit, which are characterized by basaltic andesite/andesite and rhyolite with their pyroclastic equivalents.

The Kösedağ lithologies are intensely deformed and sheared, and they display well-developed deformation. As they are located very close to the NAFZ, this appears to have influenced the Kösedağ metavolcanic rocks. This effect is seen as dynamic metamorphism, which has resulted in mylonitization of the Kösedağ lithologies. The effect of mylonitinic deformation is especially well observed at micro-scale by the presence of porphyroclasts that have developed in the close vicinity of the North Anatolian Fault Zone lying just to the north of the study area. Therefore, in addition to low-grade metamorphism, the later developed dynamic effects give rise to a complex nature on these rocks. Tüysüz (1985) also mentioned that the Kösdağ metamorphics is situated in an area which has been heavily affected from the NAFZ.

The northern boundary of the Kösedağ Metavolcanics is tectonic, which is bounded by the NAF and the CPSC (Tekin et al., 2012). The southern boundary, however, is controversial, which arises from the diverse views on the nature of contact relationship between the Kösedağ Metavolcanics and metacarbonates of the Dikmen Formation. Hakyemez et al. (1986) suggest a stratigraphic boundary between these units and propose that the metavolcanic assemblage transitionally passes to the Dikmen Formation upward in the sequence. This idea is also favored by the recent study of Aygül et al. (2015) who suggest that the metavolcanics are stratigraphically overlain by the metacarbonates of the Dikmen Formation. According to Sevin and Uğuz (2011), however, this is also claimed as a tectonic contact. In the present study, however, the contact relationship between the

Kösedağ and Dikmen units was observed to be tectonic, which is in contrast with the view that the metacarbonates are transitional to the underlying metavolcanics.

5.2. Age of the Kösedağ Metavolcanics and their cover

The age of the Kösedağ Metavolcanics is also debated. Hakyemez et al. (1986) propose an age of Late Jurassic-Early Cretaceous by fossil data. It must also be noted that these carbonates from which Hakyemez and his co-workers acquired the fossil data are not from the Kösedağ region, but collected from the unit further to the west (the Akbayır Formation of Akyürek et al., 1982) that these authors regard them as equivalents of the Yaylacık Formation. Therefore, first, it is not clear that the units they regarded as similar actually correspond to the same units. Second, even if assuming that these two carbonate units are their equivalents, no stratigraphic relationship is found between the metavolcanics and carbonates. Hence, the age data acquired from Akbayır Formation may not reflect the age of Kösedağ Metavolcanics.

In this study, no fossil finding could be obtained from recrystallized limestones of the Dikmen Formation. Therefore, there exists no reliable biostratigraphical data that can reflect the age of metacarbonates in the study area. However, if the carbonates lying to the west are indeed comparable to the Dikmen Formation, this would constrain the age of the Dikmen Formation to Late Jurassic-Early Cretaceous interval. On the other hand, Aygül et al. (2015) in their recent study, reported the radiometric ages that they acquired from two metarhyolite samples. These authors interpreted 93.8±1.9 and 94.4±1.9 Ma zircon U-Pb ages as the protolith ages. This age finding is of particular importance, since it entirely differs with the view that the Kösedağ Metavolcanics are Late Jurassic as suggested by the previous studies (e.g. Hakyemez et al., 1986). Aygül et al. (2015) also suggested an age of 69.9±0.4 Ma (Maastrichtian) for the age of low-grade metamorphism based on $^{40}Ar/^{39}Ar$ muscovite dating.

5.3. Source and Magmatic Evolution

The Kösedağ metavolcanic rocks have been subjected to alteration as displayed by high and variable LOI contents. On the basis of immobile trace element systematics, the Kösedağ metavolcanic rocks are characterized by three compositional groups; basalts, andesites and rhyodacites/dacites (Fig. 4-1). Harker diagrams reveal that fractional crystallization of olivine, pyroxene, plagioclase and Fe-Ti oxides may have been an important process during the magmatic history of Kösedağ metavolcanic rocks. (Fig. 4-3, Fig. 4-4). The Kösedağ metavolcanic rocks can be subdivided into two distinct chemical groups as Type 1 and Type 2 based on trace element systematics. Both groups of the Kösedağ Metavolcanics reflect inclusion of a depleted spinel-bearing mantle source which has been modified by subduction component (Fig. 4-7). The overall trace element characteristics of Kösedağ Metavolcanics suggest that they have been generated above a subduction zone, probably in an island-arc setting.

The geological observations are also consistent with the idea that the Kösedağ metavolcanic rocks represent relicts of an intra-oceanic arc. The sedimentary material within the Kösedağ Metavolcanics is entirely oceanic-derived; no terrigenous detritus is present in the unit, which is also reported by Aygül et al. (2015). Therefore, this may suggest that the Kösedağ metavolcanic rocks were developed in an oceanic environment and based on geochemistry is it is consistent with an island-arc setting. This idea seems to be in agreement with a number of studies who regarded the Kösedağ Metavolcanics as remnants of an island-arc (Yoldaş, 1982; Tüysüz, 1985; Aygül et al., 2015).

5.4. Regional Correlation of the Kösedağ Metavolcanics

As mentioned above, the Kösedağ Metavolcanics display arc-type geochemical signatures, thus they do not resemble to the metabasic lithologies from the Karakaya Complex (the Nilüfer Unit sensu Sayit et al., 2010) that display OIB and E-MORB type signatures. On the other hand, the metavolcanic rocks from the Çangaldağ Complex have been reported to show arc-like characteristics (Ustaömer

and Robertson 1999), which suggest a similarity to the Kösedağ Metavolcanics. However, the Early Cretaceous metamorphism on the Çangaldağ Complex as suggested by Okay et al. (2013) is in contrast with the Late Cretaceous protolith ages of the Kösedağ Metavolcanics. Therefore, on the basis of these data, it appears that the Kösedağ Metavolcanics cannot be the equivalent of the Çangaldağ Complex. The Kösedağ-like lithologies also crops out to west and east of the study area. These volcano-sedimentary assemblages are known as the Mudurnu Volcanics, which are composed of mafic and felsic volcanic rocks interbedded with volcaniclastics, limestone and mudstone. Apart from this lithological similarity, the Mudurnu Volcanics also display similar geochemical features to the Kösedağ metavolcanic rocks (Fig. 5-1). The main difference between these two units, however, is the metamorphic nature of the latter. Another important point is the age of the Mudurnu Volcanics. These non-metamorphosed volcanics are stratigraphically overlain by the Sogukçam Limestone of Late Jurassic-Early Cretaceous age, which constrain the age of the volcanics to Middle Jurassic. This is an important issue, because Aygül et al. (2015) ascribed the age of the Kösedağ Metavolcanics to Late Cretaceous on the basis of U-Pb radiometric ages. If this age finding is confirmed, it would indicate that the Kösedağ Metavolcanics are clearly not the equivalents of the Mudurnu volcanic rocks. On the other hand, if the Upper Jurassic-Lower Cretaceous age suggested by Hakyemez et al. (1986) is confirmed, then it may be possible that the Kösedağ metavolcanic rocks are the metamorphic equivalents of the Mudurnu Volcanics.

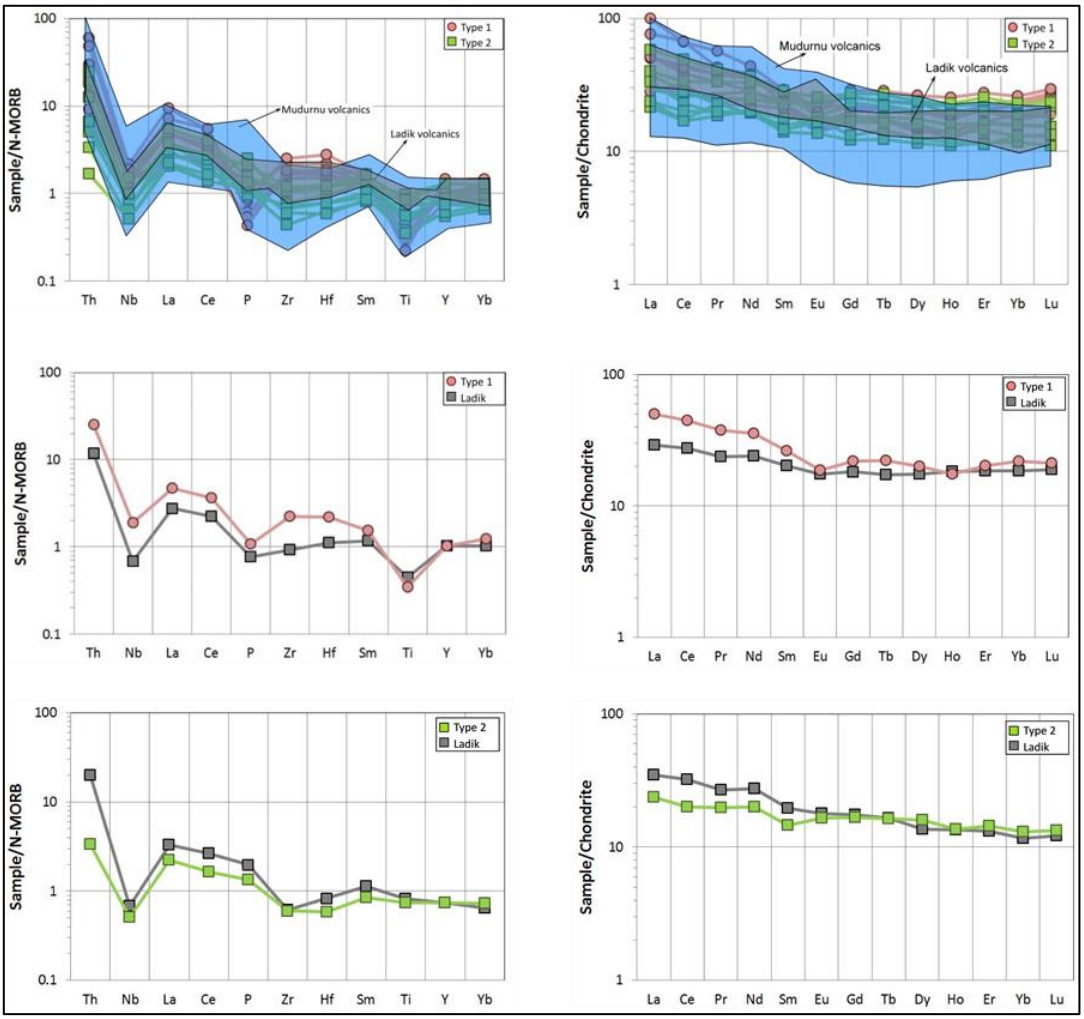

Figure 5-1: Comparison of Mudurnu and Ladik volcanics with Kösedağ metavolcanic rocks (Mudurnu and Ladik data from Genç and Tüysüz, 2010).

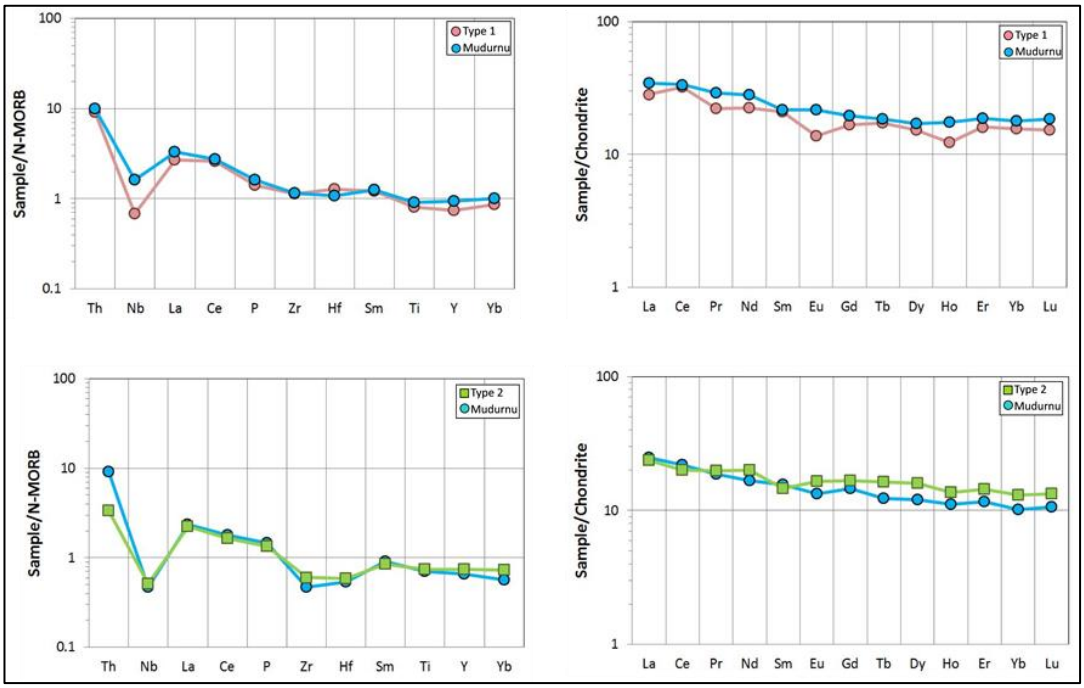

Figure 5-1: (continued).

5.5. Geodynamic Evolution

There are several geodynamic models proposed for the studies Kösedağ Metavolcanics. Regarding the geodynamic scenarios proposed for the Jurassic-Cretaceous evolution of the Pontide region, Genç and Tüysüz (2010) proposed two alternative models based on the geology and geochemistry of the Mudurnu Volcanics, which they believed to be the equivalent of the Kösedağ Metavolcanics. In their first model, the Sakarya Continent was situated to the south of the Palaeotethys. During the Early Triassic, Paleotethys was subducted beneath Cimmerian continent situated in south (Şengör et al., 1980, 1984), giving rise to the Karakaya back-arc basin. At the end of Triassic, this basin was closed, and the back-arc extension led to rifting of the Neotethys (Izmir-Ankara-Erzincan Ocean) to south of the Sakarya zone. This rifting process generated the Mudurnu Volcanics (Şengör and Yılmaz, 1981; Görür et al., 1983) (Fig. 5-2a, Fig. 5-2b).

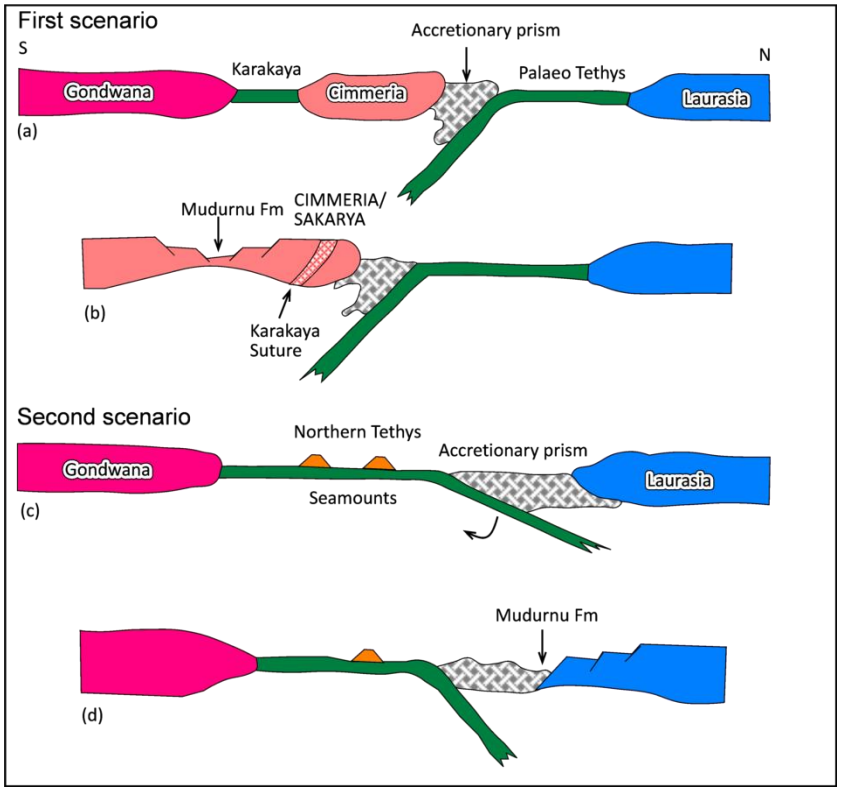

Figure 5-2: Geodynamic models for northern Turkey during the Triassic to Jurassic period. a, b) Palaeotethys Ocean subducted to southward, Karakaya back arc basin opened, and Mudurnu Formation generated on Cimmeria c, d) Illustration displaying the opening of the rift basin on the complex basement (Genç and Tüysüz, 2010).

In their second scenario, these authors regarded a continuous subduction process during the Mesozoic. In this model, the Tethys Ocean subducted northwards beneath Laurasia to form a wide accretionary prism (Fig. 5-2c and d). This accretionary prism was interpreted as pre-Liassic basement of the Sakarya Continent. According to this model, northward subduction of Tethys during the Liassic formed a rift basin above the accreationary prism and the Laurasian Continent, which is represented by the Mudurnu Formation. However, this rift model is not supported owing to the arc-related geochemistry of the Kösedağ Metavolcanics.

Berber et al. (2014) suggested that during the closure of the Paleotethys, the southward subduction created the Karakaya Complex that accreted to the Sakarya

Continent in the Late Triassic. During the Liassic, the Karakaya Complex was covered by the Bayırköy Formation. During the same period, the subduction direction changed in the northerly located ocean, which in turn formed the Kösedağ Arc. With ongoing subduction, the roll-back of the subducting slab gave way to the formation of a back-arc type ocean which was named as Aylı Dağ ophiolite (Göncüoğlu et al., 2012). During the Malm and Early Cretaceous, the Kösedağ Arc accreated to the Sakarya continent and disconformably overlain by the slope type Soğukçam limestone (Fig. 5-3).

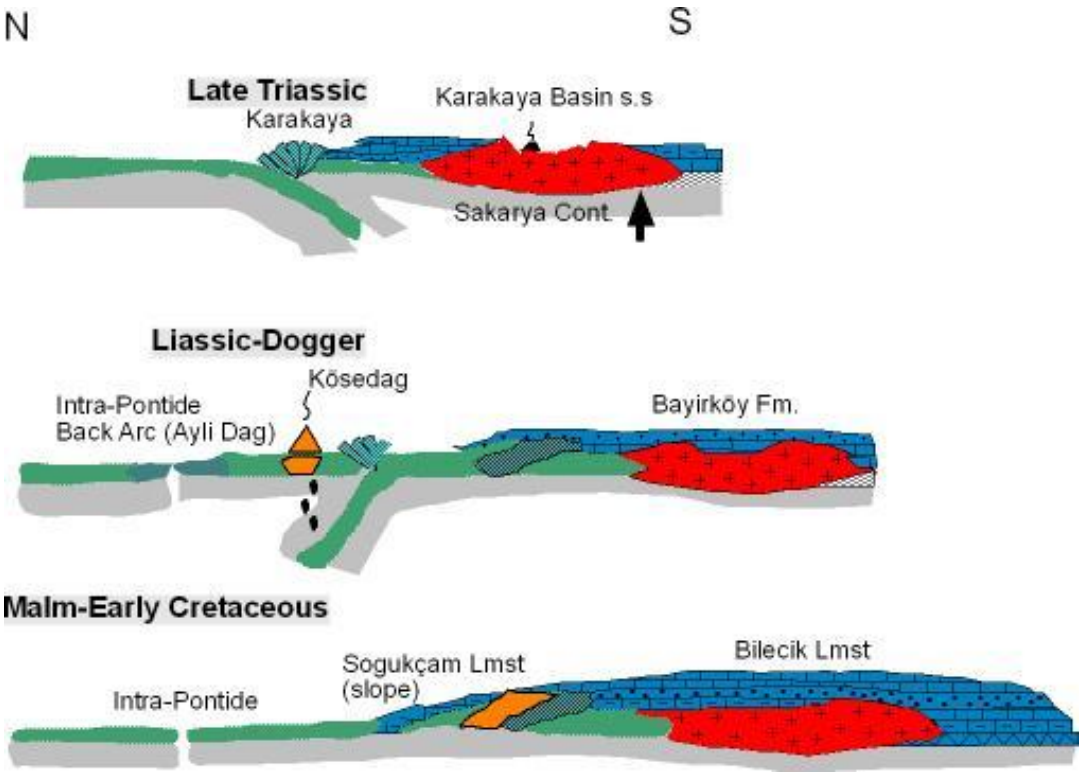

Figure 5-3: Geodynamic model of Berber et al (2014) for the evolution of Kösedağ Metavolcanics.

Aygül et al. (2015), in their geodynamic model, envisioned the Kösedağ Metavolcanics as an island-arc formed as a result of northward intra-oceanic subduction of the Neotethys within the Izmir-Ankara-Erzincan Ocean during the early Late Cretaceous. During this period, another subduction was beneath the northerly located SCT, and generated the Albian-Turonian accretionary wedge

CPSC. At the end of Cretaceous, the Kösedağ Arc incorporated into this wedge (Fig. 5-4).

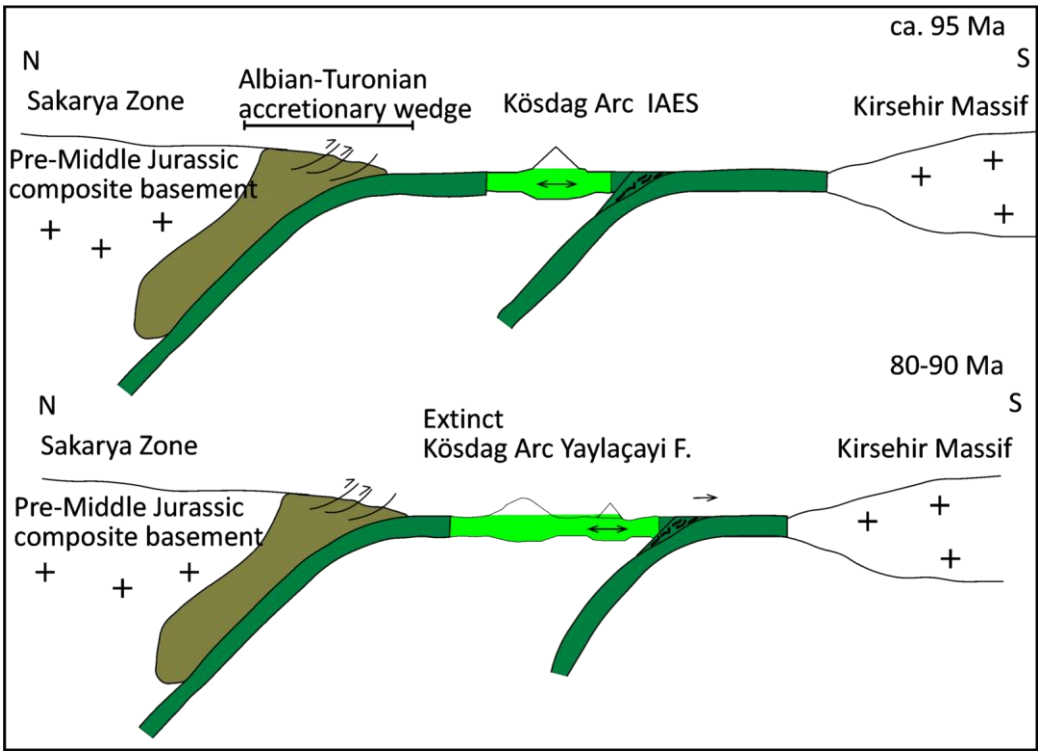

Figure 5-4: Schematic model showing the geodynamic evolution of Central Pontide in Late Cretaceous and formation of the Kösdağ Arc (Aygül et al., 2015).

As mentioned before, there is no paleontological age data acquired from the Kösedağ Metavolcanics. The only age data come from the study of Aygül et al. (2015), which suggests that the Kösdağ Arc was formed in the early Late Cretaceous. If this age finding is taken into consideration, it does not seem possible that the Kösedağ and Mudurnu volcanics were the result of the same magmatic event. Thus, if this is indeed the case, a Late Jurassic-Early Cretaceous origin does not seem likely for the formation of the Kösedağ Metavolcanics. Furthermore, a rift-related origin as suggested for the Mudurnu volcanics is not consistent with the arc-related geochemistry of the Kösedağ Metavolcanics. Because of these reasons, based on the available data, it seems more likely that the Kösedağ Metavolcanics

were representing an island-arc during the Late Cretaceous time. At this point, however, whether the Kösedağ magmatism was a part of the IAO or Intra-Pontide Ocean is hard to solve. If the latter scenario is assumed, however, the Kösedağ lithologies can be envisioned as representing an intra-oceanic arc system within the Intra Pontide Ocean during the Late Cretaceous (considering the age finding Aygül et al., 2015).

Alternatively, if the age of Kösedağ magmatism is assumed as Late Jurassic-Late Cretaceous, the following geodynamic scenario can be proposed (Fig. 5-6). During the Late Triassic, the southward closure of Palaeotethys to the North of the Sakarya Composite generated the Karakaya Complex. During the Liassic and Dogger, the Karakaya Complex accreted to the Sakarya Continent and subsequently covered by the Bayırköy Formation. Following this, the subduction polarity changed in the northerly located oceanic plate of the Intra-Pontide Ocean, creating the Kösedağ arc. The ongoing subduction associated with the rollback of the subducted slab led to formation of a back-arc basin represented by the Aylı Dağ ophiolite (Göncüoğlu et al., 2012). During the Late Cretaceous the Kösedağ arc incorporated into the Intra-Pontide subduction-prism and affected by metamorphism. It collided with the rest of the Sakarya continent at the end of Cretaceous.

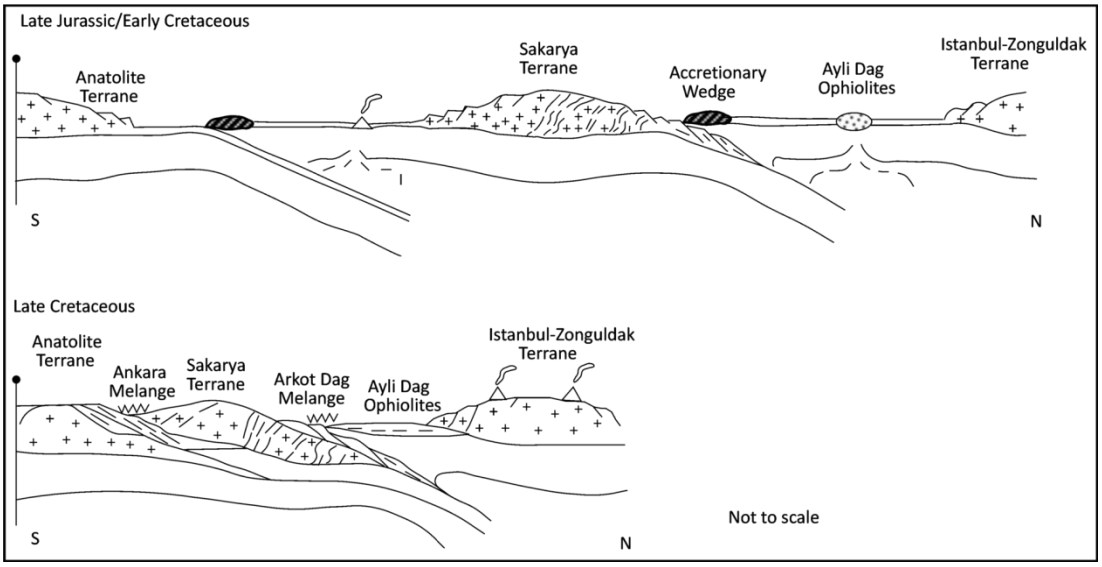

Figure 5-5: Two dimensional geodynamic reconstruction of the Intra-Pontide oceanic domain during the boundary between the Late Jurassic/Early Cretaceous and the Late Cretaceous (Göncüoğlu et al., 2014).

Among these possible geodynamic scenarios, none of them is yet acceptable without any doubt and additional studies, including acquisition of precise age data from the Kösedağ Metavolcanics, isotopic analysis of different type of metavolcanic rocks and the relationship and age of the metacarbonate unit are needed to get an answer for the problems discussed above.

CHAPTER 6

CONCLUSION

1. In the study area, two units are exposed; Kösedağ Metavolcanics and Dikmen Formation. The Kösedağ Metavolcanics consist of metadacite, metaandesite, metabasalt intercalated with volcaniclastics, mudstone, pelagic limestone and chert. The Dikmen Formation is represented by metacarbonates.
2. A primary contact relationship between the Kösedağ Metavolcanics and Dikmen Formation could not be observed in this study. The Kösedağ Metavolcanics tectonically overlie the Dikmen Formation.
3. There is no data on the primary juxtaposition of the Kösedağ-Dikmen and Ophiolitic Mélange units.
4. The Kösedağ metavolcanic rocks include a range of chemical compositions; basalt, andesite, and dacite. The Kösedağ Metavolcanics have derived from a depleted spinel lherzolite source modified by subduction component.
5. On the basis of trace element systematics, there are two distinct chemical groups as Type 1 and Type 2. Although Type 1 samples include felsic products, basaltic members are present in both groups. Geochemically, while Type 1 display depletion in P, Type 2 is characterized by depletion in Zr and Hf. Type 2 seems to have derived from a more depleted mantle source relative to Type 1.
6. No paleontological age could be obtained during this study. The only precise age data on the extrusion and metamorphism ages come from the

zircon U-Pb study of Aygül et al. (2015). The age data relies only on very few single zirzon ages and needs to be confirmed by additional data. Thus, the age of the Kösedağ Metavolcanics remains still not clear.

7. Overall geological and geochemical features indicate that the Kösedağ metavolcanic rocks represent an intra-oceanic arc that has formed above a Neotethyan subduction zone. Available data suggests that this Neotethyan Ocean may be the Intra-Pontide Ocean or, alternatively, the Izmir-Ankara-Erzincan Ocean.
8. The recent location of the Kösedağ Metamorphic Unit is controlled to a great extent by the North Anatolian Fault Zone with several active faults. Considering their strike-slip character of the NAF and without any information on the character and amount of off-sets along these faults during the Neotectonic Period, the original association of the unit to one of the main larger tectonic units of Turkey is very difficult to prove.

REFERENCES

Akyürek, B., Bilginer, E., Akbaş, B., Hepşen, N., Pehlivan, Ş., Sunu, O., Soysal, Y., Dağer, Z., Çatal, E., Sözeri, B., Yıldırım, H., Hakyemez, Y,. 1982. Ankara-Elmadağ-Kalecik Dolayının Jeolojisi. Maden Tetkik ve Arama Dergisi Rapor No:7298, Ankara (unpublished).

Ayaroğlu, H., 1980. Tosya kuzeybatısının (Karadere) jeolojisi ve ekonomik olanakları. Jeoloji Mühendisliği, 10, 65-73 pp, (In Turkish).

Aydın, M., Demir, O., Özçelik, Y., Terzioğlu, N., and Satır, M., (1995). A geological revision of Inebolu, Devrekani, Ağlı and Küre areas: New observations in Paleo-Tethys–Neo-Tethys sedimentary successions, in Erler, A., et al., (eds.) Geology of the Black Sea region: Maden Tetkik ve Arama Genel Müdürlüğü, 33–38, Ankara.

Aygül, M., Okay, A.I., Oberhansli, R., Schmidt, A., and Sudo, Masafumi., 2015. Late Cretaceous infant intra-oceanic arc volcanism, the Central Pontides, Turkey: Petrogenetic and tectonic implications. Journal of Asian Earth Sciences.

Baier, J., Andreas A., and Hans K., 2008. The origin of the negative niobium tantalum anomaly in subduction zone magmas. Earth and Planetary Science Letters 267.1: 290-300.

Barka, A.A., 1992. The north Anatolian fault zone. Annales tectonicae. Vol, 6. 164-195.

Barker, A.J., 1990. Introduction to metamorphic textures and microstructures. Glasgow: Blackie; Blackie, New York: Chapman and Hall, pp. 162.

Becker, H., Klaus P. J., and Richard W., 2000. Trace element fractionation during dehydration of eclogites from high-pressure terranes and the implications for element fluxes in subduction zones. Chemical Geology, 163.1, 65-99.

Berber, F., Göncüoğlu, M.C., and Sayit, K., 2014. Geochemistry and Tectonic Significance of the Kösedağ Metavolcanic Rocks from the Sakarya Zone, Northern Turkey. In: Proceedings of 20th CBGA Congress, Abstract Book, vol.1, 161-163, Tirana, Albania.

Best, M.G., 1975. Migration of hydrous fluids in the upper mantle and potassium variation in calc-alkalic rocks. Geology 3.8, 429-432.

Blumental, M., 1939. Über den stand der geologischen aufnahmen im Ilgaz Dağ. Maden Tetkik Arama Genel Müdürlüğü Rapor No: 842, pp, 35. Ankara (unpublished).

Blumenthal, M., 1948. Bolu civarı ile Aşağı Kızılırmak arasındaki Kuzey Anadolu Silsilelerinin jeolojisi. Maden Tetkik Arama Genel Müdürlüğü yayınları seri B, no, 13, 71-119, (In Turkish).

Blumenthal, M., 1950. Orta ve aşağı Yeşilırmak bölgelerinin jeolojisi. Maden Tetkik Arama Genel Müdürlüğü Yayınları seri D, no, 4, pp, 153. (In Turkish), Ankara.

Bortolotti, V., and Gianfranco P., 2005. Tethyan ophiolites and Pangea break-up. Island Arc 14.4, 442-470.

Bortolotti, V., Chiari, M., Göncüoğlu, M.C., Marcucci, M., Principi, G., Tekin, U. K., Saccani, E., and Tassinari, R., 2013. Age and geochemistry of basalt-chert associations in the ophiolites of the Izmir-Ankara Mélange, east of Ankara, Turkey: Preliminary data. Ofioliti 38, 2, 157-173.

Chen, F., Siebel, W., Satir, M. Terzioğlu, M.N., Saka, K., 2002. Geochronology of the Karadere basement (NW Turkey) and implications for the geological evolution of the Istanbul zone. International Journal of Earth Sciences 91.3, 469-481.

Chorowicz, J., Damien D., and Niyazi G., 1999. Neotectonics in the eastern North Anatolian fault region (Turkey) advocates crustal extension: mapping from SAR ERS imagery and Digital Elevation Model. Journal of Structural Geology 21.5, 511-532.

Clark, A.H., Pearce, T.H., Roeder, P.L., and Wolfson, I., 1986. Oscillatory zoning and other microstructures in magmatic olivine and augite: Nomarski Interference Contrast Observations on Ethec Polished Surfaces. American Mineralogist, 71(5-6), 734-741.

Coulant, E., 1894. Kastamonu vilayeti Çiban Köyü Nikel Yatakları. Maden Tetkik Arama Genel Müdürlüðü Report No: 1398, 12s. Ankara (in Turkish) (unpublished).

Creasey, 1966, Hydrothermal alteration, ir• Titley, S. R., and Hicks, C. L., eds., Geology of the porphyry copper deposits, south•vestern North America: Tucson, Univ. Arizona Press, p. 51-74.

Çelik, Ö.F., Marzoli, A., Marschik, R., Chiaradia, M., Neubauer, F., and Öz, İlknur., 2011. Early-Middle Jurassic intra-oceanic subduction in the İzmir-Ankara-Erzincan Ocean, Northern Turkey, Tectonophysics, 120-134.

Dercourt, J., Zonenshain, L.P., Ricou, L.E., Kazmin, V.G., Pichon, X.L., Knipper, A.L., Grandjacquet, Sbortshikov, I.M., Geyssant, J., Lepvrier, C., Pechersky, D.H., Boulin, J., Sibuet, J.C., Savostin, L.A., Sorokhtin, O., Westphal, M., Bazhenov, M.L., Lauer, J.P., and Duval, B.B., 1986. Geological evolution of the Tethys belt from the Atlantic to the Pamirs since the Lias." Elsevier Science Publishers B.V., Amsterdam, Tectonophysics 123,1, 241-315.

Dewey, J.F., Hempton, M.R., Kidd, W.S.F., Saroglu, F., and Şengör, A.M.C., 1986. Shortening of continental lithosphere: the tectonics of Eastern Anatolia-young collision zone. In Collision Tectonics Edited by: J.Coward & A.C. Ries. Geological Society Special Publication, London, 19, 3-36.

Dilek, Y., Thy, P., Hacker, B., and Grundvig, S., 1999. Structure and petrology of Tauride ophiolites and mafic dike intrusions (Turkey): Implications for the Neotethyan ocean. Geological Society of America Bulletin, 111.8, 1192-1216.

Floyd, P.A., and Winchester, J.A., 1978. Identification and discrimination of altered and metamorphosed volcanic rocks using immobile elements. , 21, 291-306.

Floyd, P.A., Yaliniz, M.K., and Goncuoglu, M. C., 1998. Geochemistry and petrogenesis of intrusive and extrusive ophiolitic plagiogranites, Central Anatolian Crystalline Complex, Turkey. Lithos 42.3, 225-241.

Furman, T., Kaleta, K.M., Bryce, J.G., and Hanan, B.B., 2006. Tetrtiary mafic lavas of Turkana, Kenya: Constraints on East African Plume Structure and the Occurence of high-μ volcanism in Africa. Journal of Petrology, 47.6, 1221-1244.

Genç, Ş.C., and Tüysüz, O., 2010. Tectonic setting of the Jurassic bimodal magmatism in the Sakarya Zone (Central and Western Pontides), Northern Turkey: a geochemical and isotopic approach. Lithos, 118, 95-111.

Gibson, S.A., Thompson, R.N., Leat, P.T., Morrison, M.A., Hendry, G.L., Dickin, A.P., and Mitchell., J.G. 1993. Ultrapotassic magmas along the flanks of the oligo-miocene Rio Grance Rift, USA: monitors of the zone of lithospheric mantle extension and thinning beneath a continental rift. Oxford University Press, Journal of Petrology, vol 34. Part 1, pp. 187-228.

Gökten, E., and Floyd., P.A., 2007. Stratigraphy and geochemistry of pillow basalts within the ophiolitic mélange of the Izmir–Ankara–Erzincan suture zone: implications for the geotectonic character of the northern branch of Neotethys. International Journal of Earth Sciences, 96, 725-741.

Göncüoğlu, M.C., Toprak, V., Erler, A., and Kuşçu, İ., 1991. Orta Anadolu Masifinin Batı Bölümünün Jeolojisi, Bölüm 1, Güney Kesim TPAO Rap no: 2909, pp.176.

Göncüoğlu, M.C., and Türeli, K., 1993. Petrology and geodynamic interpretation of plagiogranites from Central Anatolian Ophiolites (Aksaray-Turkey). Turkish Journal of Earth Sciences, 195-203.

Göncüoglu, M.C., Dirik, K., and Kozlu, H., 1997. General characteristics of pre-Alpine and Alpine Terranes in Turkey: explanatory notes to the terrane map of Turkey, 515-537.

Göncüoğlu, M.C., Turhan, N., Şentürk, K., Özcan, A., Uysal, Ş., and Yaliniz, M.K., 2000. A geotraverse across northwestern Turkey: tectonic units of the Central Sakarya region and their tectonic evolution. Geological Society of London, Special Publications, 173, 139-161.

Göncüoglu, M.C., Yaliniz, M.K., and Tekin, U., K., 2006. Geochemistry, tectono-magmatic discrimination and radiolarian ages of basic extrusives within the Izmir-Ankara suture belt (NW Turkey); time constraints for the Neotethyan evolution. Ofioliti, 31, 25-38.

Göncüoglu, M. C., Gürsu, S., Tekin, U.K., and Köksal, S., 2008. New data on the evolution of the Neotethyan oceanic branches in Turkey: Late Jurassic ridge spreading in the Intra-Pontide branch. Ofioliti, 33.2, 153-164.

Göncüoglu, M.C., Sayit, K., and Tekin, U.K., 2010. Oceanization of the northern Neotethys: geochemical evidence from ophiolitic melange basalts within the Izmir–Ankara suture belt, NW Turkey. Lithos, 116.1, 175-187.

Göncüoglu, M.C., Marroni, M., Sayit, K., Tekin, U.K., Ottria, G., and Pandolfi, L., 2012. The Ayli dag ophiolite sequence (central Northern Turkey): a fragment of middle jurassic oceanic lithosphere within the intra-pontide suture zone. Ofioliti, 37.2, 77-92.

Göncüoglu, M.C., Marroni, M., Pandolfi, L., Ellero, A., Ottria, G., Catanzariti, R., Tekin, U.K., Sayit, K., 2014. The Arkot Dağ Mélange in Araç area, central Turkey: Evidence of its origin within the geodynamic evolution of the Intra-Pontide suture zone. Journal of Asian Earth Sciences, 85, 117-139.

Görür, N., Şengör, A.M.C., Akkök, R., and Yılmaz, Y., 1983. Pontidlerde Neo-Tetis' in kuzey kolunun açılmasına ilişkin sedimentolojik veriler. Bulletin of the Geological Society of Turkey 26, pp. 11-20.

Görür, N.,Monod, O., Sengör, A.M.C., Tüysüz, O., Sakınç, E., Akkök, R., 1997. Palaeogeographic and tectonic position of the Carboniferous rocks of the western Pontides (Turkey) in the frame of the Variscan belt. Bulletın la Socıete geologıque de France 168, pp. 197-206.

Hakyemez, Y., Barkurt, M.Y., Bilginer, E., Pehlivan, Ş., Can, B., Dağer, Z., ve Sözeri, B., 1986. Yapraklı-llgaz-Çankırı-Çveır dolayının jeolojisi: MTA Rap. 7966 (unpublished).

Hawkesworth, C. J., O'nions, R.K., Pankhurst, P.J., Hamilton, P.J., Evensen, N.M., 1977. A geochemical study of island arc and back arc tholeiites from Scotia Sea. Earth Planet. Sci. Lett., 36, 253-62.

Irving, Anthony J., and Frederick A. Frey. Distribution of trace elements between garnet megacrysts and host volcanic liquids of kimberlitic to rhyolitic composition. Geochimica et Cosmochimica Acta 42.6 (1978): 771-787.

Jolly, W.T., Lidiak, E.G., Dickin, A.P., and Wu, T.W., 1998. Geochemical diversity ofMesozoic island arc tectonic blocks in eastern Puerto Rico. Geological Society of America, 322, pp.67.

Jolly, Wayne T., Lidiak, E.G., Dickin, A.P., and Wu, T.S., 2001. Secular geochemistry of central Puerto Rican island arc lavas: Constraints on Mesozoic tectonism in the eastern Greater Antilles.Journal of Petrology, 42.12, pp. 2197-2214.

Kaya, O., and Mostler, H., 1992. A Middle Triassic age for Low-Grade Greenschist Fades Metamorphic Sequence in Bergama (Izmir), Western Turkey: the First Paleontological Age Assignment and Structural-Stratigraphic Implications. Newsletters on Stratigraphy, pp. 1-17.

Ketin, I., 1966. Tectonic units of Anatolia (Asia Minor). Min Res Expl Inst Turkey, 66, pp. 22-34.

Kozur, H.W., Aydın, M., Demir, O., Yakar, H., Göncüoğlu, M.C., and Kuru, F., 2000. New stratigraphic and palaeogeographic results from the Palaeozoic and early Mesozoic of the Middle Pontides (northern Turkey) in the Azdavay, Devrekani, Küre and Inebolu areas: implications for the Carboniferous-Early Cretaceous geodynamic evolution and some related remarks to the Karakaya oceanic rift basin. Geologia Croatica, 53.2, pp. 209-268.

Köksal, S., Möller, A., Göncüoglu, M.C., Frei, D., and Gerdes, A., 2012. Crustal homogenization revealed by U–Pb zircon ages and Hf isotope evidence from the Late Cretaceous granitoids of the Agac¸ ören intrusive suite (Central Anatolia/Turkey). Contributions to Mineralogy and Petrology,

Köksal, S., Köksal, F.T., Göncüoğlu, M.C., 2013. Crustal source of the Late Cretaceous Satansarı monzonite stock (central Anatolia–Turkey) and its significance for the Alpine geodynamic evolution. Journal of Geodynamics, 65 pp. 82-93.

Meyer, C., and Hemley, J.J., 1967. Wall Rock Alteration. Geochemistry of Hydrothermal Ore Deposits, pp. 166-235.

Marroni, M., Frassi, C., Göncüoğlu, M.C., Di Vincenzo, G., Pandolfi, L., Rebay. G., Ellero, A., Ottria, G., (2014). Late Jurassic amphibolite-facies metamorphism in the Intra-Pontide Suture Zone (Turkey): an eastward extension of the Vardar Ocean from the Balkans into Anatolia, J Geol. Soc. 171, 605-609.

McDougall, I., and Lovering, J. F., 1963. Fractionation of chromium, nickel, cobalt and copper in a differentiated dolerite-granophyre sequence at Red Hill, Tasmania. Journal of the Geological Society of Australia, 10.2, 325-338.

McKenzie, D., and O'nions, R.K., 1991. Partial melt distributions from inversion of rare earth element concentrations. Journal of Petrology, 32, 1021-1091.

Meschede, M., 1986. A method of discriminating between different types of mid-ocean ridge basalts and continental tholeiites with the Nb-Zr-Y diagram. Chemical Geology, 56, 207-218.

Moix, P., Beccaletto, L., Kozur, H.W., Hochard, C., Rosselet, F., and Stampfli, G.M., 2008. A new classification of the Turkish terranes and sutures and its implication for the paleotectonic history of the region. Tectonophysics, 451.1, pp. 7-39.

O'Brien, H.E., Irving, A.J., and McCallum, I.S., 1988. Complex zoning and resorption of phenocrysts in mixed potassic mafic magmas of the Highwood Mountains, Montana. Amer. Mineral. 73, 1007-1024.

Okay, A.I., and Tüysüz, O, 1999. Tethyan sutures of northern Turkey, in The Mediterranean Basins: Tertiary Extension Within the Alpine Orogen, vol. 156, Geological Society, London, Special Publication, pp. 475-515, Oxford, UK.

Okay, A.I., 2000, Was the Late Triassic orogeny in Turkey caused by the collision of an oceanic plateau?, in Bozkurt, E., et al., (eds)., Tectonics and magmatism in Turkey and surrounding area: Geological Society [London] Special Publication 173, p. 25–41.

Okay, Aral I., and Göncüoğlu, M.C., 2004. The Karakaya Complex: a review of data and concepts. Turkish Journal of Earth Sciences, 13.2, 75-95.

Okay, A.I., Tüysüz, O., Satır, M., Altıner, S.Ö., Altıner, D., Sherlock, S., Eren, R., H., 2006. Cretaceous and Triassic subduction-accretion, high-pressure–low-temperature metamorphism, and continental growth in the Central Pontides, Turkey. Geological Society of America Bulletin, 118.9-10, pp. 1247-1269.

Okay, A.I., Sunal, G., Sherlock, S., Altıner, D., Tüysüz, O., Kylander-Clark, A.R.C., Aygül, M., 2013. Early Cretaceous sedimentation and orogeny on the active margin of Eurasia: Southern Central Pontides, Turkey. Tectonics, 32.5, 1247-1271.

Okay, A.I., Altıner, D., and Kılıç, A., 2015. Triassic limestone, turbidites and serpentinite–the Cimmeride orogeny in the Central Pontides. Geological Magazine, 152.3, 460-479.

Parlak, O., Çolakoğlu, A., Dönmez, C., Sayak, H., Yildirim, N., Türkel, A., Odabaşi, İ., 2013. Geochemistry and tectonic significance of ophiolites along the İzmir–Ankara–Erzincan Suture Zone in northeastern Anatolia.Geological Society, London, Special Publications, 372.1, 75-105.

Passchier, C.W., and R.A.J. Trouw., 2005. Microtectonics, 366 pp.

Pearce, J.A., and Cann, J.R., 1973. Tectonic setting of basic volcanic rocks determined using trace element analyses. Earth and planetary science letters,19.2, 290-300.

Pearce, J.A., 1982. The trace element characteristics of lavas from destructive plate boundaries. In: Thorpe, R.S., (ed.), Andesites, 525-548. New York: John Wiley and Sons.

Pearce, J.A., 1983. Role of the subcontinental lithosphere in magma genesis at active continental margins, 230-249.

Pearce, J.A., and Peate, D.W., 1995. Tectonic implications of the composition of volcanic arc magmas. Annual Review of Earth and Planetary Sciences, 23, 251-286.

Pearce, J.A., Stern, R.J., Bloomer, S.H., Fryer, P., 2005. Geochemical mapping of the Mariana arc-basin system: Implications for the nature and distribution of subduction components. Geochemistry, Geophysics, Geosystems. v6.7

Pickett, E.A., and Robertson, A.H.F., 2004. Significance of the volcanogenic Nilüfer Unit and related components of the Triassic Karakaya Complex for Tethyan subduction/accretion processes in NW Turkey. Turkish Journal of Earth Sciences, 13.2, v. 13, 97-143.

Pilz R., 1937. Kastamonu ve Sinop vilayetlerindeki çeþitli mineral yataklarının tetkiki. Maden Tetkik Arama Genel Müdürlüðü Report No: 644. Ankara (in Turkish) (unpublished).

Robertson, A.H.F., Dixon, J.E., Brown, S., Collins, A., Morris, A., Pickett., E., Sharp, I., and Ustaömer, T., 1996. Alternative tectonic models for the Late Palaeozoic-Early Tertiary development of Tethys in the Eastern Mediterranean region. Geological Society, London, Special Publications, 105.1, 239-263.

Robertson, A.H.F., Ustaömer, T., Pickett, E.A., Collins, A.S., Andrew, T., Dixon, J.E., 2004. Testing models of Late Palaeozoic–Early Mesozoic orogeny in Western Turkey: support for an evolving open-Tethys model. Journal of the Geological Society, 161.3, 501-511.

Rojay, B., 2013. Tectonic evolution of the Cretaceous Ankara ophiolitic mélange during the Late Cretaceous to pre-Miocene interval in Central Anatolia, Turkey. Journal of Geodynamics, 65, 66-81.

Sarıfakıoğlu, E., Özen, H., and Winchester, J.A., 2008. Petrogenesis of the Refahiye ophiolite and its tectonic significance for Neotethyan Ophiolites Along the İzmir-Ankara-Erzincan Suture Zone. Turkish Journal of Earth Science, vol. 18, 187-207.

Sarifakioglu, E., Dilek, Y., and Sevin, M., 2014. Jurassic–Paleogene intraoceanic magmatic evolution of the Ankara Mélange, north-central Anatolia, Turkey."Solid Earth, 5.1, 77-108.

Sayıt, K., and Göncüoglu, M.C., 2009. Geochemistry of mafic rocks of the Karakaya Complex, Turkey: evidence for plume-involvement in the Palaeotethyan extensional regime during the Middle and Late Triassic. International Journal of Earth Sciences, 98.2, 367-385.

Sayıt, K., and Göncüoglu, M.C., 2013. Geodynamic evolution of the Karakaya Mélange Complex, Turkey: A review of geological and petrological constraints. Journal of Geodynamics, 65, 56-65.

Sayit, K., Tekin, U.K., and Göncüoglu, M.C., 2011. Early-middle Carnian radiolarian cherts within the Eymir Unit, Central Turkey: Constraints for the age of the Palaeotethyan Karakaya Complex. Journal of Asian Earth Sciences, 42.3, 398-407.

Sayit, K., Marroni, M., Göncüoglu, M.C., Pandolfi, L., Ellero, A., Ottria, G., Frassi, C., Geological setting and geochemical signatures of the mafic rocks from the Intra-Pontide Suture Zone: implications for the geodynamic reconstruction of the Mesozoic Neotethys. International Journal of Earth Sciences, 1-26.

Scambelluri, M., and Philippot, P., 2001. Deep fluids in subduction zones. Lithos, 55.1, 213-227.

Schmid, S., Bernoulli, D., Fügenschuh, B., Matenco, L., Schefer, S., Schuster, R., Tischler, M., and Ustaszewski, K., 2008. The Alps-Carpathians-Dinarides-connection: a correlation of tectonic units. Swiss Journal of Geosciences, 101.1, 139-183.

Sevin, M., and Uğuz, M.F., 2011. Çankırı-G32 paftasına ait rapor, No: 148. Maden Tetkik ve Arama Genel Müdürlüğü, Ankara.

Stampfli, G.M., and Borel, G.D., 2002. A plate tectonic model for the Paleozoic and Mesozoic constrained by dynamic plate boundaries and restored synthetic oceanic isochrons. Earth and Planetary Science Letters, 196.1, 17-33.

Stolz, A.J., Jochum, K.P., Spettel, B., Hofman, A.W., 1996. Fluid and melt related enrichemnt in the subarc mantle: evidence from Nb/Ta variations in island arc basalts. Geology; v.24; no 7; 587-590.

Şengör, A.M.C., Yılmaz, Y., and Ketin, I., 1980. Remnants of a pre-Late Jurassic oceain in northern Turkey: Fragments of Permian-Triassic Paleo-Tethys. Geological Society of America Bulletin, 91, 599-609.

Şengör, A.M.C. and Yılmaz, Y., 1981. Tethyan evolution of Turkey: A plate tectonic approach. Tectonophysics, 75, 181-241.

Şengör, A.M.C., Burke, K., and Dewey, J.F., 1982. Tectonics of the North Anatolian Transform Fault. See Işıkara & Vogel, 1982, 3–22.

Şengör, A.M.C., Yılmaz, Y., and Sungurlu, O., 1984. Tectonics of the Mediterranean Cimmerides: nature and evolution of the western termination of Paleo-Tethys. In: Dixon, J.E., and Robertson, A.H.F., (eds.), The Geological Evolution of the Eastern Mediterranean. Geological Society, London, Special Publications, 17, 77-112.

Şengör, A.M.C., 1984. The Cimmeride orogenic system and the tectonics of Eurasia. Geological Society of America Special Papers, 195, 1-74.

Şengör, A.M.C., Görür, N., and Şaroğlu, F., 1985. Strikeslip faulting and related basin formation in zones of tectonic escape: Turkey as a case study. In Strike-slip Deformation, Basin Formation, and Sedimentation, Soc. Econ. Paleontol. Miner. Spec. Publ. 37 (in honor of J.C. Crowell), ed. KT Biddle, N Christie-Blick, 227–64.

Şengör, A. M. C., Tüysüz, O., İmren, C., Sakınç, M., Eyidoğan, H., Görür, N., Pichon, X.L., Rangin, C., 2005. The North Anatolian fault: A new look. Annu. Rev. Earth Planet. Sci. 33, 37-112.

Spath, A., Le Roex, A.P., and Duncan, R.A., 1996. The geochemistry of lavas from the Comores Archipelago, Western Indian Ocean: petrogenesis and mantle source region characteristics. Journal of Petrology, 37, 961-991.

Sun, S.S., and McDonough, W.F., 1989. Chemical and isotopic systematics of oceanic basalts: implications for mantle composition and processes. Geological Society, London, Special Publications, 42.1, 313-345.

Taylor, S.R., and McLennan, S.M., 1995. The geochemical evolution of the continental crust. Reviews of Geophysics, 33.2, 241-265.

Tekin U.K., Göncüoglu M.C. and Turhan N., 2002. First evidence of Late Carnian radiolarian fauna from the Izmir-Ankara Suture Complex, Central Sakarya, Turkey: Implications for the opening age of the Izmir-Ankara branch of Neotethys. Geobios, 35.1, 127-135.

Thompson, G., 1991. Metamorphic and hydrothermall processes: basalt-seawater interactions. In: Floyd, P.A., (ed.), Oceanic Basalts. Blackie, Glasgow and London, 148-173.

Topuz, G., Altherr, R., Kalt, A., Satır, M., Werner, O., and Schwarz, W.H., 2004. Aluminous granulites from the Pulur complex, NE Turkey: a case of partial melting, efficient melt extraction and crystallisation. Lithos, 72.3, 183-207.

Topuz, G., Altherr, R., Schwarz, W.H., Dokuz, A., Meyer, H.P., 2007. Variscan amphibolite-facies rocks from the Kurtoğlu metamorphic complex (Gümüşhane area, Eastern Pontides, Turkey). International Journal of Earth Sciences, 96.5, 861-873.

Topuz, G., Göçmengil, G., Rolland, Y., Çelik, Ö.F., Zack, T., and Schmitt, A.K., 2012. Jurassic accretionary complex and ophiolite from northeast Turkey: No evidence for the Cimmerian continental ribbon. Geology, 41.2, 255-258.

Tüysüz, O., 1985. Kargı Masifi ve dolayındaki tektonik birliklerin ayırdı ve araştırılması (petrolojik inceleme). Diss. PhD thesis, Istanbul University Institute of Science, 431 pp. (unpublished).

Tüysüz, O., 1990. Tectonic evolution of a part of the Tethyside orogenic collage: the Kargi Massif, northern Turkey. Tectonics, 9.1, 141-160.

Tüysüz, O., 1993. Karadeniz'den Orta Anadolu'ya bir jeotravers: Kuzey neo-Tetis' in tektonik evrimi: Türkiye Petrol Jeologları Derneği Bülteni, 5. 1-33.

Tüysüz, O., and Yiğitbaş, E., 1994. The Karakaya basin: a Palaeo-Tethyan marginal basin and its age of opening. Acta Geologica Hungarica, 37.3-4, 327-350.

Tüysüz, O., 1999. Geology of the Cretaceous sedimentary basins of the Western Pontides. Geological Journal, 34.1-2, 75-93.

Tüysüz, O., and Tekin, U.K., 2007. Timing of imbrication of an active continental margin facing the northern branch of Neotethys, Kargı Massif, northern Turkey. Cretaceous Research, 28.5, 754-764.

Ustaömer, T. and Robertson, A.H.F., 1993. A Late Palaeozoic-Early Mesozoic marginal basin along the actives sourthern continental margin of Eurasia: Evidence from the central Pontides (Turkey) and adjacent regions. Geological Journal, 28.3-4, 219-238.

Ustaömer, T. and Robertson, A.H.F., 1994. Late Palaeozoic marginal basin and subduction-accretion: The Palaeotethyan Küre complex, central Pontides, northern Turkey. Journal of the Geological Society, 151.2, 291-305.

Ustaömer, T. and Robertson A.H.F., 1997. Tectonic-sedimentary evolution of the north tethyan margin in the Central Pontides of northern Turkey. AAPG Mem 68, 255-290.

Ustaömer, P.A., and Rogers, G., 1999. The Bolu Massif: remnant of a pre-Early Ordovician active margin in the west Pontides, northern Turkey. Geological Magazine, 136.5, 579-592.

Ustaömer, P.A., Ustaömer, T., and Robertson, A.H.F., 2012. Ion Probe U-Pb dating of the Central Sakarya Basement: a peri-Gondwana terrane intruded by Late Lower Carboniferous subduction/collision-related granitic rocks. Turkish Journal of Earth Sciences, 21.6, 905-932.

Uğuz, M. F., Sevin, M., and Duru, M., 2002. Sinop sheet in the Geological map series of Turkey, scale 1: 500 000, Maden Tetkik ve Arama Genel Müdürlüğü, Ankara.

Uysal, İ., Şen, A.D., Ersoy, E.Y., Dilek, Y., Saka, S., Zaccarini, F., Escayola, M., Karslı, O., 2014. Geochemical make-up of oceanic peridotites from NW Turkey and the multi-stage melting history of the Tethyan upper mantle. Miner Petrol, 108, pp. 49-69.

Uysal, I., Ersoy, E.Y., Dilek, Y., Escayola, M., Sarıfakıoğlu, E., Saka, S., and Hirata, T., 2013. Depletion and refertilization of the Tethyan oceanic upper mantle as revealed by the early Jurassic Refahiye ophiolite, NE Anatolia—Turkey. Gondwana Research, 27.2, 594-611.

Vernon, R.H., 2004. A Practical Guide to Rock Microstructure. Cambridge University Press. 594 pp.

Williams, P.F., 1972. Pressure shadow'structures in foliated rocks from Bermagui, New South Wales. Journal of the Geological Society of Australia, 18.4, 371-377.

Wilson, M., 1989. Igneous Petrogenesis. London: Unwin Hyman, 466 pp.

Winchester, J.A., and Floyd, P.A., 1977. Geochemical discrimination of different magma series and their differentiation products using immobile elements. Chemical geology, 20, 325-343.

Winter, J.D., 2001. An introduction to igneous and metamorphic petrology. pp. 699

Wood, D.A., Gibson, I.L., and Thompson, R.N., 1976. Elemental mobility during zeolite facies metamorphism of the Tertiary basalts of eastern Iceland. Contributions to Mineralogy and Petrology, 55.3, 241-254.

Yalınız, M.K., Floyd, P.A., and Göncüoglu, M.C., 1996. Supra-subduction zone ophiolites of Central Anatolia: geochemical evidence from the Sarıkaraman Ophiolite, Aksaray, Turkey. Mineral. Mag., 60: 697-710

Yaliniz, K.M., Aydın, N.S., Göncüoğlu, M.C., Parlak, O., 1999. Terlemez quartz monzonite of Central Anatolia (Aksaray-Sarıkaraman): age, petrogenesis and geotectonic implications for ophiolite emplacement. Geol. J, 34, 233-242.

Yalınız M.K., Göncüoglu, M.C., and Özkan-Altıner, S., 2000a. Formation and emplacement ages of the SSZ-type Neotethyan Ophiolites in Central Anatolia, Turkey: paleotectonic implications. Geol. J., 35, 53-68.

Yalınız M.K., Göncüoglu M.C., and Floyd P.A., 2000b. Geochemistry of volcanic rocks from the Çicekdağ Ophiolite, Central Anatolia, Turkey, and their inferred tectonic setting within the northern branch of the Neotethyan ocean. In: E. Bozkurt, J. Winchester and J.A. Piper (Eds.), Tectonics and magmatism in Turkey and the surrounding area. Geol. Soc. London Spec. Publ., 173: pp. 203-218.

Yılmaz, O., 1980. Tectonics and lithostratigraphic units of the northeastern part of the Daday-Devrakani massif (in Turkish). Yerbilimleri, 5–6, 101–135.

Yılmaz, O., and Durmuş B., 1986. Kastamonu granitoid belt of northern Turkey: First arc plutonism product related to the subduction of the paleo-Tethys. Geology, 14.2, 179-183.

Yılmaz, O., 1988. L'ensemble ophiolitique de C angal (Turquie du Nord): Mise en evidence d'un metamorphisme oceanique et d'un retrometamorphisme cataclastique tardif. Geologie Alpine, 64, 113–132.

Yılmaz, Y., and Tüysüz, O., 1984. Kastamonu-BoyabatVezirköprü-Tosya arasındaki bölgenin jeolojisi (Ilgaz-Kargı masiflerinin etüdü). Maden Tetkik Arama Genel Müdürlüğü Report No:7838, pp. 275. Ankara (in Turkish) (unpublished).

Yılmaz, Y., Tüysüz, O., Yiğitbaş E., Genç, Ş.C., and Şengör, A.M.C., 1997. Geology and tectonic evolution of the Pontides. In Regional and Petroleum Geology of the Black Sea and Surrounding Region, Am. Assoc. Pet. Geol. Mem. 68, ed. AG Robinson, pp. 183–266. Tulsa, OK: Am. Assoc. Pet. Geol.

Yiğitbaş, E., Elmas, A., and Yılmaz, Y., 1999. Pre-Cenozoic tectonostratigraphic components of Western Pontides and their geological evolution Geol. J, 34, 55–74.

Yoldaş, R., 1982. Tosya (Kastamonu) ile Bayat (Çorum) arasındaki bölgenin jeolojisi: Ph.D. Thesis. İstanbul Üniversitesi, pp. 311.

APPENDIX A

GEOCHEMICAL ANALYSIS RESULTS

Table A-1: Geochemical analysis results of Kösedağ Metavolcanics

ELEMENT	6-4	6-5	6-6	6-7a	6-7b	6-7c	6-8	168
SiO_2 (%)	56.79	69.26	63.62	58.72	71.4	48.07	73.61	58.17
Al_2O_3 (%)	17.29	15.08	16.49	17.81	12.75	19.64	14.27	17.31
Fe_2O_3 (%)	11.31	5.7	8.2	7.55	5.6	12.79	2.55	11.09
MgO (%)	5.35	1.95	3.25	2.94	2.5	10.29	1.77	4.85
CaO (%)	1.74	1.77	3.54	6.82	0.87	4.05	0.87	0.55
Na_2O (%)	5.63	4.91	2.31	2.23	5.69	3.95	4.17	6.31
K_2O (%)	0.04	0.49	1.87	3.09	0.27	0.13	2.31	0.35
TiO_2 (%)	1.25	0.58	0.44	0.54	0.64	0.71	0.36	1.03
P_2O_5 (%)	0.29	0.17	0.13	0.1	0.18	0.13	0.07	0.17
MnO (%)	0.31	0.08	0.11	0.21	0.13	0.28	0.05	0.13
Cr_2O_3 (%)	0.002	b.d	b.d	0.002	b.d	0.004	b.d	0.01
LOI (%)	4.4	2.2	5	5.5	2	5.4	2.8	3.2
Sum (%)	99.88	99.9	99.83	99.77	99.91	99.86	99.85	99.89
Ni (ppm)	7.4	1.2	3.9	11.7	3.3	19.6	1.9	3.8
Sc (ppm)	38	21	14	12	20	35	9	29
Ba (ppm)	15	103	498	535	58	38	520	53
Co (ppm)	22.1	5.3	7	7.3	7	30.8	2.7	23
Cs (ppm)	b.d	0.2	0.8	0.5	b.d	b.d	0.6	0.2

Table A-1: (continued).

Hf (ppm)	2	2.4	4.5	5.7	2.3	1.3	3.4	2.6
Nb (ppm)	1.8	2.4	4.4	5	3.5	1.5	4.3	1.6
Rb (ppm)	0.6	6.7	27.2	35.3	3.7	1.4	37.2	4.7
Sr (ppm)	84.3	119.5	162.2	524.7	42.8	270	60.6	66.8
Ta (ppm)	b.d	0.1	0.3	0.4	0.2	b.d	0.2	b.d
Th (ppm)	0.6	0.7	3	7.2	2.3	2.9	5.8	1.1
U (ppm)	0.1	0.2	0.7	0.8	0.6	0.7	1	0.4
V (ppm)	226	35	17	124	62	236	31	244
Zr (ppm)	57.5	79.3	164.2	185.4	78.9	32.7	126	84.6
Y(ppm)	36.3	29.9	28.8	26.9	29.3	15.4	22.4	20.8
La (ppm)	5.5	7	11.8	23.5	13.8	8.9	18.1	6.7
Ce (ppm)	10.6	15.9	27.4	40.7	29.8	17.3	41.2	19.6
Pr (ppm)	2.19	2.55	3.59	5.4	3.9	2.15	4.04	2.1
Nd (ppm)	11.6	13.1	16.6	20.4	17	9	17.7	10.5
Sm (ppm)	3.42	3.64	4.02	4.43	4.25	2.13	3.42	3.2
Eu (ppm)	1.38	1.28	1.08	1.23	1.05	0.79	0.92	0.8
Gd (ppm)	5.13	5.36	4.49	4.61	4.78	2.51	3.81	3.42
Tb (ppm)	0.91	0.88	0.83	0.82	0.82	0.46	0.65	0.65
Dy (ppm)	5.69	5.86	5.07	4.92	4.97	2.91	3.53	3.86
Ho (ppm)	1.26	1.08	0.99	1.06	1.14	0.62	0.8	0.7
Er (ppm)	3.75	3.41	3.37	3.67	3.3	1.93	2.74	2.66
Tm (ppm)	0.59	0.48	0.51	0.57	0.49	0.29	0.43	0.35
Yb (ppm)	3.81	3.23	3.74	4.06	3.2	2	3.23	2.65
Lu (ppm)	0.61	0.46	0.54	0.69	0.56	0.28	0.51	0.39
ELEMENT	**44**	**49**	**32**	**50**	**169**	**182**	**214**	
SiO_2 (%)	76.88	68.73	56.09	54.82	54.19	60.96	78.35	
Al_2O_3 (%)	12	15	23.93	15.38	18.63	15.93	12.37	
Fe_2O_3 (%)	3.15	5.49	7.19	13.15	10.35	8.78	1.56	
MgO (%)	1.17	2.87	5.21	4.93	5.53	4.35	0.57	
CaO (%)	2.54	1.56	1.24	7.08	4.15	3.64	1.8	
Na_2O (%)	1.43	4.83	0.74	3.15	5.55	4.43	4.27	

Table A-1: (continued).

K_2O (%)	2.22	0.76	4.28	0.03	0.24	0.35	0.7
TiO_2 (%)	0.39	0.45	0.73	1.1	0.95	1.07	0.28
P_2O_5 (%)	0.1	0.11	0.06	0.14	0.16	0.25	0.05
MnO (%)	0.05	0.12	0.06	0.19	0.2	0.18	0.01
Cr_2O_3 (%)	0.005	0.008	0.005	0.002	0.006	b.d.	0.003
LOI (%)	2.4	2	4.8	3.7	4	3.3	1.4
Sum (%)	99.89	99.92	99.8	99.8	99.81	99.85	99.93
Ni (ppm)	1.1	3.6	7.4	9.5	8.5	0.9	1
Sc (ppm)	11	17	25	41	34	27	8
Ba (ppm)	533	156	444	36	122	123	333
Co (ppm)	3.6	8.6	9.6	35	22.2	14.1	1.1
Cs (ppm)	0.8	0.7	1	0.2	0.3	0.2	0.3
Hf (ppm)	3.1	1.6	3.9	1.6	1.2	2.5	3.7
Nb (ppm)	4.4	2.3	3.2	1.2	1.2	2.3	3.1
Rb (ppm)	31	15.2	58	0.4	2.9	5.2	10
Sr (ppm)	74.7	135.4	258	147.9	183.4	163.2	150.9
Ta (ppm)	0.2	b.d	b.1	b.d	b.d	b.d	0.2
Th (ppm)	2.9	1.5	3.6	0.2	0.4	0.8	2.1
U (ppm)	1.1	0.1	b.d	b.d	b.d	0.2	0.4
V (ppm)	42	60	55	398	341	110	60
Zr (ppm)	110.2	54.9	121.9	49.4	44.5	88.4	136
Y (ppm)	28.8	17.1	23.2	24.5	20.8	36.3	41.1
La (ppm)	12.4	7.9	7	5.1	5.6	9.5	12.1
Ce (ppm)	23.5	14	17.3	10.4	12.3	20.6	25.9
Pr (ppm)	3.17	1.84	2.39	1.76	1.89	3.15	3.68
Nd (ppm)	13.2	9	11.6	9.3	9.4	15.4	17.4
Sm (ppm)	3.35	2.39	3.48	2.71	2.24	4.35	4.4
Eu (ppm)	0.81	1.01	0.95	1.04	0.96	1.48	1.14
Gd (ppm)	4.27	2.72	4.05	3.69	3.43	5.6	5.89
Tb (ppm)	0.8	0.54	0.78	0.68	0.61	1	1.06
Dy (ppm)	4.95	3.15	4.74	4.45	4.06	6.01	6.65

Table A-1: (continued).

Ho (ppm)	1.07	0.67	1.14	0.89	0.77	1.3	1.43
Er (ppm)	3.36	1.87	3.37	2.69	2.39	4.19	4.55
Tm (ppm)	0.47	0.32	0.58	0.4	0.36	0.62	0.63
Yb (ppm)	2.95	2.21	3.9	2.7	2.2	3.89	4.43
Lu (ppm)	0.48	0.33	0.65	0.39	0.34	0.59	0.75

* b.d: below detection limit.